POLITECNICO DI TORINO

Dipartimento di Ingegneria Meccanica ed Aerospaziale

Tesi di Laurea Magistrale

# ASSESSMENT OF THE IMPACT OF MINIATURIZED ELECTRIC PROPULSION SYSTEMS ON SMALL SATELLITES TECHNOLOGY



**Relatori**

Prof. Sabrina Corpino

Ing. Fabrizio Stesina

**Candidato**

Sergio Zanola

Ottobre 2019

# ACKNOWLEDGEMENTS

# ABSTRACT

The present thesis was born as part of a joint project between the CubeSat Team of Politecnico di Torino and the European Space Agency (ESA). This project, named ESA-Prop has the goal to design a platform devoted to the test and qualification of miniaturized electrical propulsion systems for CubeSats. The idea is to increase the devices Technology Readiness Level (TRL) and to study the mutual interaction occurring between the propulsion system and the host platform. The ultimate goal of the project is to provide a one-stop test facility for the qualification of CubeSats featuring propulsion systems on board.

This thesis covers the last part of the phase one of the project, with the feasibility concept and the integration and test of the prototype, and the early stages of phase two, with the definition of tests and the upgrade of the prototype to host the ePS and collect relevant data. Its focus is on the assessment of the impact and mutual interaction of an ePS on a CubeSat platform, particularly on the thermal aspects.

The first part of this thesis focuses on an overview of the State-of-the-Art of miniaturized electric propulsion. most prominent solutions have been identified and their capabilities and limitation analysed. They were cross checked with a preliminary analysis of different mission scenarios, creating a matrix summarizing ePS capability to fulfil different roles.

An overview of the different aspects an ePS will impact over the CubeSat is then analysed, and then measurements of interest are identified. In order to define qualification tests and test platform design, sensors to be used are identified and discussed, with a focus on those measurements that have been defined as priority during a meeting with ESA customers.

The thesis then covers the integration and testing phases of the prototype both in Turin and at the Electric Propulsion Laboratory at ESA/ESTEC. It provides a status of the project at prototype phase, that is the starting point for the upgraded version that will implement the sensors to acquire the measurements discussed in the previous chapter.

A focus is then put on the assessment of the thermal aspects of the interaction between the ePS and the platform. The operational environment and the test environment are defined and discrepancies between the two identified. It is then described the thermal model of the platform designed with thermal desktop to define the optimal points for temperature sensors. The model provides a firs approximation of the heat loads and temperature map of the test platform, enabling test designers to position thermistors accordingly.

Thermal model outputs are then verified and corrected empirically thanks to an ePS thermal load emulator, composed by an aluminium structure with dissipating resistors simulating the dissipated power of the ePS.

Next phases of the project will see the completion of the new avionics design, with more acquisition lines, allowing other sensors to be tested. At the end of test definition and platform upgrade the new test platform will be integrated with an ePS and actual tests will be conducted in a vacuum chamber.

# CONTENTS

# LIST OF FIGURES

# LIST OF TABLES

# ABBREVIATIONS

**ADC**: Analog to Digital Conversion

**ADC**: Analog to Digital Converted

**AU:** Astronomical Unit

**C&DH**: Command and Data Handling

**CTP**: CubeSat Test Platform

**EPL**: Electric Propulsion Laboratory

**EPS**: Electric Power System

**ePS**: Electric Propulsion System

**ESA**: European Space Agency

**FEEP**: Field Emission Electric Propulsion

**GSE**: Ground Support Equipment

**GUI**: Graphic User Interface

**HPT**: Helicon Plasma Thruster

**LEO**: Low Earth Orbit

**LS**: Load Switch

**MLI**: Multi-Layer Insulation

**MRIT**: Miniaturized Radiofrequency Ion Thruster

**NEO**: Near Earth Object

**NTC**: Negative Temperature Coefficient

**OBC**: On-Board Computer

**PEEK**: Poly-Ether Ether Ketone (plastic material)

**PPT**: Pulsed Plasma Thruster

**PWM**: Pulse Width Modulation

**QCM**: Quartz Crystal Microbalance

**RBT**: Remove Before Test

**RBT:** Remove Before Test

**RCS**: Reaction Control System

**RFT**: Reduced Functional Test

**RPA**: Retarding Potential Analyser

**SPF**: Small Plasma Facility

**TCS**: Thermal Control System

**TNC**: Terminal Node Controller

**TRL**: Technology Readiness Level

**tvac**: Thermal Vacuum

**vac**: Vacuum

# INTRODUCTION

## 1.1 CONTEXT

Nano-satellites represent an emerging opportunity to pursue a broad set of mission goals, including science, technology demonstration, Earth Observation, and communications, at low cost and fast delivery. For this reason, the last years have seen an increase of interest from both the public and private sector in the development of missions and technologies tailored for small satellites in general and CubeSats in particular.

Since the standard creation in 1999 CubeSats have developed from Education tools to technology demonstrators and now as actual science or service platforms, able to perform tasks like bigger spacecraft. Those services are provided both from single CubeSats, often released as secondary objectives from bigger missions, and from constellations of tens or even hundreds of small satellites, able to provide a far superior coverage than a single platform. This has been made possible thanks to the miniaturization of spacecraft technology and payloads. One of the most discussed new application of CubeSat and nanosats is the creation of constellations composed by thousands of satellites to provide broad band internet connection all over the world, such as SpaceX's Starlink constellation.

European Space Agency (ESA) interest in CubeSat is also growing, seeing they have various promising applications in ESA context [1]:

- As a driver for drastic miniaturization of systems, "systems-on-chip" and totally new approach to packaging and integration, multi-functional structures and embedded propulsion
- As an affordable means of demonstrating such technologies, together with novel techniques such as formation flying, close inspection and rendezvous and docking
- As an opportunity to carry out distributed multiple in-situ measurements, such as obtaining simultaneous multi point observations of the space environment
- As a means of deploying small payloads

- As a means of augmenting solar system exploration with – for instance, a standalone fleet capable of rendezvous with multiple targets (e.g. NEOs) or a swarm carried by a larger spacecraft and deployed at the destination (e.g. Moon, asteroids and comets, Mars)

The development of standardised subsystems for CubeSat represents a clear niche for scientists and industry alike. Many progresses have been done in most fields but there is still a significant gap between current technology and the theoretical limits. One of the systems that have gained more and more attention is micropropulsion[2]. This is both one of the less developed fields of CubeSat technology and one of the most interesting to reach near future goals. For this reason, there is an increasing number of agencies, universities and private companies that are miniaturizing existing PS or developing brand new ones, specifically dedicated to small satellites.

A particular interest is given to Electric propulsion, that can achieve much higher Isp than traditional propulsion, thus requiring less propellant in order to complete the same mission. This is particularly important for CubeSats missions where both mass and volume of the systems is particularly critical due to the small form factor of the standard. To give an order of measure while for small Earth orbit changes a few hundred seconds are enough, in order to have standalone CubeSats missions to the NEOs the ideal specific impulse of about 2500-3000 seconds is required. A specific impulse this high is only achievable through advanced propulsion such as ion propulsion or other electric technologies.

## 1.2 TECHNOLOGY READINESS LEVEL

Electric propulsion is quite a new addition to spacecraft propulsion systems in use even for bigger spacecraft and are almost completely new in their miniaturized form. Some of the so called "potentially disruptive technologies" have just reached a laboratory research level and will still need much research and work before they develop to their full potential. The maturity of a technology is usually referred to as Technology Readiness Level, or TRL. Miniaturized propulsion technology has at the moment low TRL and little to no actual launches to space.

This thesis exists in the picture of a Politecnico di Torino project funded by the Electric Propulsion Laboratory of ESA-ESTEC facility for the design, integration, testing and operation of a CubeSat Test Platform (CTP) enabling an easy to integrate way of testing propulsion systems in relevant conditions such as vacuum and thermovacuum while integrated in an

actual CubeSat-like platform, with all its critical subsystems and a set of sensor to study the actual impact of the ePS during various phase missions.

The use of ESA-Prop platform to test not only electric propulsion but any type of CubeSat sized miniaturized propulsion will increase the Technology Readiness Level of the technology to TRL6. In Figure 1 is reported a table of TRL from NASA, as shown TRL6 is the higher TRL achievable before launching and testing in space the technology and is usually required to perform TRL7 space test.

**TRL 9**
•Actual system "flight proven" through successful mission operations

**TRL 8**
•Actual system completed and "flight qualified" through test and demonstration (ground or space)

**TRL 7**
•System prototype demonstration in a space environment

**TRL 6**
•System/subsystem model or prototype demonstration in a relevant environment (ground or space)

**TRL 5**
•Component and/or breadboard validation in relevant environment

**TRL 4**
•Component and/or breadboard validation in laboratory environment

**TRL 3**
•Analytical and experimental critical function and/or characteristic proof-of-concept

**TRL 2**
•Technology concept and/or application formulated

**TRL 1**
•Basic principles observed and reported

*Figure 1 Technology Readiness Level (TRL). Credits: NASA*

## 1.3 The CubeSat gap

As stated in the previous paragraph, miniaturized electric propulsion is being developed at an increasing rate from many different actors on the international industry scene. Many of the technologies are at laboratory testing level and the first results are encouraging, with good performances and compact form factors. All seems to indicate that in a few years CubeSat relying on electric propulsion for several applications could be an established asset for both space agencies and private actors.

However, one aspect of the application of electric propulsion to CubeSat platforms still remains unexplored. There has not yet been an assessment of the mutual interaction between electric propulsion technology and CubeSat technology. This causes an important knowledge gap that should be filled before any actual mission featuring electrically propelled CubeSats can be launched. It is critical for both the safety and the success of the mission that the extent of the mutual interaction is fully understood, especially considering a CubeSat system has usually fewer fail-safe systems and redundancies than a traditional, bigger platform.

## 1.4 Motivation and Objectives

This thesis, as the whole ESA-Prop program, aims at filling the above-mentioned knowledge gap, and to provide a wider, clearer view on the application of electric propulsion to CubeSat and its impact on the system at every level. Specifically, ESA-Prop goals are:

- Goal of the whole activity: to provide a one-stop facility for the qualification of CubeSat platforms featuring electric propulsion systems, including functional, performances and environmental tests.
- Objective I: to build a platform devoted to CubeSats qualification
- Objective II: to evaluate ePS impact on CubeSat technology

This thesis, while supporting the development of the ESA-Prop program and collaborating in achieving its objective as a whole, focusing on certain aspects. The objectives driving this work where:

- To support the development, integration and testing of the CubeSat Test Platform

4

- To provide an overview of the impact of ePS at mission level, by investigating propulsion technologies and analysing their mission applicability
- To provide an overview of the impact of ePS system at system level, with a focus on electro-thermal aspects.

# ELECTRIC PROPULSION FOR CUBESATS

CHAPTER 2

## 2.1 MINIATURIZED ELECTRIC PROPULSION: STATE OF THE ART

As a preliminary activity for this project a study on the state of the art of miniaturized ePS was performed, identifying the most promising technologies and their capabilities as well as the most advanced propulsion systems based on them.

The platform is designed to be compatible with almost any CubeSat sized ePS whose power needs are met from the dedicated electric power system. Plans are ongoing to further extend the power range in order to follow the trend for more powerful ePS in the future. However different ePS could present different characteristics both regarding its demands from the CTP and its impact on the system. For example, it is likely a PS relying on hot gas or plasma to generate thrust will have much higher heat loads than a purely electromagnetic thruster, while the latter could have more issues with EMC.

In order to assess the impact of a certain ePS on the spacecraft when in use it is important to understand the physical principles behind the engine. This knowledge combined with a model simulation should help optimizing the number and positioning of different sensors as well as adapting to the specific test object.

The important parameters for the assessment of the impact of a certain ePS on a CubeSat mission are:

- **Mass:** the mass of the entire ePS considering the standard propellant mass when declared by the manufacturer. Where possible mass can vary depending on propellant needs.
- **Power:** The average power required when firing, this is an important parameter since power itself must be provided by the CTP for the tests and must be generated on board during the actual mission. This parameter is also responsible, along with

thermal efficiency for the thermal loads on the spacecraft. It will be defined in Watts.

- **Propellant:** the propellant used by the thruster. Different propellants might have different storing needs, as well as show different advantages and drawbacks.
- **Size:** the actual volume occupied in a CubeSat by the Propulsion System, based on data available for prototypes being developed or on the market if any. This is only indicative since development in technology or manufacturing or mission driver on total delta-V could significantly change the actual value. It will be defined in millimetres.
- **Specific Impulse (Isp):** again, a term interesting from a mission point of view, it's the most important parameter from the ePS point of view since it represents the efficiency with whom propellant is exchanged for thrust. It is defined in seconds.
- **Thermal efficiency:** the amount of power in percentage that is lost by the thruster to heat. The mission will need to dispose of the excess heat through radiation to the environment.
- **Thrust:** only interesting from a mission's point of view, it is the actual force generated by the thruster at a certain power at net of all losses. It will be defined in submultiples of the Newton.
- **Total impulse:** it is the force generated in the whole firing time of the thruster. It is important for mission design and depends on thruster performances and the amount of stored propellant. Measured in Newton per second.
- **TRL:** maximum TRL reached by the technology, not necessarily by every single considered ePS in the category. It gives an idea on how developed a certain technology is.
- **Voltage:** the voltage at which the electric current should be provided to the ePS for it to work. Measured in Volt.

In order to assess the capabilities of different ePS on a mission level, delta-V for two different configurations has been calculated with the Edelbaum approximation for low thrust circular orbit transfer:

- **6U:** A six units CubeSat with a total mass of 12 kg, that is the standard imposed limit for this category
- **12U:** A twelve units CubeSat with a total mass of 24 kg, that is the standard imposed limit for this category

The results of this research are only indicative, and all the values might change while the technology is ongoing constant and rapid maturation and since there is no need for the actual mission to exactly match the maximum mass.

## 2.1.1 Helicon Plasma Thruster

Helicons are reliable, highly efficient plasma sources that are now being explored as standalone thrusters. Its first application in spacecraft propulsion is as a plasma source for VASIMR propulsion system, that has however thus to be demonstrated in space due to the huge amount of power required.

Helicons however are being developed to create a new kind of small, compact propulsion system, composed by very few elements thus increasing reliability. The lack of electrodes and neutralizer means this system is not subject to erosion issues and is able to properly work with a wide variety of propellants. HPT can use any noble gas as well as Iodine, that can be stored in solid state thus reducing propellant tanks requirements. Some studies are also being conducted on the idea of air propelled HPT for very low orbit/ very high atmospheric orbit maintenance. Those would use an air intake for refuelling and then the HPT would create plasma out of the air and use it to propel the spacecraft. It would be possible since there are no exposed parts in the flux that would deteriorate when contacting the propellant.



1. Discharge chamber
2. RF antenna
3. Magnetic system
4. Gas injector
5. Outlet diaphragm
6. Plume screen
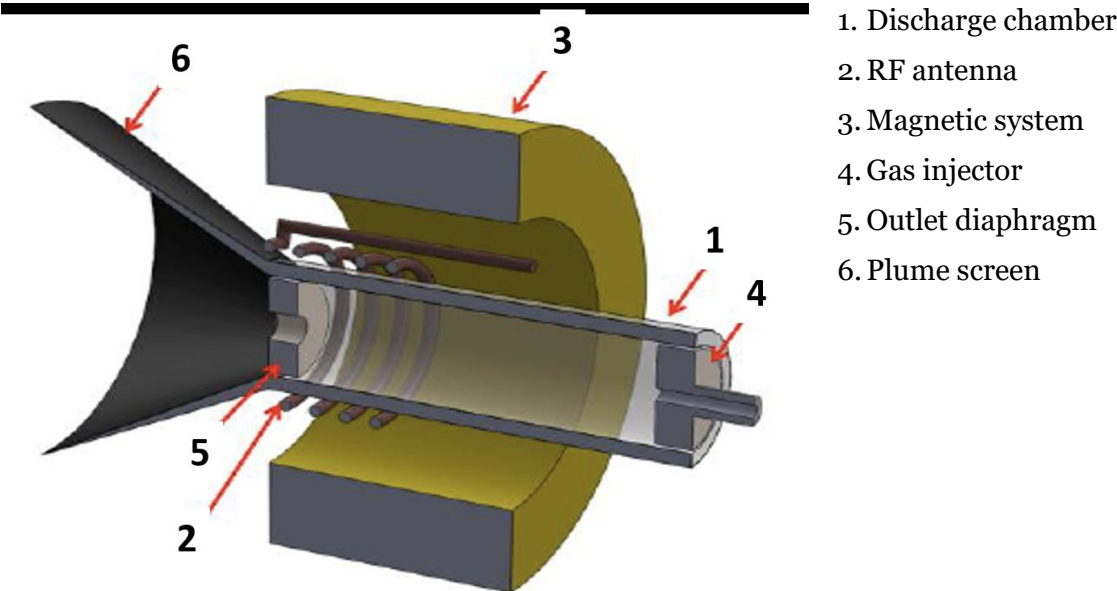
*Figure 2 Helicon Plasma Thruster diagram*

The thruster architecture is based on a dielectric tube surrounded by an antenna and a magnetic arrangement. The antenna is fed by Radio Frequency Power. The source is fed by

propellant gas provided by a distribution line. The antenna ionizes plasmas inside the source, heating up also electrons. Electrons, being lighter and at higher temperature, come out faster than ions from the source generating an ambipolar field which in turn accelerates the ions. The motor ejects a neutral plasma thus no neutralizer is needed. The magnetic field is necessary for three main reasons: (I) plasma confinement within the source, (II) optimization of antenna plasma coupling, (III) plasma acceleration through a magnetic nozzle.



*Figure 3 REGULUS HPT from T4i*

The cooperation between Politecnico di Torino and T4i for the European commission Horizon 2020 contest EPIC gave us access to early data on T4i's HPT REGULUS, so this has been used as a reference model not only for HPTs in this document but also for the design of ESA-Prop CTP platform itself. In Table 1 are reported REGULUS specifications at our last update, further improvements are likely as the technology is under development. This is the only known HPT in Europe at this stage of design, while a similar concept although not exactly an HPT can be found in the USA. The propulsion company PHASEFOUR has developed an RF plasma thruster called MAXWELL. The technology is similar since it uses radiofrequencies to ionize the plasma, but it does not use helicon waves. The proposed MAXWELL thruster shows a much higher thrust than REGULUS at the cost of an Isp that is quite low, scoring in the field of traditional chemical propulsion. MAXWELL is quite scalable in size and performances, with a power requirement ranging from 160W up to 450W. A CubeSat platform won't be able to

sustain more than 160W of power generation, that is actually quite the high end of the future trend. At this power level a thrust of about 3.6mN is achieved, at a specific impulse of 374s. The Maxwell will probably score higher for small, not CubeSat spacecraft in the order of a hundred kilograms of mass.

*Table 1 HPT specifications*

### REGULUS Qualification Model Specifications (12/2018)

| | |
|---|---|
| *Thrust* | 0.5 mN@30W (0.2-0.7 mN) |
| *Isp* | 600 s@30W (220-900 s) |
| *Total impulse* | 3000-11000 (up to unlimited) Ns |
| *Required power* | 50 W (20-80 W) |
| *Volume* | 150x100x100@3000Ns |
| | 200x100x100@11000Ns |
| *Propellant* | Iodine, Xenon |
| *Voltage* | 12-24 V DC |
| *Weight* | 2.4 kg @ 3000Ns |
| *TRL* | 6 |
| *Reference mission delta-V* | 0.25-0.91 km/s for 6U |
| | 0.125-0.45 km/s for 12U |

## 2.1.2 Electron Cyclotron Resonance Thruster

This ePS is based on an ECR plasma source, ionizing power is supplied via Electron-Cyclotron Resonance absorption of microwaves by the propellant. Plasma is confined radially by a DC magnetic field generated by coils and the B-field is maintained at the required strength for ECR to occur in the central area of the chamber. The plasma is contained axially by two magnetic Dynamic Gas Mirrors. The downstream magnetic mirror acts as a magnetic nozzle for charged particles powerful enough to cross the mirror, thus providing thrust.
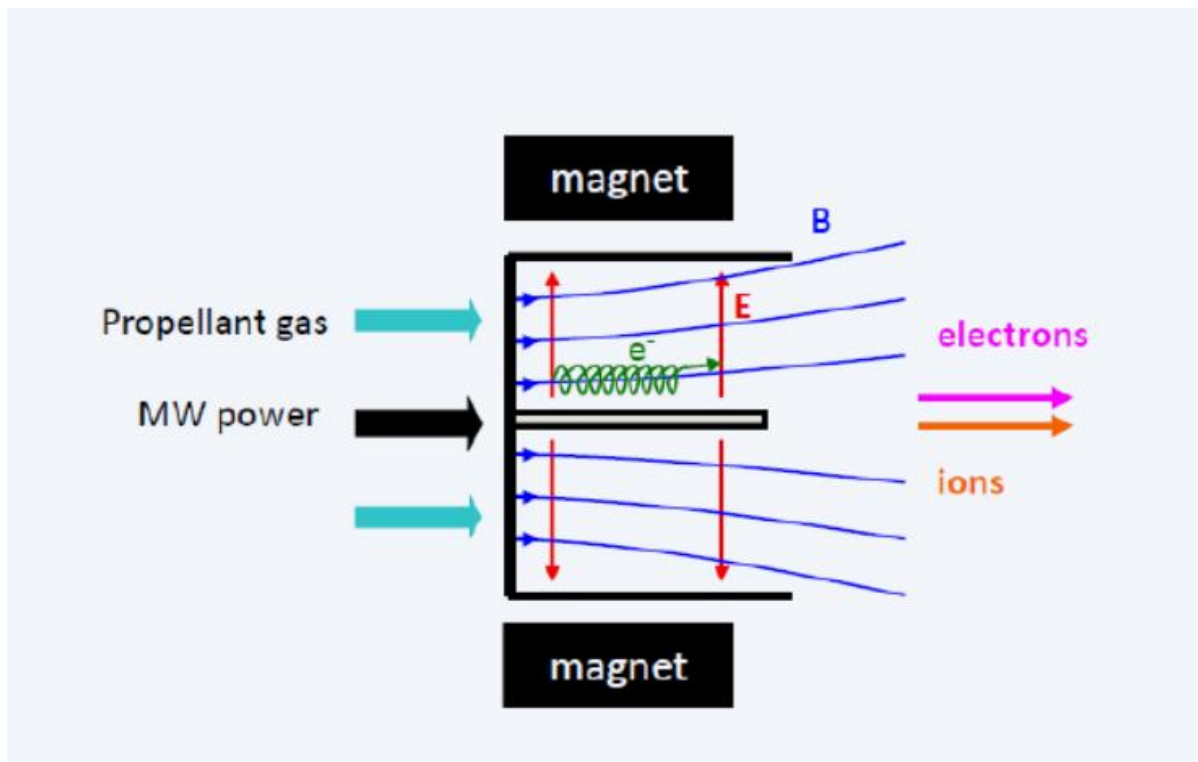
*Figure 4 ECR thruster schematic. credits: www.minotor-project.eu*

Developed ECRs for small spacecraft applications are at the moment beyond CubeSat capabilities in terms of power requirements. With a power requirement of about 150W only bigger spacecraft can afford ECR propulsion. Anyway, as the trend for CubeSats seems to be developing high power generation and relatively high-power propulsion ECR could become a viable technology for the CubeSats of tomorrow.

It is also to consider the possibility that as the technology continues to improve ECR thrusters at a lower power consumption may appear on the market. As an example, a European consortium also competing in the EPIC call has the goal to develop its now TRL3 MINOTOR ECR up to market release in different sizes, one being 30W and thus well into CubeSat achievable levels. There are few actual data about ECR performance since they are at early stages of development, but an overview of the known parameters [3] is given in Table 2.

*Table 2 LECR-50*

### 150W class LECR-50 ePS

| | |
|---|---|
| *Thrust* | 2.3 mN |
| *Isp* | 4010 |
| *Required power* | 150 W |
| *Diameter* | 50 mm |

# 2.1.3 Pulsed Plasma Thruster

The PPT is an impulsive thruster that relies on electric pulses in order to create the plasma and accelerates it thanks to Lorentz forces. Every burst of plasma provides a finite force and the total thrust level can by accurately controlled via the frequency of the pulses.
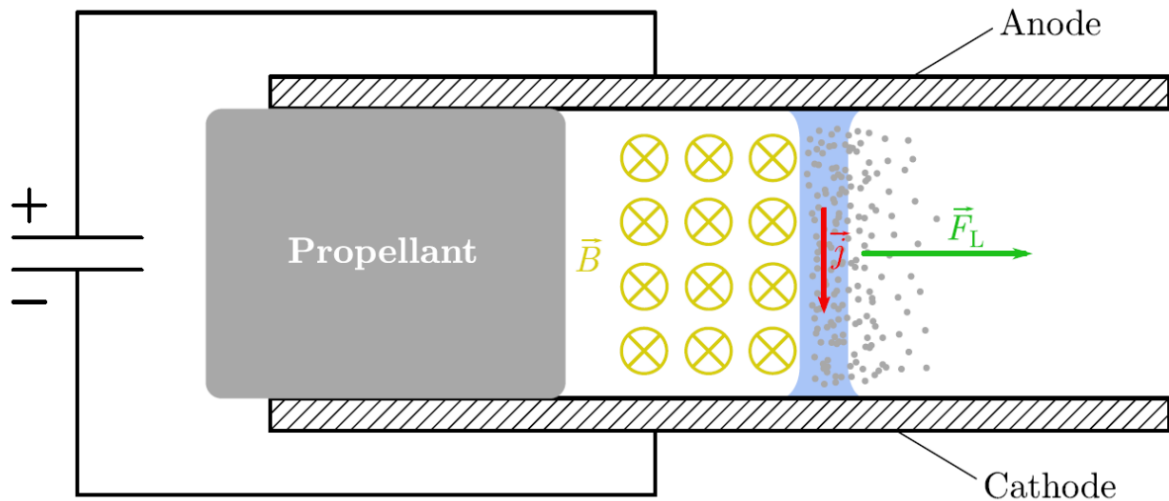


*Figure 5 PPT schematics. credits: IRS- Universität Stuttgart*

PPTs have a very compact and simple design, usually using solid state propellant like Teflon bars (PTF) that are pushed in position by a spring to close the circuit. The electric pulse discharge sublimates, ionizes and accelerates surface propellant, providing the thrust. This solution removes the need for propellant tanks and feed system, thus removing mass and volume and increasing the reliability of the system. The downside is the complexity of the PPU that must include a Pulse Generation Network composed by capacitors. The ability of the PPU to recharge the capacitors will be the main limitation on pulse frequency and thus on maximal thrust achievable [4], [5].

Another limitation of this system is the total impulse achievable, since it is not possible to increase propellant mass at will without mounting more PPTs. This is the reason why typical total impulses and thus delta-V capabilities of PPTs are quite low. Research on liquid or gas propellant PPTs are being conducted, but this removes the advantage of not having a propellant feed system.

PPTs are some of the most developed small electric thrusters since due to their characteristics they were viable precision RCS on bigger spacecraft, and now the know how to transform them in main propulsion systems for CubeSats is quite advanced. Typical values for PPTs are reported in Table 3.

12

*Table 3 PPTs specifications. data from manufacturer datasheets*

## PPTs specifications

| Manufacturer | Mars Space (UK) | Busek (USA) |
|---|---|---|
| Pulse bit | 90 µNs | 20 µNs |
| Isp | 650 s | 536 s |
| Total impulse | 190 Ns | 220 Ns |
| Required power | 6.7 W | 7.5 W |
| Volume | 100x100x35 mm | 100x100x70 mm |
| Propellant | PTF | PTF |
| Weight | 0.35 kg | 0.5 kg |
| TRL | 8 | 9 |
| Reference mission delta-V | 0.015 km/s for 6U<br>0.0079 km/s for 12U | 0.018 km/s for 6U<br>0.0091 km/s for 12U |

# 2.1.4 Electrospray thruster

Electrospray thrusters works by feeding propellant to an emitter where a strong electrostatic field is applied between the emitter and an opposing electrode. There are two kinds of electrospray thrusters depending on the propellant type: colloid thrusters and Field Emission Electric Propulsion (FEEP) thrusters. Both ePS exploit the nature of specific propellants to spontaneously emit charged particles when strong electric fields are applied [4], [5].

Electrospray thrusters don't rely on plasma discharge in order to provide thrust, thus eliminating the efficiency losses of vacuum plasma discharge chambers, usually quite high for miniaturized systems. The emitters are usually in the micrometre order of size and thus they are perfect for CubeSat miniaturization. Single emitters provide thrust in the order of the micronewton or even less, so array configurations of emitters are used for the actual propulsion system.

Colloid thrusters rely on molten salt mixtures that contains ions, fed to the emitter both with a pressure fed or directly thanks to liquid capillarity, the strong electrostatic field separates charged droplets of ions and accelerates them to provide thrust. The emitters in colloid thrusters can be disposed in order to accelerate from different emitters both positive and negative particles or change in time the emission sign of the particle, thus achieving a neutral beam and avoiding the need for external neutralization.
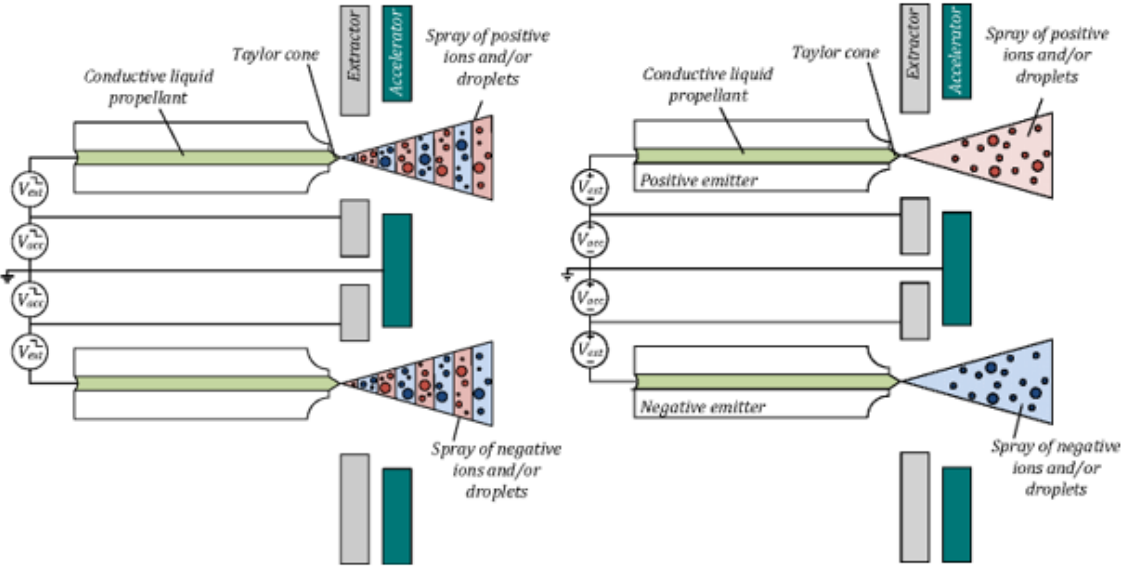


*Figure 6 Electrospray schematics for alternating and constant emission*

FEEPS function similarly to colloid thrusters, but use liquid metal as a propellant, Indium and Caesium are the most common ones and adapt to different kinds of emitters. The propellant in this case is always fed thanks to capillary forces, thus creating a very compact system. Indium is preferable than Caesium due to the latter handling difficulties, it being very reactive with even small traces of water or oxygen. When not handled properly it can form oxides that can clutter the emitters slides and ducts. Indium requires heaters since it's melting point is at 154°C but can be handled with no difficulty. Another advantage is Indium is not corrosive, while Caesium is highly corrosive and can compromise the thruster and electrodes.
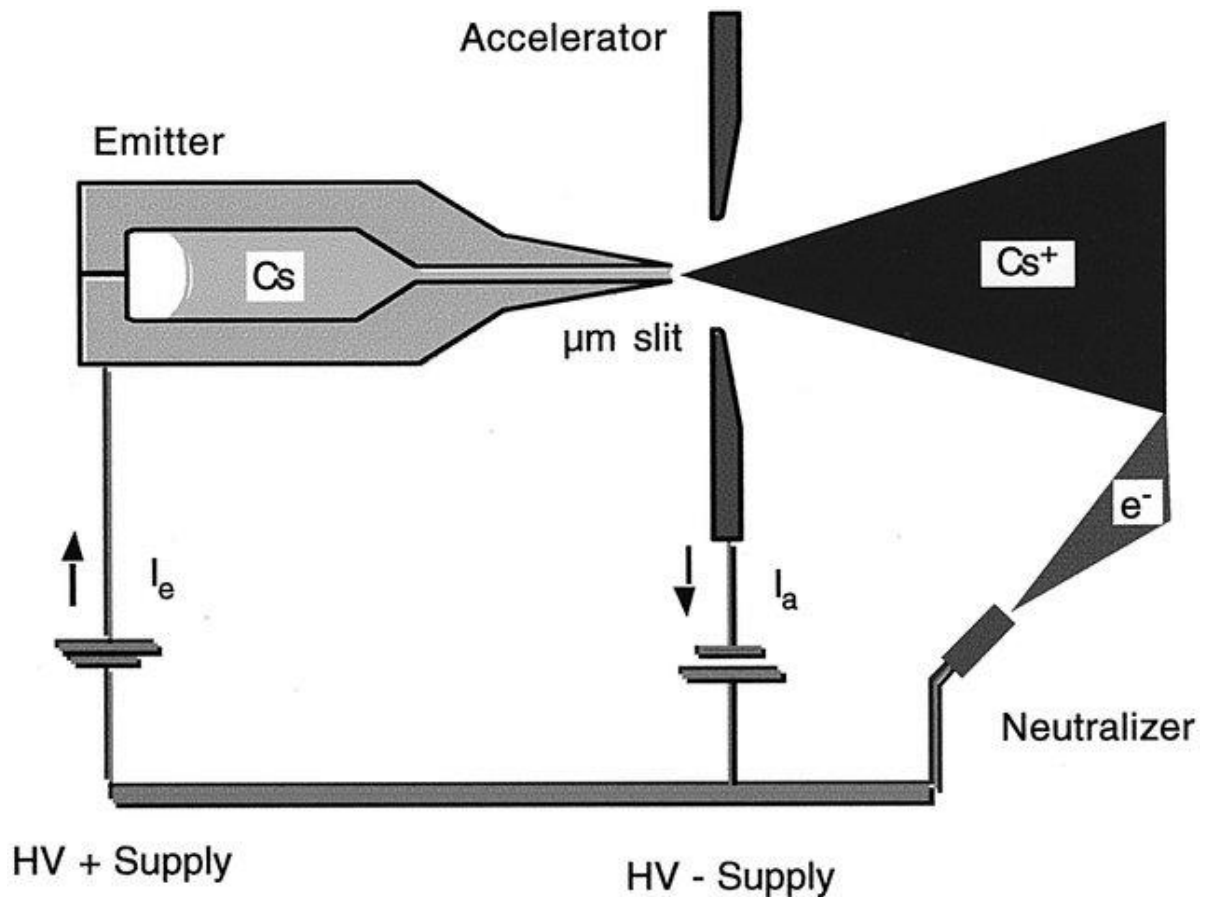
Electrospray thrusters have been developed mostly as precision attitude control RCS for bigger space systems, and colloid thrusters have been used on board LISA Pathfinder. There are many electrospray thrusters being developed for CubeSats around the world, thanks to their compact form factor and easy scalability due to the emitters array configuration. One of the most advanced FEEP solution to date is that of Austrian company ENPUSION.

*Table 4 Electrospray thruster*

### ENPULSION IFN Nano Thruster specifications

| | |
|---|---|
| *Thrust* | 0.01-0.4 mN (nominal 0.35 mN) |
| *Isp* | 2000-6000 s |
| *Total impulse* | 5000 Ns |
| *Required power* | 8-40 W (40W @ 0.35 mN) |
| *Volume* | 100x100x82.5 mm |
| *Propellant* | Indium |

| | |
|---|---|
| *Voltage* | 12-28 V DC |
| *Weight* | ~1 kg |
| *TRL* | 9 |
| *Reference mission delta-V* | 0.417 km/s for 6U |
| | 0.208 km/s for 12U |

## 2.1.5 Ion Thruster

Ion Engines are a wide family of thrusters relying on an electrostatic field to extract and accelerate ions from a plasma magnetically confined in a chamber. There are two main families depending on the ionization process, DC Ion thrusters use a direct current of electrons to ionize the propellant, while RF ion thrusters rely on radiofrequencies to transfer power to the gas. DC solutions requires less power per ion generated but requires also more delicate components such as an internal cathode for electron production. A couple of gridded electrodes extracts and accelerates the ions, then an external cathode neutralizes the beam. This poses some issues with electrodes erosion and the cathode itself is quite delicate as well as critical for the thruster.

Ion engines have been developed for and used on traditional spacecraft and thus in this case it is a matter of miniaturization. The challenges derive from the plasma chamber losses, that grow higher with the miniaturization of the chamber itself, and the thrust provided that is dependent on the exit area since there are limits on the current density of ions.
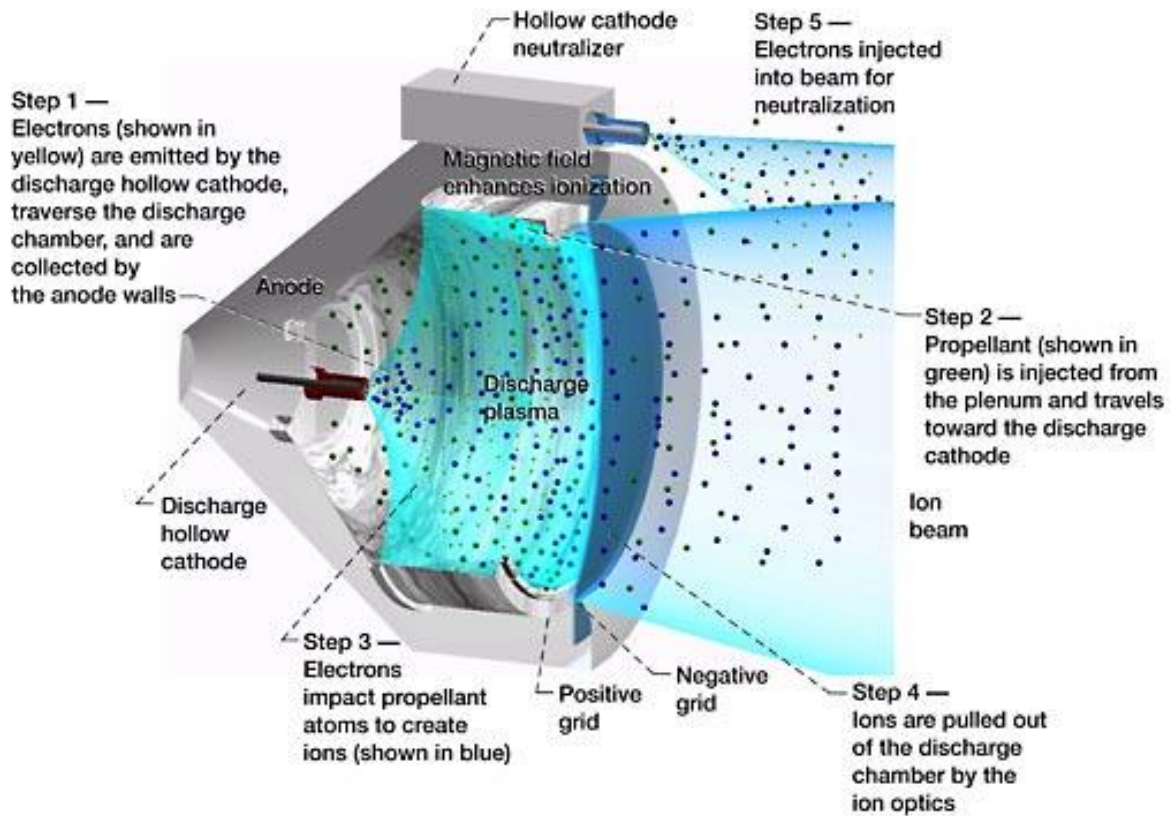
*Figure 8 Gridded Ion engine working schematic for DC plasma ionization. credits: NASA*

CubeSat designed ion thrusters rely mostly on RF ionization and some manufacturers such as THRUSTME are also developing RF technology not only as a plasma source but also as an acceleration method. This solution [6] uses an RF to apply the voltages on the grids instead of the common DC used by ion engines. Thanks to RF usage the grids will go through a cycle of voltages thus alternating between ion emission and electron emission, not requiring an external neutralizer for the ion beam.

Great interest has been shown by ESA in Miniaturized Radiofrequency Ion Thrusters (MRIT) for future standalone CubeSat exploration missions thanks to their high Isp that could enable a 6U or more likely a 12U CubeSat to autonomously transfer from LEO to at least NEO. For this to happen higher power level should be reached and ePS in the order of 150W are expected to be used.

The main issues of DC Ion engines integration in CubeSats is due to the complexity to miniaturize the PPU, that must provide not only a certain amount of power but must provide it with very high voltages in order to effectively accelerate ions. Even the RF solution requires a quite complex PPU and RF generation system, thus most of the miniaturization challenges are not thruster technology but power management technologies [4], [5], [7].

17

Table 5 Ion Engines specifications

## Ion Engines

| Manufacturer | JPL (USA) | Astrium (EU) | Thrustme (FR) |
|---|---|---|---|
| Name | MiXI | µNRIT-2.5 | Neptune |
| Type | DC gridded Ion Engine | RF gridded Ion Engine | RF ion engine with RF acceleration |
| Thrust | 0.01-1.5 mN | 0.05-0.6 mN | 0.3-0.9 mN |
| Isp | 2500-3200 s | 2861 s | >1000 s |
| Required power | 13-50 W | 13-34 W | 30-60 W |
| Propellant | Xenon | Xenon | Xenon, Iodine |
| Weight | 200 g | 210 g | 1 kg |

| Manufacturer | Busek (USA) | Airbus (EU) | Airbus (FR) |
|---|---|---|---|
| Name | BIT-3 | RIT-µX | RIT 10 EVO |
| Type | RF gridded Ion Engine | RF gridded Ion Engine | RF gridded ion engine |
| Thrust | 1.15 mN | 0.05-0.5 mN | 5, 15, 25 mN |
| Isp | 2500s | 300-3000 s | >1900, >3000,>3200 s |
| Required power | 75 W | <50 W | 145 W |
| Propellant | Iodine | Xenon | Xenon |
| remark | Due to fly with lunar IceCube | | 3 designs available |

## 2.1.6 Hall Thruster

In a Hall thruster the electrons emitted by an external hollow cathode are accelerated by an anode positioned at the end of an annular channel. On their way to the anode electrons cross

a radial magnetic field and Lorentz forces cause them to gyrate around the magnetic field lines and drift azimuthally through the annular channel, ionizing the propellant by collision along their trajectory. Ions are accelerated out of the thruster from the same electric field that accelerates the electrons, but due to their much higher inertia they are significantly less influenced by the magnetic field and thus can leave the chamber generating thrust. other electrons from the same external cathode will then neutralize the beam.
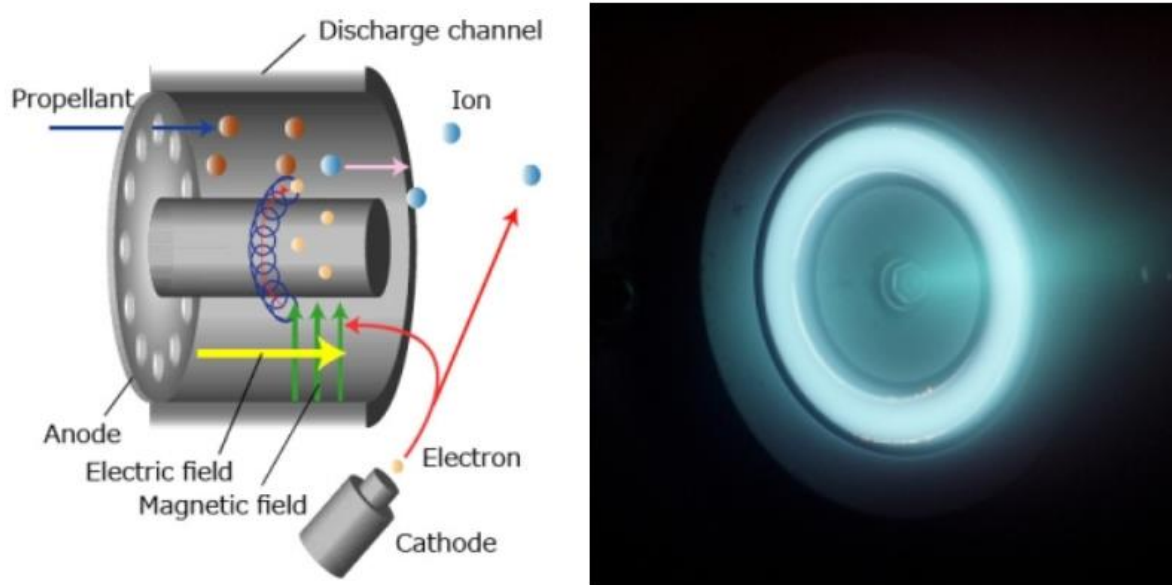


*Figure 9 Hall thruster schematics and operating view. Credits: Komurasaki-Koizumi Laboratory*

For traditional spacecraft Hall thrusters' specific impulses vary around 1500-2000 seconds, thus making it a better choice than ion thrusters for near Earth missions, while they are not optimal for Earth orbit operations or long interplanetary missions. Obviously for micro technologies slight differences might arise and the optimum could shift, thus making interesting Hall thrusters even for Earth orbit operations.

Hall thrusters are quite challenging to miniaturize due to their plasma generation principle, reducing the overall size of the thruster entails a reduction of Larmor radius, thus requiring stronger magnetic fields to curve electrons in their trajectories. At the same time smaller dimensions imply less distance between confined plasma and thruster walls, that will also cause more particles to escape the containment and hit the walls, causing higher heating to the magnets, with the risk of demagnetization and thus further reduced containment.

Those problems presented major challenges in Hall thrusters' miniaturization and caused first attempts to have low efficiencies. To overcome most of the issues presented by miniaturizing conventional Hall thrusters a new geometry specifically designed for small propulsion systems has been designed. Those cylindrical Hall thrusters use a cylindrical rather than annular flow channel with a mostly axial rather than radial magnetic field. Axial magnetic

field concentration in the anode region mirrors back electrons approaching the anode, creating an area of high-density electrons not thanks to Lorentz forces but thanks to an equilibrium between electrostatic attractive forces and magnetic mirroring [4], [5], [7].
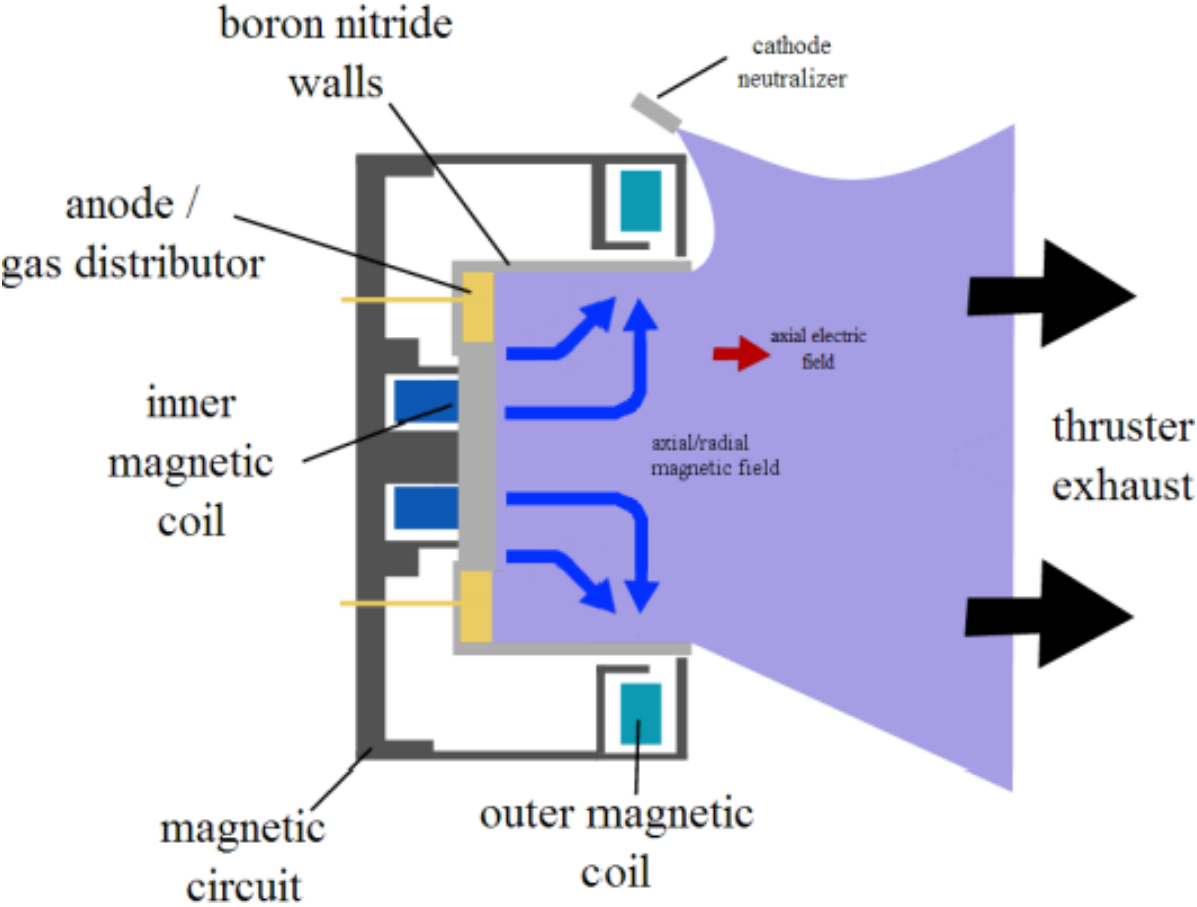


*Figure 10 Cylindric Hall thruster schematics. credits: Semantic Scholars*

Hall thrusters, like ion engines, require a complex PPU that is challenging to miniaturize, even if slightly easier since the voltage required is smaller and fewer power supplies are needed in a Hall engine.

*Table 6 Hall effect engines specifications*

### Hall effect Engines

| Manufacturer | Busek (USA) | Sitael (IT) | UTIAS-SFL (Canada) |
|---|---|---|---|
| Name | BHT-200 | HT 100 | CHT |
| Thrust | 12.8 mN | 10 mN | 1-10 mN |
| Isp | 1390 s | 1100 s | 1139 s |

| Required power | 200 W | 100 W | <200 W |
|---|---|---|---|
| Propellant | Xenon, Iodine, Krypton | Xenon, Krypton | Xenon, Argon |

## 2.1.7 Electrothermal thrusters

Electrothermal propulsion is mainly represented by resistojet, whose basic principle is like traditional chemical propulsion, with the difference that energy is not self-contained in the propellant chemical bindings but is provided by an external electrically powered heat source. As deducible by the name, resistojet provide heat thanks to a resistance that dissipates electric power into heat, that is then passed to the propellant due to forced convection. This implies that actual temperatures are limited by the maximum operative temperatures of the materials composing the resistance and suffer from low efficiency due to thermal losses.
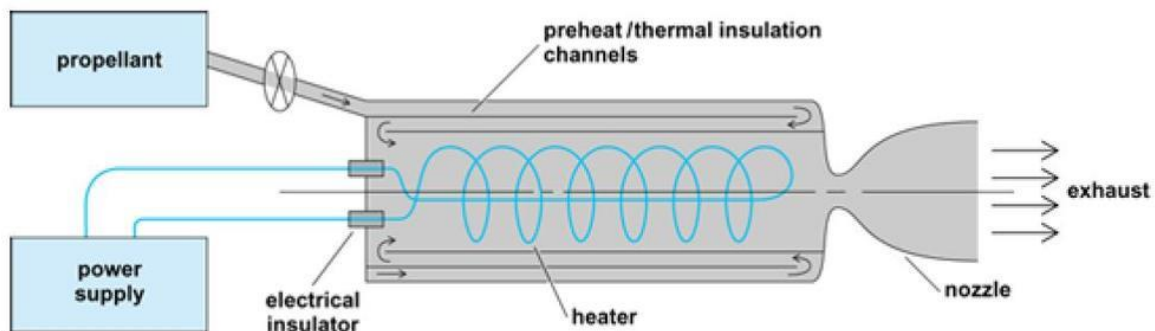


*Figure 11 Resistojet thruster schematics. credits: ESA*

A particular development of the resistojet is the arcjet, that overcomes the resistance temperature limit by removing the resistance and replacing it with a direct electrical discharge in the propellant that dissipates heat in it. This solution enables the propellant to reach higher temperatures and thus higher exhaust velocities and efficiency. There are no current uses of arcjets for CubeSat propulsion at the moment though.

While all electrothermal engines provide thrust by heating gaseous propellant and expelling it to space, its storage on board can vary quite consistently. Different devices store propellant in different ways. We can find propellant that is stored as a gas, but also in liquid or solid phase. In those cases a phase-change accompanies the heating of the gas, and is usually performed by e pre-heater in contact with a part of the propellant that is kept at the right conditions of pressure and temperature for the process (vaporisation, sublimation) to occur [2].

When resistojet are scaled down to CubeSat size we have limitation on the power as well as managing high thermal loads, thus making for resistojet having performances below same size chemical thrusters. The big advantage of resistojet systems over chemical propulsion is they don't need explosive propellants or combustion to occur on the satellite, that is not accepted by most CubeSat guidelines. They use cold gas system like propellant or even inert liquids such as water, but they performance is usually only slightly better than cold gas systems, that does not require the extra power. For this reason, they have not been used on CubeSat despite the technology being well developed [5], [7].

*Table 7 Resistojet specifications*

### *Resistojet Engines*

| *Manufacturer* | VACCO (USA) | GomSpace (EU) | SSTL (UK) |
|---|---|---|---|
| *Name* | CHIPS | MEMS | LPR |
| *Thrust* | 20 mN | 1-10 mN | 18mN |
| *Isp* | 82 s | 60-92 s | 48 |
| *Required power* | 30 W | 2 W/nozzle | 30 W |
| *Size* | 1U+ | 0.44U | - |
| *Propellant* | R134a | Butane | Xenon |

## 2.2 MISSION CAPABILITIES

As stated in the introduction CubeSat standard was created in 1999 from Cal Poly and Stanford universities as a mean to develop students' skill in the design, integration and testing of space systems. For some years that was the CubeSat primary goal and the idea spread to many universities all around the world. As space technology evolved, CubeSat platforms grew more and more complex, and some universities started to use the platform as a cheap technology demonstrator for both software and hardware in miniaturized form.

Following a strong development in technology and the resulting miniaturization of various on-board systems and payloads both space agencies and private societies have demonstrated a large interest in CubeSat application to a wide variety of missions. Exploiting a bigger form

factor than the common educational 1U CubeSat, there are nowadays many examples of multi-U CubeSat platform performing both services providing and science missions. Those missions come in many forms, both as support missions to space exploration, such as the use of MarCO as both a technology demonstrator and a support to Insight mission, launched in May 2018, and as standalone platforms, often in a constellation, such as Planet constellation for distributed Earth observation on a daily basis.

The range of mission opportunities for CubeSat could be extended by the introduction of propulsion systems. The use of chemical propulsion creates many concerns due to the risk posed by CubeSat, usually launched as a piggyback cargo, to the main mission. A safer solution can be cold gas propulsion, that however has really low Isp and thus only enables missions requiring a few m/s of delta-V. The future trend seems to be the use of electric propulsion, that makes it possible to use inert propellant such as in cold gas propulsion but reaching an Isp that is even higher than chemical propulsion.

For electric propulsion CubeSats larger form factors are going to be used both in order to host all the subsystems related and leaving the space for actual payload and for energy generation needs, that will probably require deployable solar panels. The most promising form factor for those missions seems to be 6U CubeSats for relatively small delta-V and 12U for the most demanding missions such as standalone missions to the Moon or NEOs. Those cases define the reference mission for which certain ePS, where total impulse of commercial engine was declared. In the following section possible application of ePS and their expected performances will be briefly discussed.

## 2.2.1 In-plane manoeuvres: altitude change

This is one of the basic manoeuvres a spacecraft could perform, by applying a burn in the orbital plane along its velocity vector a spacecraft can vary its velocity and thus its altitude. If the acceleration is provided concordant with the velocity (prograde burn) altitude will increase, if it is provided opposing the velocity (retrograde burn) altitude will decrease. For impulsive thrusters two manoeuvres are needed to perform an altitude change, while ePS rely on finite burns that slightly change the velocity along the entire orbit, thus achieving an ascending or descending spiral. The following formula states the relation between a circular orbit radius and the velocity of the spacecraft.

$$v = \sqrt{\frac{GM}{r}}$$

*Where GM is the standard gravitational parameter depending on the central body considered, v is the orbiting body velocity and r is the radius of the orbit.*

Calculating exact changes for finite burn transfer is challenging and goes beyond the needs of a general statement on mission capabilities, thus Edelbaum assumptions has been used for approximation. The Edelbaum approximation is valid for the transfer between two circular orbits, solving the two-body problem with the assumption that in every moment of the manoeuvre the orbit remains circular. If the assumptions are respected such is the case of circular orbit altitude change in Earth orbit, Edelbaum calculations are quite accurate with an error varying between 1% and 3%. For elliptical orbits or when the two-body problem is not enough error can reach 10% or 20% of the value returned by the calculation.

To assess mission capabilities of the reference CubeSats in different situation assuming they use standard commercial versions of ePS as stated from the manufacturers the altitude change achievable has been calculated in the most plausible scenarios. Those are LEO orbit change; Lunar orbit altitude change and Mars orbit change. Since the actual gain is dependant both on the delta-V and the starting radius, the following values have been used for all the engines:

- **Earth:** the spacecraft starts on a 6571 km radius circular orbit
- **Moon:** the spacecraft starts on a 2000 km radius circular orbit
- **Mars:** the spacecraft starts on a 4000 km radius circular orbit

*Table 8 Altitude changes for 6U CubeSat*

| ePS | Delta-V [km/s] | Earth delta-R [km] | Moon delta-R [km] | Mars delta-R [km] |
|---|---|---|---|---|
| *REGULUS* | 0.91 | 1866 | 9638 | 3719 |
| *MAXWELL* | 0.305 | 544 | 1086 | 865 |
| *Mars space PPT* | 0.015 | 24 | 41 | 39 |
| *Busek PPT Bmp220* | 0.018 | 29 | 48 | 45 |
| *ENPULSION* | 0.417 | 760 | 1713 | 1252 |
| *THRUSTME* | 0.417 | 760 | 1713 | 1252 |

Table 9 Altitude changes for 12U CubeSats

| ePS | Delta-V [km/s] | Earth delta-R [km] | Moon delta-R [km] | Mars delta-R [km] |
|---|---|---|---|---|
| REGULUS | 0.45 | 844 | 1998 | 1409 |
| MAXWELL | 0.153 | 263 | 455 | 401 |
| Mars space PPT | 0.0018 | 0.58 | 5 | 4 |
| Busek PPT Bmp220 | 0.0092 | 13 | 24 | 23 |
| ENPULSION | 0.208 | 363 | 661 | 562 |
| THRUSTME | 0.208 | 363 | 661 | 562 |

The values in the table are dependent on total impulse capacity of the ePS, and thus for engines with a separate tank and feed system they can be tailored for a specific mission. It is easy to see that PPTs, which are also only extensible to a certain degree due to their design, are not suitable for significant manoeuvres.

## 2.2.2 Off-plane manoeuvres: inclination change

This is one of the costliest manoeuvres to perform, especially at low altitudes since the delta-V required is proportional to the velocity. The inclination change can be performed by burning perpendicularly to the plane. If impulsive thrust is used it should be performed at the ascending and descending nodes in order not to vary the other parameters of the orbit, in case of electrical propulsion the burn is distributed again on the whole trajectory, but it is to be noted that thrust direction is to be changed every half period.

The best performing ePS considered would achieve at best a couple degrees of inclination change in LEO, and thus a limitation remains on CubeSat inclination changes. The manoeuvre could be achievable for high orbit CubeSats orbiting lower mass central bodies such as the Moon and Mars.

## 2.2.3 Interplanetary transfer

As for plane changes a very high delta-V is required in order to reach escape velocity from Earth and provide enough energy to reach another planet, so standalone interplanetary CubeSats are

not an option, at least at the moment. Solutions could be implemented where one or more CubeSats are deployed on an intercept trajectory to another planet like MarCO, and a propulsion system could enable small trajectory corrections as well as a planetary capture on arrival.

Standalone missions traveling autonomously from LEO could be possible with high Isp solutions such as Ion engines with larger propellant tank going to the Moon or NEOs. Mission concepts are being studied by agencies especially for NEOs, since there is great interest in their study and the low budget solution represented by CubeSats could be a key factor in obtaining the funding. This is the example of ESA M-ARGO (Miniaturized Asteroid Remote Geophysical Observer) that as stated in [8] would use a mini-RIT gridded ion engine to reach NEOs. This solution will require a mini-RIT able to provide about 3750 km/s of delta-V to a 12U CubeSat, with an Isp higher than 3000 seconds. Another example is NASA NEO-Scout spacecraft, that as from [9] would use an Iodine mini Hall thruster to transfer again a 12U CubeSat to selected NEOs.

The use of high Isp high total impulse engines for this kind of missions requires the use of technologies like ion engines or Hall thrusters. Possible new disruptive technologies are at the moment unable to match the requirements. The identification and promotion of the most promising ones could however accelerate the advancement and open new possibilities for this kind of missions.

## 2.2.4 Orbit maintenance

In an ideal scenario when a spacecraft is launched into space and reach orbit, it will perpetually maintain its trajectory except for manoeuvres. In reality many factors vary the orbit during time, they are called perturbations. They come from atmospheric drag caused by the higher layers of the atmosphere, that although is conventionally considered to end at an altitude of 100 km in reality is not neglectable until thousands of kilometres, from solar pressure, gravitational perturbations and other factors. The sum of the perturbations, and for LEO mostly the atmospheric drag, causes the satellites to change their orbit with time, and even re-enter in the atmosphere in a few years for the lowest ones.

The lowering of the orbit is more important the lower the orbit is, and thus a low satellite will fall sooner than a similar satellite in a higher orbit. In order to prevent this from happening some satellites use their propulsion systems to exchange delta-V for time in operative orbit. This is not done at the moment for CubeSats, that are usually left to drift freely and fall after a few years. The implementation of a cheap, reliable ePS could enable station keeping so that the

satellite can remain operative for longer time. For example, a total impulse capability of 3000 Ns could enable a mission prolongment of about 5 years for a 6U CubeSat.

This is where simple, low cost, medium Isp ePS could carve out their place in the market. They could extend significantly mission duration without having an excessive impact on the budget, spacecraft design and form factor.

## 2.2.5 Formation Flight: Differential drag compensation

CubeSat missions often rely on constellations to acquire data in a distributed way, for certain tasks or to maximize the constellation's efficiency each satellite should be at a certain, well defined, relative position from the others. Another case of formation flight is wen a satellite, that will be called the follower, must remain in a certain relative position relative to another spacecraft, that is called the leader, for example as an inspection tool or part of a two-spacecraft system.

Since perturbations are different depending on the position above the main body, the cross-section of the satellite and even random effects such as climate on the planet, each satellite in the constellation will drift from its starting orbit. While this is useful for the deployment of a constellation, since the satellites can be released in a single launch and will naturally spread out, it makes a constellation to require a lot more satellites in order to assure coverage on a certain area.

The solution can be to constantly correct the position of the satellites as to maintain the relative positions and velocities, but this could require quite a large amount of delta-V. Another approach has been analysed and proposed for missions such as Planet Lab [10] and QB50 [11] constellations, this solution is called differential drag. It exploits the drag forces to vary the velocity, by changing the attitude of a CubeSat in order to change its ballistic coefficient. This makes it possible to keep relative distances, but using this solution accelerates the falling process due to atmospheric drag intentionally higher than the minimal.

Differential drag compensation is a hybrid solution, combining the passive solution of differential drag with the ability of a propelled spacecraft to compensate for it in order to maintain both the orbit and the relative position with the other satellites. According to [11] an esteem of the delta-V necessary for this kind of control on a low orbit of 300 km is about 6.2 m/s every 30 days.

Again, medium Isp low cost ePS could provide years of optimal operations to a constellation of CubeSats requiring well defined relative positions, and thus could shine in this application.

## 2.2.6 Inspection and Proximity Operations

As it was said in the previous paragraph inspection can be considered a particular case of formation flight. It has anyway some important characteristics that can differ from generic formation flight. The first thing that comes with inspection missions is the necessity that the follower is spatially confined in a small volume close to the leader, while constellations often does not require satellites to be near one to the other. The follower should move in space, by exploiting small differences in the orbits, to fly around the leader and provide the desired coverage of the latter.

The ensemble of the operations occurring in the area close to the other spacecraft is called Proximity Operations and is composed of manoeuvres to change the relative velocity and thus position between the leader that is commonly fixed and the follower that is the one performing the manoeuvres. Other possible proximity operations to be considered are collision avoidance manoeuvres to be performed if an error causes the follower to enter a collision course to the leader and eventually docking and undocking manoeuvres, that require a great degree of precision and are some of the most complicated manoeuvres that can be performed in space.

From a mission point of view the main constraint about inspections comes from the degree of coverage required, that is the percentage of the leader spacecraft to be inspected, and the time to achieve said coverage. It is possible, by slight variation of the orbital parameters, to perform a complete 'orbit' around the leader in an orbital period. Depending on the spacecraft architecture and the instruments used more than one period can be necessary, covering different surfaces. The small changes in orbital parameters is also the most efficient solution from a propellant point of view. Another solution that could potentially save time is to actively move around the spacecraft, thanks to a continuous thrust to make continuous changes to the orbit of the follower. This solution is going to consume a significantly higher amount of fuel and should only be used if really necessary, also because the continued fire of the engine is more likely to contaminate not only the CubeSat, but even the inspected object.

The wide variety of proximity operations and mission design makes it possible to have very different delta-V requirements for proximity operations. From the usual trade-off between specific impulse and thrust level the latter results more important, especially if the small orbital fluctuations approach is used for inspection. A higher thrust lowers the time needed before achieving the desired course relative to the leader spacecraft, thus allowing better reaction time. Another important thing to note can be the necessity of providing collision avoidance manoeuvres effective enough even with short notice. This is an operation where there could be

competition even with cold gas systems, where the added value of ePS could be the higher mission duration allowed.

## 2.2.7 Attitude control and desaturation

Using propulsion for attitude determination or desaturation on CubeSats is something that was and still is unlikely on most applications, since the cost and complexity of the system gives no significative advantages with respect to the combination of reaction wheels and magnetic torquer, that are also almost unlimited not consuming any propellant to be used.

This was true for most of the launched CubeSats and for most of the upcoming ones, at least for those meant to operate in Earth orbit. For interplanetary CubeSats meant for the Moon, Mars or NEOs another solution should be found. Reaction wheels are an excellent way to have a fine control on the attitude but suffer from saturation, and without the Earth magnetic field the only known way for a spacecraft to generate momentum in space is the use of a propulsion system. A study in the mission should assess if it is more efficient to use reaction wheels for control or to completely replace them with a Reaction Control System (RCS).

The optimal candidates for this purpose are characterized by small, controllable forces, with a high specific impulse for mission time maximisation provided by a compact, lightweight propulsion system featuring a distribution of small thrusters in a configuration enabling the development of torque around the spacecraft's three body axes. For this reason, optimal solutions could be PPTs and electrospray thrusters. The requirements could be fulfilled even by cold gas and electrothermal thrusters, but the low specific impulse can negatively impact the mission duration, and the pressure fed line impulses cannot be finely tuned as the former solutions.

## 2.2.8 Conclusions

As seen, there are multiple technologies to cover the different mission applications, and often the same mission requirements can be successfully fulfilled by different technologies. There are different technologies that share almost all their possible applications with similar performances. In Figure 12 is reported a matrix summarizing the study on the possible application of different technologies to CubeSat missions. The Technology-Mission couple is summarized by a symbol, where a green button defines a technology that is nowadays ready (even if eventually not yet tested for space) and that can accomplish the mission; a yellow

button defines a technology that is either not yet developed at an operative level but that will likely be in a few years or a technology that provided some expected improvements could in a few years be ready even for that mission; a red button defines a technology that is not suitable for the selected mission and will probably never been; a yellow rhombus defines technology that would be suitable for the mission but usually comes with relatively low total impulses, due to built-in storages and thus will be suitable for the mission only if there is the possibility to overcome the limit and increase the propellant storage capability.

After the mission is defined and a few suitable technologies are selected the decision between different engines will follow a trade-off criterion between different parameters such as cost, reliability, flight heritage, technology maturity, availability, even politics related to manufacturers nationality for ESA programs. It is likely that some developing technologies will be selected as most promising, as happening with the EPIC programme of H2020 for disruptive propulsion, and thus will be sponsored and developed faster and better than others. For this reason, it is suggested to keep the technology study updated and to account for advancements and program drawbacks.



Figure 12 Summary matrix of ePS technologies for different operative scenarios

# DEFINITION OF THE CUBESAT-ePS INTERACTION

## 3.1 TEST OBJECTIVES

In order to define the mutual interaction between CubeSat and ePS technologies and to evaluate the impact on system and subsystem level it is necessary to define test procedures and to identify the measurements of interest. This has been done in the feasibility phase of ESA-Prop program and later discussed with ESA experts in order to design a proper test platform.

With the feasibility phase a prototype has been developed, whose detailed description will be provided in chapter 4, and at the end of the phase a meeting was held with the customer, the European Space Agency. During the meeting various aspects of the ESA-Prop programme were discussed, mostly on the medium- and long-term goals. It is expected to reach the ability to fully simulate a CubeSat mission with electric propulsion, enabling the collection of relevant data all along the mission. This will require the system to integrate a sun simulator, a suspended structure inside the vacuum chamber and various sensors to collect a large amount of data.

Since ESA-Prop is a step-by-step, multiphase programme the implementation will not be done for every subsystem and test capability at the same time but will follow a progression. During the meeting some priorities emerged and thus those will be the first to be addressed during phase two.

This chapter will provide an overview of SPF vacuum chamber and of the GSE available at EPL facilities. The main part of the chapter will be about the measurements to be done, as defined in the first study reported in TN01, and the description of the different aspects of the impact of an ePS on the CubeSat, integrating that study with subsequent research and the feedback of both external experts and ESA members.

## 3.2 ELECTRIC PROPULSION LABORATORY

The program was commissioned from the department of Space Propulsion and Thermodynamics of ESA/ESTEC. The CTP will be an upgrade to test facilities Tests will be conducted at ESA/ESTEC EPL facilities in Nordwjik, Netherland. This is a propulsion laboratory dedicated to the study and testing of electric propulsion and is part of the Space Propulsion and Thermodynamics department of ESA/ESTEC, that is the customer of ESA-Prop program.

The EPL, as described in [12] has seven vacuum facilities at disposal, each consisting of a vacuum tank and a dedicated pumping system and sensors system. Flanges of various sizes on the tanks are provided to accommodate a variety of different feedthroughs. The EPL also contains a flow bench and working table for small integration and manufacture tasks. If necessary, the laboratory can implement an ISO8 certified clean room on the area containing the vacuum chambers and workbench.

The selected vacuum chamber for the ESA-Prop program is the Small Plasma Facility. SPF consists of a 3.35 x Ø2 meter main chamber with a 1 x Ø1 meter hatch. CTP's functional tests were conducted in the hatch of the chamber. One of the flanges has been used for the feedthrough and the GSE was mounted on a desk near the vacuum chamber. SPF can achieve a minimal pressure of $10^{-7}$ mbar with a nominal pumping capacity of 128000 L/s $N_2$. It is equipped with a liquid nitrogen cooled shroud and the entire system is controlled by dedicated software. The intended uses of the facility are Aerothermodynamics experiments, EP contamination experiments and overall testing of electric propulsion devices.

The EPL has several test and measurement equipment at disposal, with some of this GSE dedicated to specific vacuum facilities and others more versatile. Thrust balances, reported in Figure 13, will be used to test thruster performances with CTP, that will have a mechanical interface for balance integration.

Some of the vacuum facilities have plasma diagnostic systems mounted on arms for plasma beam measurements. Those are GIGANTIC, CORONA and SPF. The latter is also equipped with a back-flow diagnostic system. Mounted on a metallic arm inside SPF are 12 Faraday cups and one 1.25kV RPA (Retarding Potential Analyser). Those sensors are disposed radially on a half-circumference (Figure 14) to define beam properties at different angles. Sensors capture charged particles and analysing the produced current it is possible to measure charged particle density, and thus characterize the plasma.

| Balance | Reference Document | Picture | Manufacturer | Range/ Resolution | Facility compatibility | Calibrated | Measurement procedure |
|---|---|---|---|---|---|---|---|
| AX504 | RD13 | Figure 13 | Mettler Toledo | 500 g / 0.1 mg | All | Yes | Certified |
| XP2004S | - | Figure 13 | Mettler Toledo | 2300 g / 1 mg | All | Yes | Certified |
| 1-Axis optical thrust stand | RD14 | Figure 14 | ALTA | 500 mN / 0.4 mN (thruster mass = 3 kg), 0.75 mN (thruster mass = 15 kg) [RD45] | Corona, SPF | Yes (in house using a load cell) | Certified |
| Low Thrust Balance (LTB) | RD15 | Figure 15 | ALTA | 40 mN / 0.2 mN | Corona, SPF | Yes (in house using a load cell) | Certified |
| Micro Newton Thrust Balance (μNTB) | RD31 | Figure 16 | NPL | 500 μN / 0.1 μN | GALILEO | Yes | Certified |

*Figure 13 Thrust balances at EPL as reported in the document "EPL General Description"*

The back-flow diagnosis set (also in Figure 14) can be useful to relate beam properties and detected contamination on CTP surfaces. It is composed by multiple sensors to cover a wide variety of functions. Two low voltage (100 Volts) RPA probes and two Faraday cups similar to the diagnostic arm are used to measure ions backfiring ions density. A Langmuir probe operating either in 2 or 3 electrodes mode enables the measurements of electron density and temperature and of the plasma potential. The detection set is completed by a spectrometric system for optical emission measurements and a QCM (Quartz Crystal Microbalance) sensor to measure the mass variation due to the deposition of particles on the receptor surface.
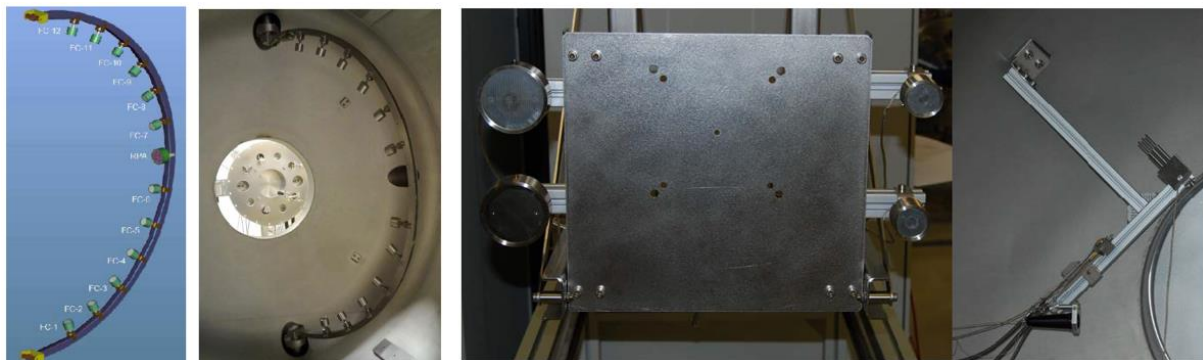


*Figure 14 SPF plasma diagnostic arm and backflow diagnostic system, as from "EPL General Description"*

The EPL also provides a wide variety of GSE for most applications. all necessary GSE for correct vacuum testing is provided and integrated with the facilities. Many generic sensors are also at disposal, such as spectrometers, microscopes, accelerometers, a thermal camera and others. standard GSE such as power supplies, multimeters, oscilloscopes and electric and electronic equipment and components are also available.

Tests conducted in the SPF will rely on both CTP sensors and EPL sensors and GSE compatible with SPF, as required by the tests. It will be possible to use CTP in other vacuum chambers previous manufacturing of a compatible integration structure.

*Figure 15 Small Plasma Facility vacuum chamber at ESA/ESTEC EPL*

## 3.3 DEFINITION OF ePS IMPACT ON CUBESATS

The introduction of ePS on CubeSat platforms impacts heavily on the whole system design and operations. It was shown how different ePS impacts at mission level in Chapter 2, and now the system level impact will be assessed. Designers will need to account for the ePS affecting both the configuration layout and the other subsystem's performances and the effects and mutual interactions occurring between ePS and other subsystems during operations.

For this reason, main impacts on design level and operation level have been identified and briefly assessed in this chapter. Measurements identified in the TN01 – Test Platform Design are also reported with the first iteration on measurements of interest and possible equipment. Some equipment has been discussed later during a meeting with ESA experts and other meetings with area experts and thus some of the considered solutions will not appear in the table of measurements and equipment from TN01. They will be further investigated and, if compliant with what is needed, they will be integrated in an issue for ESA-Prop phase two documentation.

# 3.3.1 Impact on design

This section will cover the main aspects affected by the ePS when estimating the preliminary budgets and configuration of the satellite. This is a 'fixed impact', not connected to the operation of the ePS, but only determined by its presence on board and little to no mitigation can be done by the designers other than changing the utilised ePS accordingly to their requirements.

*Encumbrance*

The whole CubeSat idea was born on the concept of very small spacecraft, and most of them to this day are actually in the class of 1U or 2U. Introducing an ePS will change this since the subsystem will usually require 1U or more only by itself. Moreover, propulsion's significant power needs will heavily impact required solar panel surface and storage batteries dimensioning. Thus, ePS are considered to be viable from the 6U form factor to bigger satellites.

But even with a 6U form factor the ePS can occupy a considerable percentage of the volume, usually 1 to 2 units. The volume occupied by it will not be available for avionics, power systems or payloads. An important factor to consider when designing a CubeSat featuring electric propulsion will be the volume required for a certain amount of total impulse.

*Mass Budget*

As for encumbrance, another important constraint for CubeSats is the mass, that should be limited as much as possible. Introducing an ePS will significantly increase the spacecraft mass both directly and indirectly. Adding any subsystem at the spacecraft will of course cause a mass increase, but in the case of the ePS the increase can be quite important. The propulsion system itself is usually quite heavy, due to both its volume and the extreme operative condition not allowing to use lightweight materials and techniques. Propulsion systems are also usually composed by several parts that are difficult to miniaturise.

For ePS especially the mass is not only increased by the thruster itself, but an important figure is due to the PPU. Even simple PPU have usually considerable weight due to transformers miniaturisation issues, the smallest the transformer the higher the loss, that is something we want to avoid on the spacecraft. If the ePS need some kind of RF generator or pulse generator the weight will increase even more.

Another important figure is the propellant, its tank and the feed system. Most of the propulsion systems rely on liquid or gas propellant contained in pressurized tanks, fed to the thruster by a feed line regulated by one or more valves. Even simpler, solid state propellant architectures will have the propellant mass and some kind of tank or feed system. The propellant mass is directly proportional to the amount of delta-V required by the mission, but an increase in propellant mass (and thus volume) will also increase the propellant tank mass.

Introducing an ePS is not only affecting the system with the additional mass of the ePS itself but will also impact on other systems for their mutual interaction, causing them to increase their weight. The ePS usually need a large amount of power, higher that the power traditionally needed and provided by classical CubeSat platforms. This will require the propelled platform to have a larger surface of solar panels, thus increasing the weight of the Electric Power System. The batteries could also be affected if a direct drive approach is not considered, requiring bigger batteries for energy storage.

The last mass increase possible is the one required if the necessity of thermal insulation or electromagnetic screening arises. In this case also this mass is to account on the decision of using a particular ePS.


*Power supply*

The common problem of ePS, even for traditional space systems, is the huge amount of electric power consumed and the high voltages required to accelerate the propellant. Miniaturized ePS present the same problems, even if scaled down, since they require power levels and voltages higher than those commonly available on a CubeSat platform.

The challenge here is to produce and provide enough power for the ePS within the strict constraints of CubeSats. This makes problematic the use of batteries, that would greatly increase the mass and would only provide power for a very limited time due to the high-power absorption from the ePS. The solution here is in firing the ePS only when in daylight, feeding power directly from the solar panels, either using an accumulator or direct drive technology. The latter is mostly seen as the possible solution for solar electric propulsion. Solar energy is harnessed by high voltage solar arrays and then directly fed to the ePS, with minimal regulation needs.

Whatever the solution, it is obvious that extensive solar panel surfaces will be needed. CubeSats with electric propulsion will need EPS enabling the generation, storage and management of powers ranging from the tens of Watts to the target power of 100-150W. At the moment the average power required by most ePS is around 50W. This is more than any other CubeSat before, and thus EPS will need to be reconfigured to meet the new requirements.

*Cost*

The use of ePS for CubeSats will not be neglectable at cost level either. Even if miniaturized electric propulsion is all about developing innovative ideas to make ePS cheaper and more available, the propulsion system will remain one of the major figures of cost, along with the payload.

Different ePS will likely come with different prices, so an important part of the design will be identifying not only the best ePS for the mission, but also the most cost efficient one. For constellations or observation satellites it could even be less cost effective to implement propulsion on board, increasing the spacecraft size and cost for both assembly and launch, or to allow the mission to decay earlier and then relaunching new, potentially updated satellites a few years later. Cost effectiveness will be thus an important parameter when considering ePS or even chemical propulsion on a CubeSat.

The decision about the actual propulsion system will need a trade-off between needs and costs. It comes to no advantage to integrate the most efficient ePS on the market on a CubeSat whose mission simply does not require it, while it will be more cost effective to select a less efficient system that is able to satisfy the requirements but costs less than the other solutions.

## 3.3.2 Impact during operations

This section will cover the main aspects of the impact of ePS operations on a CubeSat. It is important that during the design phases these aspects are accounted for in order to guarantee the correct operations of the satellite. If an ePS has a negative impact that exceeds the constraints of the satellite for one of these aspects it is possible for the designers to mitigate its impact, thus making sure the spacecraft can be operational.

*Thermal loads*

Strong thermal loads can be really difficult to manage on a satellite due to the limited heat dissipation in space and the harsh thermal environment. Luckily there are a lot of solutions enabling thermal engineers to cope with thermal issues by designing a proper thermal system. Traditionally on CubeSat TCS only use passive solutions, reducing complexity but also limiting the extent of the system's effectiveness. For this reason, it is important to define the thermal loads on board in the different mission phases, in order to adapt the mission and TCS accordingly. Thermal issues are considered one of the major concerns about ePS from both

polytechnic and ESA experts, and thus this is one of the main aspects considered by ESA-Prop phase two and this thesis.

The most intuitive source of thermal loads in the spacecraft is the thruster itself, especially for electrothermal or plasma propulsion. The heated-up or ionized propellant will heat the discharge chamber's walls and the nozzle due to irradiated heat and, for electrothermal thrusters, also convection. Ion and plasma engines will also suffer of a not perfect containment of the ionized propellant, and thus single particles heat up are also possible when a particle escapes the magnetic confinement. Whatever is the source of heat, part of the power will be lost from the propellant flux to the walls, defining what is called as the thermal efficiency of the thruster. The power loss due to imperfect thermal efficiency will heat-up the thruster, and from it the entire spacecraft, and thus it will need dissipation to deep space.

For thrusters exploiting radiofrequencies as plasma sources or ion accelerators another important dissipation point is the RF plasma generator. According to the Third Law of Thermodynamics no processes is ideal, so we will have again an efficiency that is less than unity, and part of the energy will be dissipated as heat. This will also happen for most of the electric power transformation processes and transfers, for batteries and accumulators charge and discharge cycles and even for power generation inside the solar cells. Since dissipated energy increases with the increase in power managed by the system, ePS elevated power demand will cause most of the electric system to dissipate a larger amount of energy than in traditional CubeSats. Critical items will be the step-up circuit components, devoted to voltage increase or regulation. Those suffer from difficulties in miniaturization resulting in a loss of efficiency.

For certain propulsion technologies neutralization is also needed, and it usually is achieved through a hollow cathode. This device emits electrons due to thermionic effect, where a cathode under a strong current and at high temperature will spontaneously emit electrons. Obviously, an incandescent cathode on board can be a considerable added thermal load.


*Electro-Magnetic compatibility*

Electro-Magnetic compatibility is one of the most concerning aspect to be considered when designing complex electronic systems. The small volume all the different avionics subsystems, electric components and the ePS are going to share makes it even more challenging too assure no compatibility issues arise. EMC/EMI issues are divided into two categories: Radiated and Conducted. The study of EMC/EMI should assure none of those issues exceeds safety constraints, and if it is not the case, actions should be taken to mitigate the problem.

- **Radiated:** every wire crossed by accelerated electric charges acts as an antenna. This means avionics and cables can be seen as a bunch of antennas always emitting and receiving a noise signal. If the signals emitted are too high in amplitude or have the proper frequency can cause failures or be interpreted as actual data when they are not, for this reason many data cables are shielded to reduce signal interferences over long distances.

- **Conducted:** these issues are due to the nature of the interaction between power supply unit and electric load. Power supply usually provide a fixed voltage with a constraint on maximum power, the load absorbs the power it requires, thus defining the current. If a load was purely resistive the current absorbed would be constant, but a real load is not a perfect resistance, and thus the current intensity varies in time. Those oscillations can pose a problem for the power supply and can cause issues for their amplitude and their frequency.

The ePS impacts on both aspects heavily. It is a load requiring a high amount of power, provided by a power supply that will need to cope with conducted EMC/EMI issues. The current will also be provided to the ePS through a wire, that will act as an antenna. All the dedicated electronics and the ePS itself are actually small antennas. But this is not the only thing to be kept into account. Many ePS rely on plasma as a source of charged particles or directly as a propellant. Currents in a plasma can act as antennas as well as currents in metallic elements, as demonstrated by the increasing interest in plasma antennas for space applications. this makes the thruster a big antenna, producing noise and potentially affected by the actual antenna from the Comsys. To conclude, some ePS rely on RF as a plasma source or acceleration method, and this can cause compatibility issues too.

EMC/EMI studies are important to make sure precautions are taken in design phase to mitigate the effects of interferences, and to insert an adequate amount of stiffness to compatibility issues. As part of ESA-Prop phase two proper actions for EMC/EMI environment characterisations will be conducted.


*Spacecraft charging*

Electric charges loading up in the spacecraft and not being able to be discharged can be a problem for certain ePS systems. Except for thermoelectric thrusters and plasma thrusters, that rely on the expulsion of plasma, that is neutral in overall charge, most ePS use ions or charged particles to accelerate. This creates an unbalance of charges and a subsequent overall charge build up on the spacecraft. To avoid this, it is necessary to perform beam neutralization,

by emitting in the charged beam opposite charges from a neutralizer (usually electrons from a hollow cathode) thus maintaining constant the overall charge of the spacecraft.

A malfunctioning in the neutralizing system can cause the spacecraft to build-up electrostatic charge. In space this can be a problem since the isolation of the spacecraft prevents the discharge to the outside. Thus, there is the risk of an electric arc forming between different parts of the spacecraft having different potential energies. This can have catastrophic effects on the spacecraft itself and even cause the mission failure. To avoid this redundant neutralization is usually implemented, but it is important to verify the system ability to keep the spacecraft neutral.

Charge build-up can also be due to charged particles hitting the spacecraft, and this is an issue even for spacecraft not using ePS, since there are charged particles in the upper layers of atmosphere and in space. Having a source of charged particles on board raises the risk even further for the spacecraft, with backfiring propellant particles or parts exposed to the beam potentially causing a rapid charge build-up.

*Contamination*

We have contamination when particles deposits on surfaces that are supposed to be clean. This can occur both for outgassing issues or, in the case of propulsion systems, for propellant release issues in the thruster configuration. Contamination can degrade optical properties of surfaces, corrode the materials or even lower the efficiency of the solar panels. A surface contamination on an optics can completely disable the capacity of the mission to collect relevant data, and if the contamination occurs from ions or charged particles it will also cause charge build up on the spacecraft.

Contamination should be limited as much as possible by design phases. There should not be susceptible surfaces exposed to thruster plumes, and eventual outgassing of the materials should be considered. If a configuration reveals to have too much contamination issues the problem should be addressed by a change in configuration.

For propulsion systems contamination usually comes from the propellant, that sometimes is also reactive and thus can further deteriorate the spacecraft. Contaminants can come from the exhaust plume, or the beam as usually referred to for plasma and ion engines, where low energy particles and not ionized propellant escaping the magnetic trap at low velocity can deposit on cold surfaces. Another source of contaminants is the eventuality of propellant leaks, where the gas escaping the propellant system can contaminate other systems.

# 3.4 MEASUREMENTS

The issues reported in the previous section will be evaluated by taking multiple samples in relevant environment and simulated operations. This will be done by several different sensors located on the CTP and provided by the EPL and located in the chamber. Measurements of interest and resolution, as well as some possible sensors have been defined in ESA-Prop phase one. Table 10 summarises the measurements identified as interesting during the feasibility and early design phase of ESA-Prop program, Table 11 summarises measurements actually collected by the prototype developed for ESA-Prop phase one.

In the two tables some aspects have been highlighted for each parameter:

- The instrument(s) required for the measurement
- Range and accuracy of the measurement
- The sampling time required for processing analysis
- The test object: PS, CTP or CTP+PS depending on the test object
- Test point: where the measurement is physically taken
- Evaluation method: PP – post Processing, RT – Real Time

Measurements parameters have been divided into four categories:

- Thrust performances
- Mass flow and variations
- Electrical and diagnostics
- Other parameters, that are specific to a certain ePS

Many parameters, as well as test ranges, instruments and accuracies are susceptible to changes during phase two and three to adapt to test requirements. From the very beginning of phase two instruments and measures are being discussed with experts in order to optimize the solutions.

*Table 10 List of measurable parameters from TN01 - Test Platform Design*

| Parameter | Instrument | Range | Accuracy | Sampling rate [s] | Test Object | Test Point | Note |
|---|---|---|---|---|---|---|---|
| | | | *Thrust* | | | | |
| *Thrust [mN]* | Torsional thrust balance (GSE), strain gauge (CTP) | 10 uN - 1mN | 1 uN | 1 | PS+ CTP | G SE + CTP | RT + PP |

| | | | | | | | |
|---|---|---|---|---|---|---|---|
| *Specific Impulse [s] and effective specific impulse [s]* | Indirect from thrust measurement | [0 – 5000] s | 1 s | - | PS | G SE | PP |
| *Impulse bit [µN/s]* | Indirect from thrust measurement | [0 5000] µN/s | 1 s | - | PS | G SE | PP |
| *Beam divergence [deg]* | - | [0 30] deg | 0,1 deg | - | PS | - | PP – RT (TBC) |
| | | ***Mass*** | | | | | |
| *Mass flow rate [mg/s]* | GSE: Mass flow sensors, High frame rate camera | [1 10] mg/s | 0,1 mg/s | 1 | PS | G SE | RT + PP |
| *Flux mapping (plume residual contamination)* | Kapton tape (CTP) + Microscope (GSE), Spectrometer (GSE) | TBD | TBD | 1 | PS | CPT | RT (TBC) + PP |
| *Propellant mass variation per area [g/cm²]* | GSE: Quartz Crystal Microbalance | [0 10] g/cm² | 0,1 g/cm² | TBD | PS | G SE | PP + RT (TBC) |
| *Propellant mass consumption [g]* | GSE: Balance | [0 1000] g | 10 g | 1 | PS | CTP | PP |
| | | ***Electrical and diagnostics*** | | | | | |
| *Current [mA]* | Amperometer (GSE), current sensing (CTP) | [0 5000] mA | 10 mA | 1 | PS+ CTP | CTP | RT + PP |
| *Voltage [V]* | Voltmeter (GSE), voltage sensing (CTP) | [0 50] V | 100 mV | 1 | PS+ CTP | CTP | RT + PP |
| *Temperatures [°C]* | Thermocouples | [-20; +100] °C | 0,1 °C | 1 | PS+ CTP | G SE + CTP | RT + PP |
| *Magnetic fields [T]* | Magnetic Field Mapper (GSE), Magnetometer (CTP) | [$10^{-5}$ - $10^{-2}$] T | $10^{-5}$ T | 1 | PS | G SE + CTP | RT + PP |
| *Pressure [bar]* | Pressure transducer (GSE); pressure transducer (CTP) | [0 10] bar | 0,1 bar | 1 | PS+ TP | G SE + SD card + GSS | RT + PP |
| | | ***Other parameters*** | | | | | |

| Parameter | Instrument | Range | Accuracy | Sampling rate [s] | Test Object | Test Point | Note |
|---|---|---|---|---|---|---|---|
| Radio-frequency emission [dB/Hz] | GSE: Spectrum analyser | 0 – 60 dB/Hz | 0,1 dB/Hz | 1 | PS+ TP | G SE | PP |
| Ion energy [eV] | GSE: ExB probe | 0 - 500 | 1 (TBC) | 1 | PS+ TP | G SE | RT + PP |
| Plasma (electron temperature, electron density, and electric potential) | GSE: cylindrical Langmuir probes | TBD | TBD | 1 | PS | G SE | RT + PP |
| Number of ions and electrons [#] | GSE: Faraday cup | TBD | TBD | 1 | PS | G SE | RT + PP |

*Table 11 List of measured parameters from TN01 - Test Platform Design*

| Parameter | Instrument | Range | Accuracy | Sampling rate [s] | Test Object | Test Point | Note |
|---|---|---|---|---|---|---|---|
| **Mass** | | | | | | | |
| Mass flow rate [mg/s] | GSE: Mass flow sensors, High frame rate camera | [1 10] mg/s | 0,1 mg/s | 1 | PS | G SE | RT + PP |
| Flux mapping (plume residual contamination) | Kapton tape (CTP) + Microscope (GSE), Spectrometer (GSE) | TBD | TBD | 1 | PS | CP T | RT (TBC) + PP |
| Propellant mass consumption [g] | GSE: Balance | [0 1000] g | 10 g | 1 | PS | CT P | PP |
| **Electrical and diagnostics** | | | | | | | |
| Current [mA] | Amperometer (GSE), current sensing (CTP) | [0 5000] mA | 10 mA | 1 | PS+ CTP | CT P | RT + PP |
| Voltage [V] | Voltmeter (GSE), voltage sensing (CTP) | [0 50] V | 100 mV | 1 | PS+ CTP | CT P | RT + PP |
| Temperatures [°C] | Thermocouples | [-20; +100] °C | 0,1 °C | 1 | PS+ CTP | G SE + CTP | RT + PP |
| Magnetic fields [T] | Magnetic Field Mapper (GSE), Magnetometer (CTP) | [$10^{-5}$ - $10^{-2}$] T | $10^{-5}$ T | 1 | PS | G SE + CTP | RT + PP |
| **Other parameters** | | | | | | | |

| Radio-frequency emission [dB/Hz] - TBC | GSE: Spectrum analyser | 0 - 60 | 0,1 dB | 1 | PS+ TP | G SE | PP |
|---|---|---|---|---|---|---|---|
| Ion energy [eV] - TBC | GSE: ExB probe | 0 - 500 | 1 (TBC) | 1 | PS+ TP | G SE | RT + PP |
| Plasma (electron temperature, electron density, and electric potential) - TBC | GSE: cylindrical Langmuir probes | TBD | TBD | 1 | PS | G SE | RT + PP |
| Number of ions and electrons [#] -TBC | GSE: Faraday cup | TBD | TBD | 1 | PS | G SE | RT + PP |

# 3.4.1 Thermal data collection

Thermal data are needed to create a temperature map of the CTP and thus verifying that no dangerous temperatures are reached on the electronics and batteries. The study of the temperature map will also be useful to understand heat fluxes in the platform, verifying a thermal model that can be used at design level to predict temperatures. This will enable mission designers in early phases to cope with thermal issues when the spacecraft design is still quite undefined. This can save both costs and time limiting the amount of changes to the design that could occur in latter phases of the program or even during the integration and test phase.

Thermal data will be collected by Negative Temperature Coefficient (NTC) thermistors. Those are a type of resistor whose resistance depends on temperature to a much higher extent than common resistances. As deductible from the name, NTC resistance decreases with temperature. Thermistors are usually made with ceramic or polymeric material and metal oxides and provide great accuracies for temperature logs.

Dedicated NTC thermistors are integrated in the battery packs, and a for CTP v1 up to 16 more sensors can be placed in strategic points on the CTP structure and avionics. For the phase two the number of supported thermistors will increase, and a study on positioning has been conducted with an analytical model and a thermal load emulator.

The analytical thermal model has been created with Thermal Desktop in order to create a forecast of the thermal map and define where are the key point to observe with the thermistors. NTC thermistors disposition other than those on the battery packs can be changed during ePS integration to adapt to different ePS having different characteristics, if needed.

## 3.4.2 Electromagnetic environment characterization

As previously stated, EMC/EMI is divided into two main phenomena. CTP will need to both sustain that environment without failures and to measure them. In order to sustain the environment electronic boards will integrate solutions increasing the system survivability to interferences and load variations.

Although it is important that the CTP can continue to operate when subjected to a harsh electro-magnetic environment, it is also of uttermost importance for the goals of the program to be able to detect and characterize it. To detect conducted interferences the current absorbed by the load will be monitored in order to detect oscillations in power absorbed and the frequency of the phenomenon. For radiated interferences small receiver antennas suited for the expected frequencies, that should be in the range of 300kHz to 30 MHz, will detect the signals in different points of the CTP, and then it will be amplified and processed to characterize the environment.

In the previous table other solutions have been reported for electromagnetic fields measurements, as from a first guess on the best way of detecting interferences, and magnetometers are still being considered as an useful sensor for environment characterization, but regarding interferences the best solution, according to electronics and electromagnetic compatibility experts, is to consider them as transmissions and thus using antennas as sensors.

## 3.4.3 Contamination

To assess contamination issues with ePS a passive method is proposed. The most sensitive parts of the spacecraft, the entire external surface eventually simulated fully deployed solar panels will be replaced by witness plates, able to capture contaminants particles.

Witness plates are surfaces of a specific material able to entrap contaminants which enter in contact with it for further testing. For this application silicon wafers have been suggested, since there should not be any silicon-based particle release from the spacecraft or ePS. Kapton surfaces were also considered but discarded since it is carbon based as some propellants and other components present in ePS, and thus actual contamination extent could be underestimated. After the test the witness wafer is analysed with either a spectrometer or an IR microscope for contaminants. This enables not only to assess if any contaminant particle has come into contact with the surface, but also to identify the molecule and thus define where the contaminant came from. This will enable the operators to understand if the particle was

low energy propellant, coming either from a leak or from the exhaust plume, or if it was due to outgassing/eventual sublimation of other components.

The test configuration of the witness plates will be defined for the specific case, depending on whether the test is to characterize the ePS, in which case a full coverage can be required; or it is to simulate a specific mission, in which case it could be preferable to choose a configuration matching the actual spacecraft configuration. The SPF has, as previously reported, one backfiring propellant detection device that could also help with contamination predictions.

## 3.4.4 Surface charging

Due to the risks it poses to a space mission success and even survivability, surface charging of a spacecraft can be a problematic issue. The measurement of the extent of surface charging due to thruster operation can be a useful knowledge for the design of CubeSat missions using electric propulsion. It is important anyway to consider that electric propulsion is not the only possible source of charging, that can also be caused by environmental factors and power system fails.

The measurement of this phenomenon can be assessed, as reported by ESA experts during the meeting, thanks to strips of open resistors placed on the satellite surface. Further investigation is required as to assess how this solution works and how to implement it in the platform. As part of the managing role on the project this solution is being discussed with the expert designing the avionics for ESA-Prop V2 in order to add acquisition lines for this kind of sensors, and to implement the solution on the final version of the platform.

## 3.4.5 Thrust levels and ePS performances

Although not the main goal of ESA-Prop programme, the measurement of ePS performances in relevant, operation-like environment can be of some interest for both ESA and the thruster manufacturers. Usually thruster performances are assessed on a thruster only and/or whole ePS test in vacuum chamber conducted by the manufacturers during the development of the thruster itself. From those tests all the performances analysed before about ePS are deducted and thus the system is fully characterized. What is not considered in those tests are the mutual interactions occurring between the ePS and the actual systems it will operate with.

Defining thrust performances under operation-like conditions can be the ultimate check of an ePS capabilities or help to realise eventual flaws in design. It is possible that due to platform limitation or interferences the actual start-up of the thruster is not as efficient as in the lab test with the isolated ePS, or that the plasma-generating radiofrequencies have reduced efficiency due to interferences from other electronics or the communication system. If any similar phenomena happen to the ePS during the test, designers can take mitigation actions and correct the flaws in the design.

For thrust performances definition, sensors on CTP like strain gauges or accelerometers have been discarded during the meeting at ESA/ESTEC due to the difficulty in measuring thrust effectively on board. The specialised thrust balances of the EPL are a better fitting solution for this kind of measurement and, being an external tool, can be used or not depending on the test requirements. During phase two of the program an interface is being developed enabling to mechanically interface the thrust balance and the CTP, allowing precise thrust measuring. It is nonetheless possible that strain gauges will be mounted on specific parts of the CTP to investigate the stress on the structure under firing condition.

From the measurement of thrust, knowing the shooting time and the consumed propellant all the thruster parameters can be deducted. From CTP housekeeping report it is possible to deduct ePS power consumption associated with those performances.

# CubeSat Test Platform: ESA-Prop

## 4.1 Project Overview

ESA-PROP is a project developed by Politecnico di Torino on behalf of the European Space Agency to design an provide the ESA-ESTEC Electric Propulsion Laboratory (EPL) with a 6U test platform for CubeSat propulsion, especially Electric propulsion. Its final goal is to test miniaturized propulsion systems to assess the effects of operations and their interaction with the platform.

Phase one of the project was the design and development of the platform, as well as its integration and functional test campaign. The phase ended with the acceptance of ESA-PROP CTP by the EPL in Noordwijk, after the integration in the Small Plasma Facility (SPF) vacuum chamber and the functional test conducted.

Phase two was discussed in a first meeting in ESA-ESRTEC during the acceptance of CTP at the end of phase one, and in subsequent reviews. It comprehends the study of required measurements and the implementation of a data acquisition system, the integration of some ePS in the structure and the test of the latter in vacuum conditions.

Phase three has also been introduced and will require the integration of measurements and technology from ESA-PROP CTP with an external CubeSat with its own ePS, in order to completely simulate its operative mission. This phase will require the integration of sun simulator and the use of external sensors.

During this work of thesis, the last part of Phase One was performed, with the integration and test of CTP and its acceptance at ESA-ESTEC EPL and the beginning of Phase Two, with the definition of the tests and the preliminary actions to further develop the CTP. Following are details on the work done and its results.

## 4.2 CUBESAT TEST PLATFORM ARCHITECTURE

The physical layout of CTP, shown in Figure 16, is composed of a 6U Aluminium structure containing two main sections. One is the PS Box, an up to 4U section of the CTP containing the ePS, composed by the thruster with its PPU, Propellant Feed System and Propellant Tank. The other is the service module, a 2U section containing 1U of avionics and support equipment for the test and 1U of PS batteries. The two sections are divided by a bulkhead.
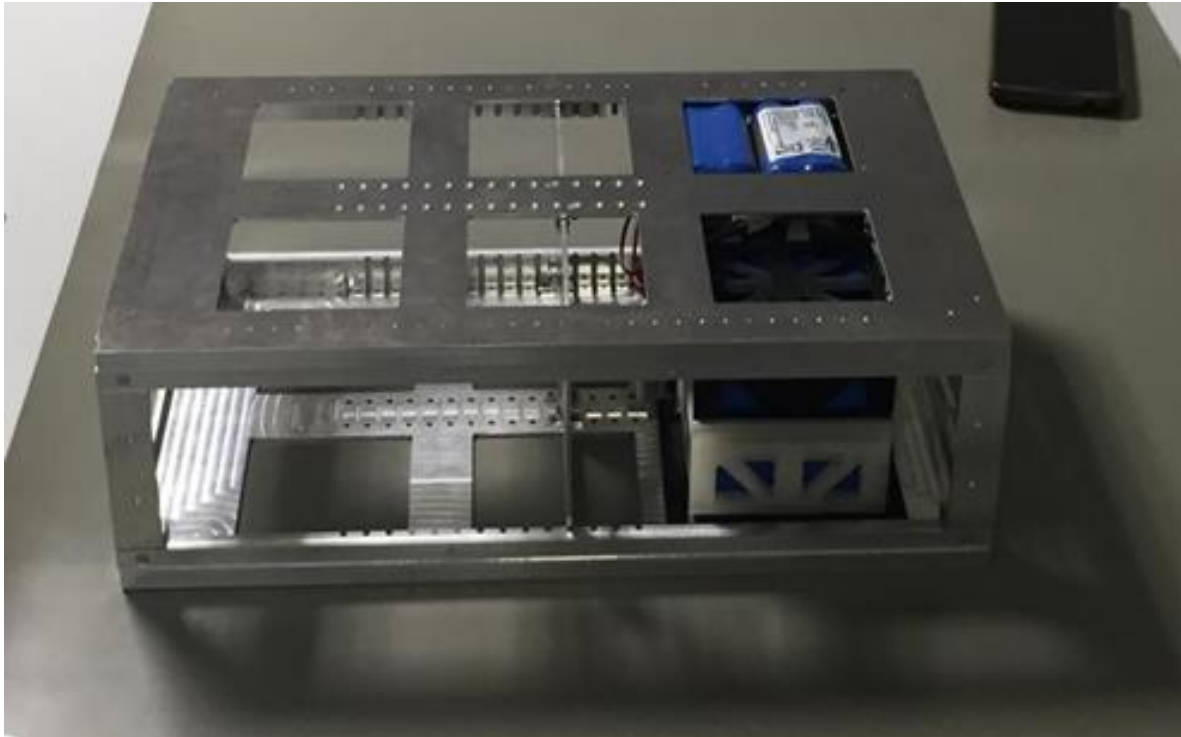


*Figure 16 CTP primary structure and interiors*

The ePS is to be fixed on the bulkhead and on the bottom of the structure. The bulkhead is moveable in order to accommodate as many propulsion systems as possible. The main structure and the internal components are covered by the secondary structure that is composed of Aluminium panels closing all the sides and leaving openings for interfaces and the ePS beam. In Figure 17 configuration is reported from design 3D CAD.
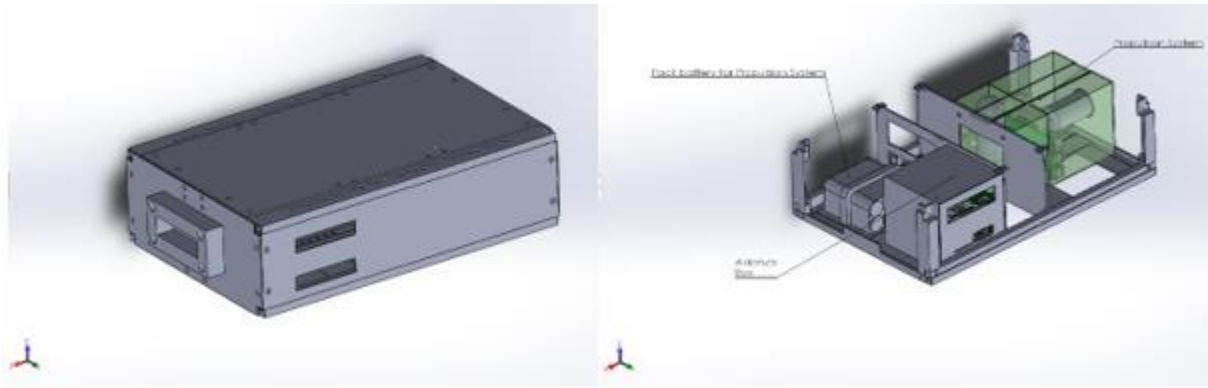
*Figure 17 External configuration with secondary structure and internal with ePS*

# 4.2.1 Service module

The service module contains all the avionics and power batteries enabling the correct functioning of CTP. Avionics are constituted of a Command and Data Handling System (C&DH), a communication System (COMSYS) and an Electric Power System. All the boards are connected by a 104-pin bus and mounted on a stack of four bars. Avionics are powered by two batteries for redundancy, mounted above the electronic boards. PS is powered by two dedicated batteries, mounted to the main structure with a 3D printed drawer made of PLA.

*Command and Data Handling*

C&DH core is a microprocessor based on ARM9 architecture located on the board itself. On C&DH board (shown in Figure 18) are also located the acquisition units, composed of multiplexers and Analog to Digital Conversion (ADC) devices. ADCs gather measurements from external sensors like NTC thermistors and strain gauges, located both in the service module and in the PS box. The board also mounts a three-axis magnetometer and three accelerometers, serial ports for interfaces and an SD-card hosting.

*Figure 18 Command and Data Handling board with ARM9 microprocessor*

The selected Real Time Operating System (RTOS) is Linux Embedded 6.32, able to accomplish software tasks without loss of synchronization thanks to a soft real-time (+/- 10µs). A customized kernel allows interfaces via different protocols such as CAN bus, UART, I2C, SPI, USB.

Application software is written in C/C++ language and cross-compiled for ARM9 architecture microcontroller, it is then uploaded on the board via USB, SD or Ethernet port. The software contains all the instructions for the CTP to perform the tests, as well as a watchdog in case anything goes wrong. The SD-card contains initialization data that can also be provided via interfaces and PS configuration. It acts also as a saving device for sensor measurements and all packets sent to the Ground Station are also written on it.

*Communication System*

CTP communicates with the GSS through a wired link and an RF link. The former is a serial connection made with RS232 protocol. The latter is composed by a qualified board equipped with a radio module operating at 437 MHz frequency, a Terminal Node Controller (TNC) able to manage KISS AX.25 protocol frames and a clock counter. The used antenna is a dipole.

*Figure 19 Comsys board*

*Electrical Power System*

EPS is composed of two main elements:

- The main board with the avionics battery pack
- The auxiliary board with the PS battery pack

Both the boards and avionics battery pack are contained in the avionics box, while the PS battery pack is contained in a dedicated section of the service module.

The EPS daughter board manages avionics power, and contains the avionics batteries recharging circuits, the regulation units and a protection circuit. Battery Charge Regulators receive up to 16W and provides energy to the two avionics battery packs, composed of four cylindrical AA-size Li-Ion cells with a capacity of 2 Ah @ 7.4 V. The Regulation Unit takes input voltage from the batteries and provides the power bus with 3.3V and 5V. Protection circuits use diodes to separate the batteries from both the recharge line and the regulation line, in case a failure occurs. A Load Switch (LS) controls the activation and deactivation of CTP and two remove before test (RBT) switches allow to isolate each battery pack from its BCR and Regulation when CTP is not used or recharging.
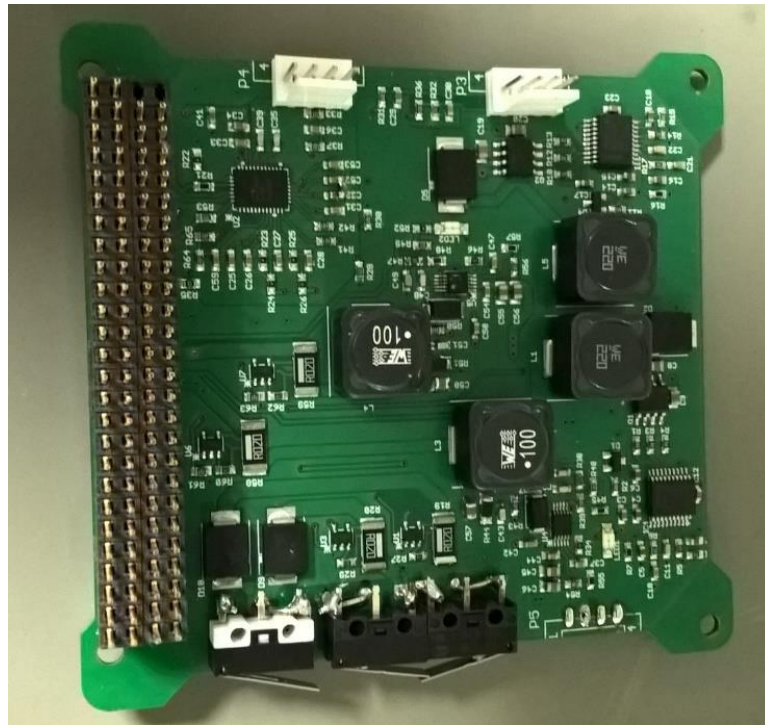
*Figure 20 EPS Daughter board*

Motherboard is dedicated to interface with the EPS. Battery Charge Regulators accept up to 30W in input and provide energy to two PS battery packs, composed by 8 cylindrical AA-sized Li-Ion cells with a capacity of 5 Ah @ 14.8 V. A step-up circuit is used to raise the 14.8V provided by the battery pack up to 28V required by the EPS. A Pulse Width Modulation (PWM) circuit, controlled by the C&DH microcontroller, regulates the step-up circuit output in the range of 5:28 V to adapt to the ePS requirements for the test. Protection circuits based on refresh fuse prevent overcurrent, overvoltage or short circuits on the power bus. Two RBT switches isolate each battery pack from the respective circuit when CTP is not used or recharging.
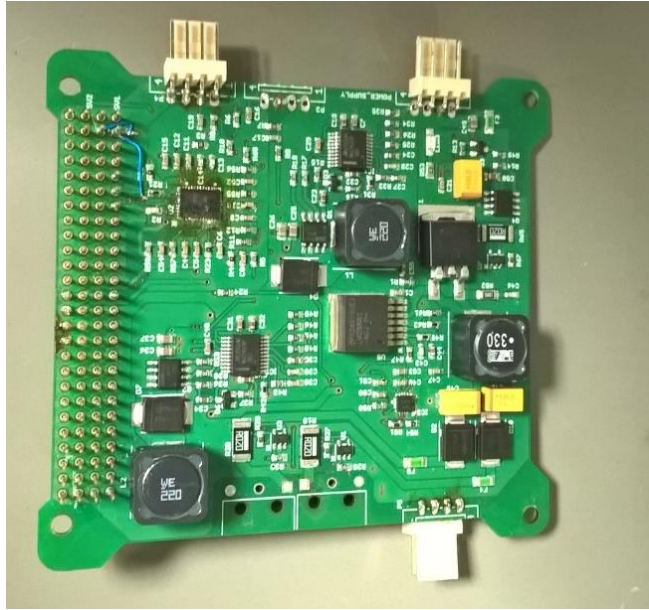
*Figure 21 EPS Motherboard*

PS batteries are sized for a peak power (accounting for a 20% margin) of 60W. Two packs are used for redundancy. Each pack provides 5.2 Ah @ 14.8V for a total power of 76.96W. this way the couple of PS batteries can provide about 154W of power. The PS battery recharge circuit can fully recharge batteries in less than 6 hours.

PS batteries are temporarily contained in a 3D printed PLA support, that is not space-grade nor vacuum-grade. For this reason, during the acceptance test in ESA/ESTEC emerged the need to replace it with a more appropriate substitute. Both a vacuum-grade plastic or an aluminium alloy solution are being considered.

Step-up circuit provides up to 60W @ 28V DC with a current of up to 2A, with a boosting efficiency of at least 95%.

Avionic batteries are sized to provide the peak power, when the PS is on and the satellite is transmitting in RF, of 9W. they can be fully charged in less than 5 hours.
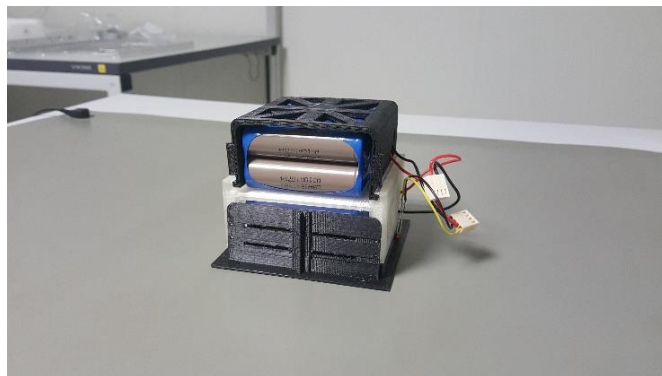


*Figure 22 PS battery packs in their 3D printed support*

# 4.2.2 CTP operational modes

By design CTP performs different tasks and has different capabilities depending on the operative mode activated. There are 5 modes of operation:

- **Dormant mode:** all the subsystems are switched off
- **Basic mode:** CTP avionics are operative, but the PS is off
- **PS mode:** CTP avionics are active; the PS is powered up
- **Burst mode:** CTP avionics and PS are active; the thruster is firing
- **Safe mode:** CTP avionics are active; diagnostics and recovery actions are performed; the PS is powered off.
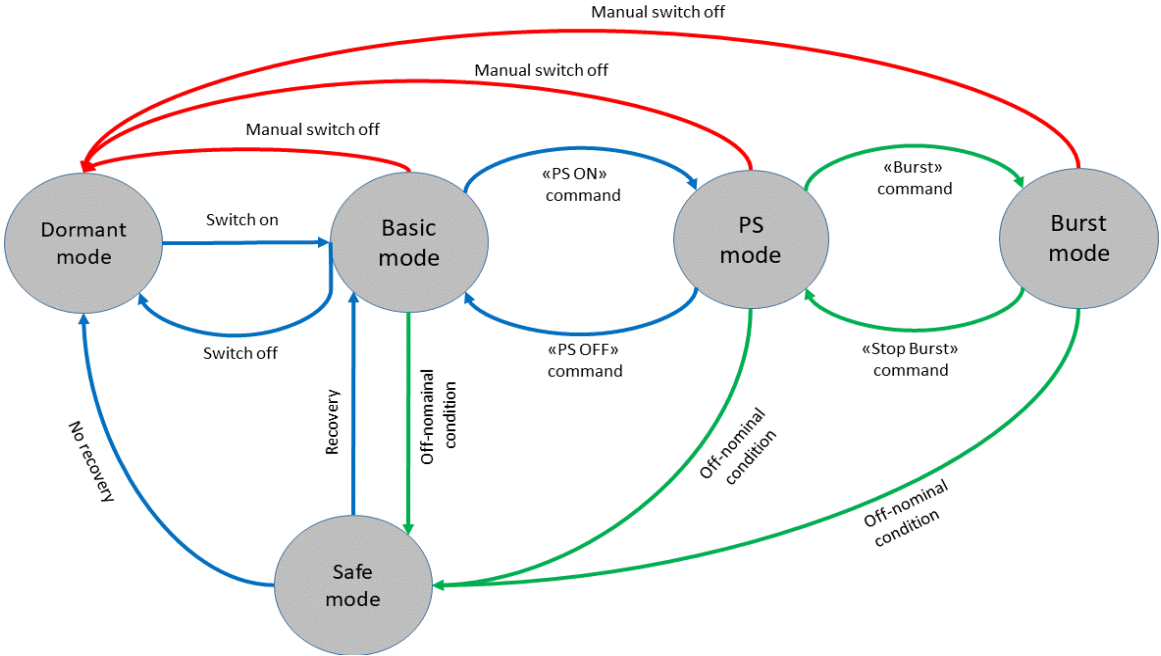


*Figure 23 CTP operative modes scheme with transitions*

In Figure 23 Red lines are used for transitions caused by the intervention of an operator; Green lines are autonomous transitions and Blue lines can be done both autonomously and/or with the intervention of an operator. Operator direct intervention (Red lines) are intended only for cases of high risk for either CTP or GSS/EPL GSE. Other transitions can be required by the GSS operator via communication link (either hard-line or RF) or can occur autonomously when certain conditions are met. Transitions to safe ode due to off-nominal conditions are autonomously performed by the CTP.

# 4.3 GROUND SUPPORT EQUIPMENT

CTP is designed to be integrated and operated at ESA/ESTEC Electric Propulsion Laboratory, using the Small Plasma Facility (SPF) or, eventually, the CORONA vacuum chambers. To properly conduct the tests several external elements other than CTP are to be used, this is the Ground Support Equipment (GSE).

Standard EPL GSE will be used and is composed by power supply units to provide electric power to CTP; sensors and acquisition units that will be discussed later in this work; a miscellanea of cables and connectors that will be used for the interfaces.

Dedicated GSS equipment has been developed specifically to complement CTP and allow the operators full control over the tests. Two computers running Ubuntu Linux are used as an interface between the operator and the platform. The workstation will use minicom on a serial port to directly control CTP and start the application. The Ground Station computer will run the GSS code, developed as part of this collaboration and later discussed with more detail, and will be the standard communication interface. The GS computer is linked to CTP both via hard-line link (HL) and radiofrequency link (RF).

Hard-line cables for both computers, along with the power supply cables and the LS button cable are connected to CTP thanks to a specifically adapted fit-through closing one of the vacuum chamber hatches. HL interfaces are shown in Figure 24 for test configuration inside SPF.
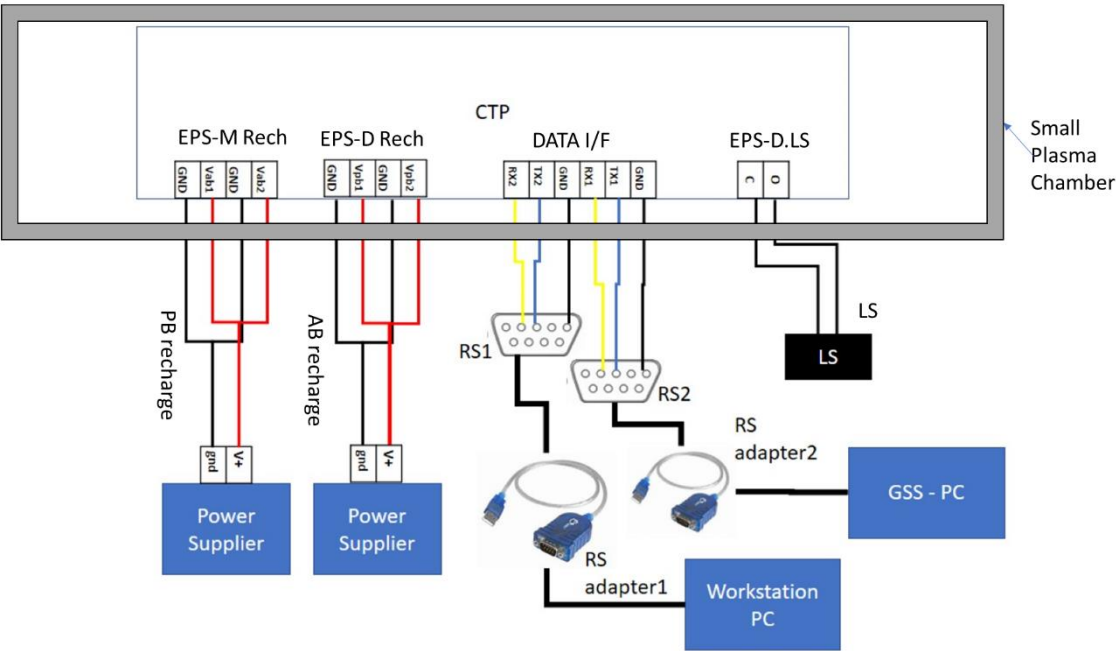


*Figure 24 CTP-GSS interfaces test configuration*

RF link is used to simulate data transmission as it would occur with an actual satellite. On the GSS side the Ground Station uses a Kenwood TH7 radio with an antenna and a TNC decoder to both receive and send packets to CTP. Communication between CTP and ground station is performed with data packets and occurs every second via HL and every 10 seconds via RF. Figure 25 shows the integration for functional test of the CTP with SPF at ESA/ESTEC EPL. It is possible to see the HL links between CTP and the fit-through. A static mat is used to prevent electronics damage, but for actual ePS tests a mechanical interface structure is to be designed and manufactured in ESA/ESTEC workshop.
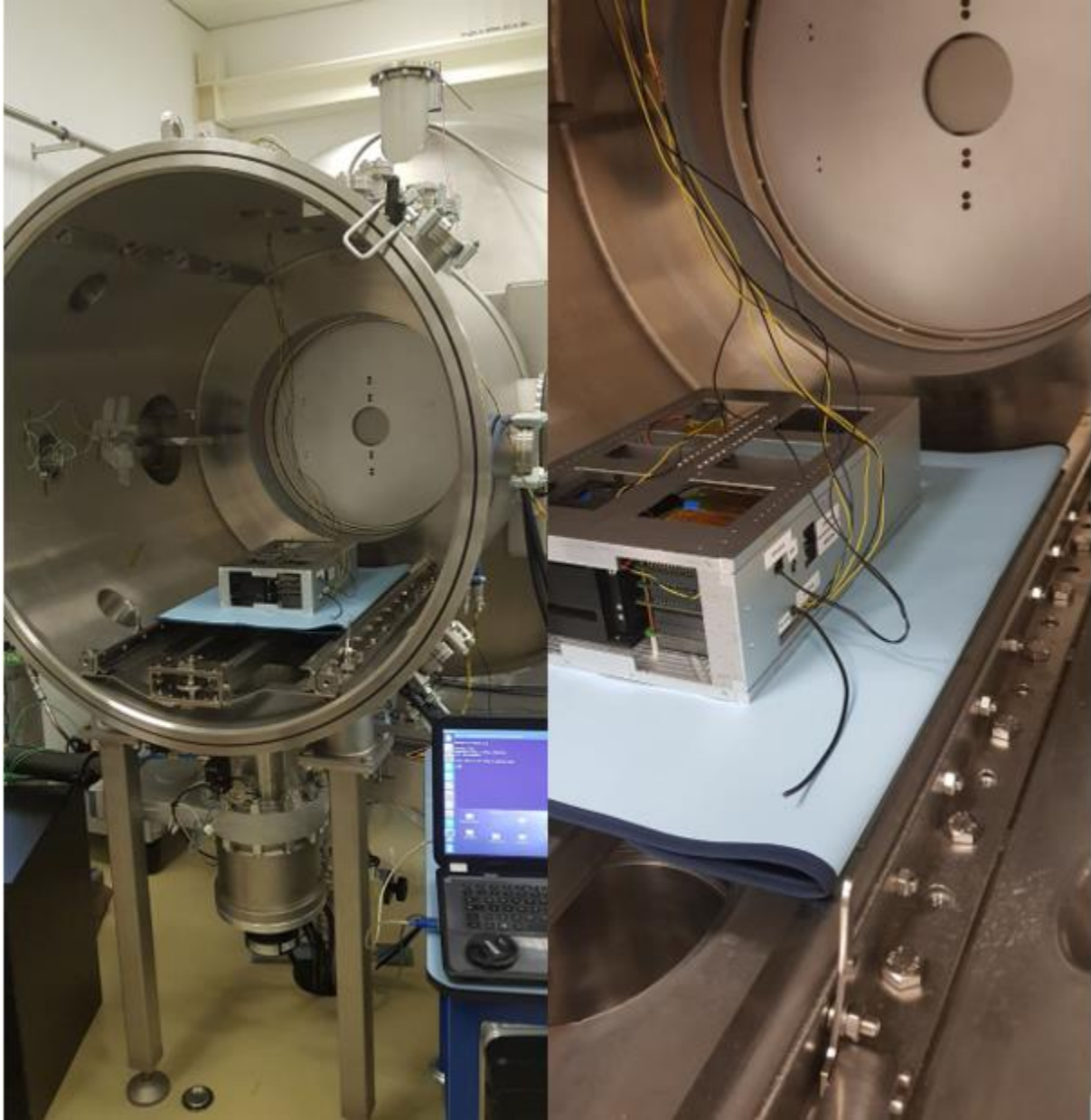


*Figure 25 CTP integration with SPF at ESA/ESTEC EPL*

# 4.3.1 Ground Support System (GSS)

The GSS is a crucial piece of Ground Segment Equipment to reach the objectives of ESA-Prop. It constitutes the main interface between the CTP and the test operators. The GSS communicates with the CTP via two lines: RF and HL.

In Figure 26 is shown the GSS PC with the two lines while it was being configured and tested at STAR Lab. On the hardware side the GSS is composed by:

- **GSS PC:** a notebook running on Ubuntu Linux
- **RS232 protocol wire:** used for HL connection
- **Level adapter:** an USB powered level adapter device to adapt voltage levels in input and output from the CTP
- **Radio + Antenna:** a Kenwood radio with either the integrated antenna or a stilo antenna, as seen in Figure 26. The radio is set at 437.445 MHz
- **TNC:** enables the coding and decoding of packets using the KISS AX25 protocol
- **Serial cable:** used to connect the TNC to the GSS PC, set at 38400 bps
- **Cables:** two cables connect the TNC to the radio, one for the receiving line and one for the transmitting one.
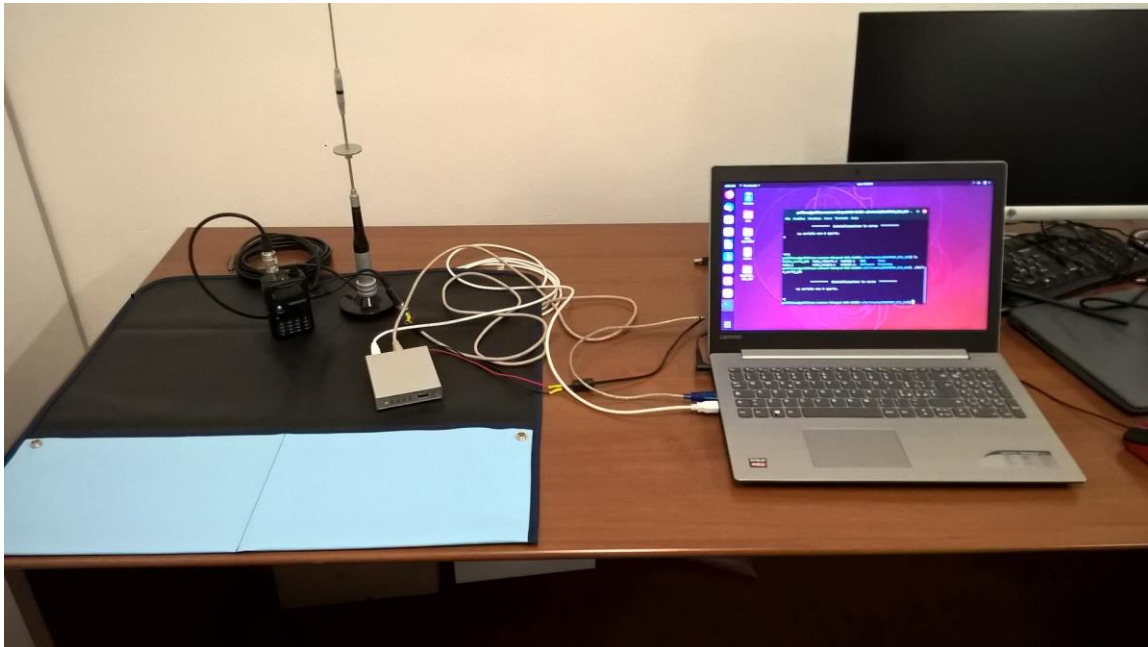


*Figure 26 Ground Support System configuration at STAR Lab*

On the GSS PC runs the core of the GSS, an application that sets and uses the two lines to communicate and control the CTP. The software was developed to provide an easy and intuitive interface for operators, while managing and both displaying and saving data from the CTP.

The software of the GSS was developed in C/C++ language and uses GTK library to create the user interface. After defining the variables, the program opens and initializes the serial ports for HL and RF links. GSS software uses a fork to create two parallel processes, one of them will monitor the two lines, read incoming packets and decoding the values, the other creates the actual Graphic User Interface (GUI). It is possible to open a second windows where it is possible to send commands to the CTP, allowing the operator to control the test.
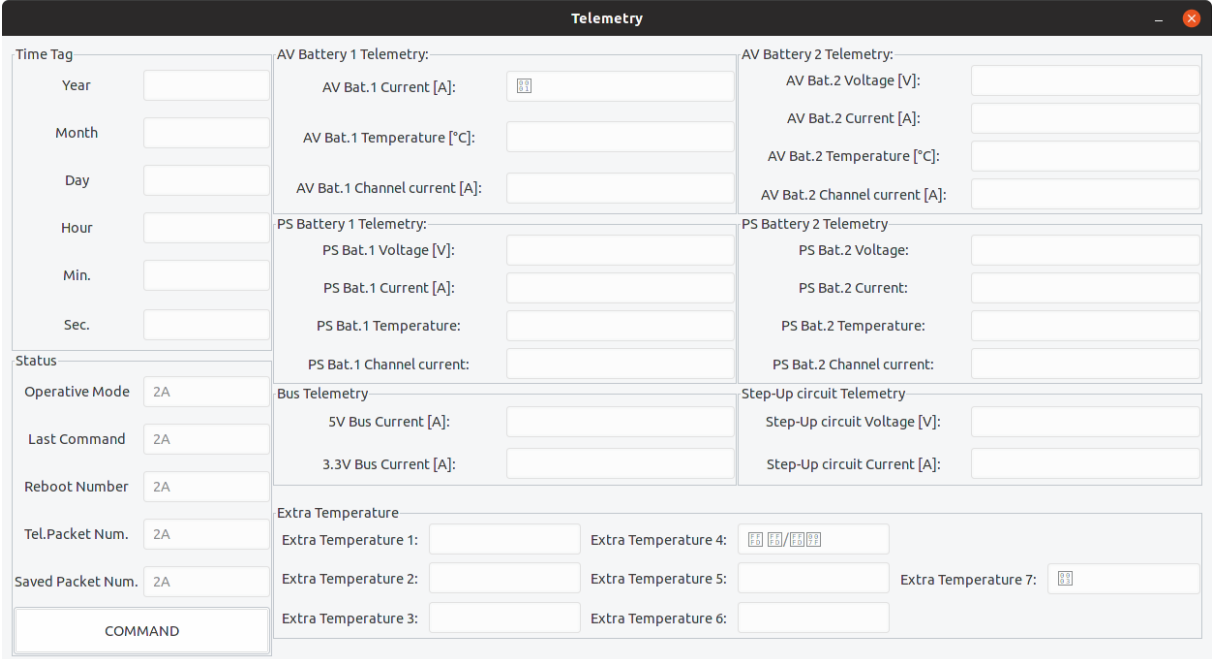


*Figure 27 GSS software GUI for telemetry and data reception*

The part of the GSS software scanning the communication lines is constantly reading HL and RF serial ports, comparing incoming values with the expected headers. Whenever a header is recognized the software saves a string of values as a packet and extracts the values from the packet to the corresponding variables. The values are then converted from 8- or 16-bit values to actual values in the expected unit of measurement. Data processed are at the moment printed on screen and will be integrated in the telemetry and data window of the GUI, shown in Figure 27.

From the telemetry window it is possible to open, by clicking on COMMAND, a second pop-up window, shown in Figure 28, enabling the operator to send commands to the CTP. When the operator selects a command to be sent to the CTP the program will create a data packet with a defined header that will be recognised by the CTP and a second part containing the command code and additional data if needed.
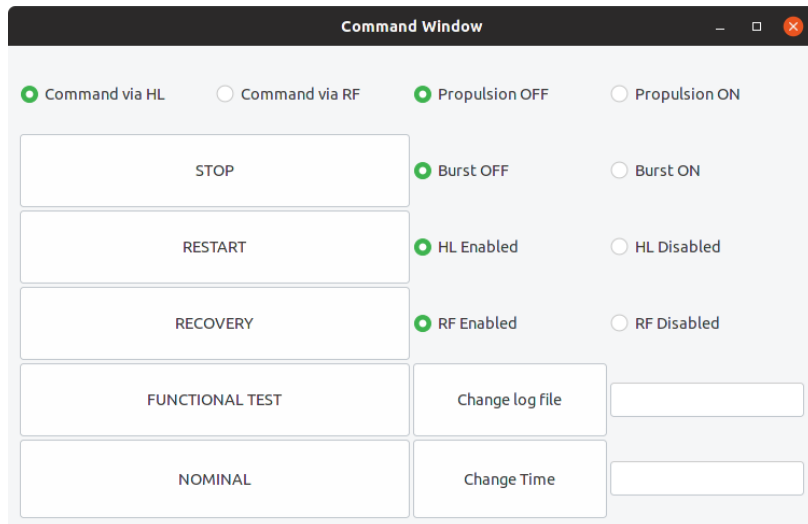
*Figure 28 GSS software GUI for sending command*

The command windows enable the operator to send commands either via HL or RF line, as defined by a radio button. The possible commands implemented are:

- **STOP:** will stop the currently running application cycle
- **RESTART:** will reboot the CTP
- **RECOVERY:** forces the CTP into recovery mode
- **FUNCTIONAL TEST:** enable the operator to perform functional tests, thus verifying the correct working of CTP
- **NOMINAL:** sets the CTP into basic mode
- **Propulsion ON/OFF:** sets the status of the ePS between not powered up (OFF) and powered up and ready to fire (ON)
- **Burst ON/OFF:** set the status of ePS between powered up (OFF) and burst mode (ON) where the thruster is firing. This command requires Propulsion ON to be enabled in order to operate.
- **HL Enabled/Disabled:** allows the operator to activate or deactivate HL communication with the CTP
- **RF Enabled/Disabled:** allows the operator to activate or deactivate RF communication with the CTP
- **Change log file:** this is used to change the file in which collected data is saved. The operator is required to write the new file name in the entry field and then select *change log file*. Doing this sends a packet containing the command code followed by the new file name to the CTP. It is recommended to use numbers in the range 0-9 as log file names.

- **Change time:** this is used to set the time of the CTP. this time will overwrite internal time data and will be used from this moment to record acquired data. The new time should be sent according to the format YYMMDDHHMMSS.

# 4.4 ASSEMBLY INTEGRATION AND VERIFICATION

CTP has been designed and assembled at Politecnico di Torino on behalf of the European Space Agency, then ESA-Prop version 1 has been delivered to ESA/ESTEC EPL for acceptance. The process of integration and functional test both at Politecnico di Torino and at EPL facility has been conducted as part of this collaboration. Integration and tests at Politecnico di Torino have been conducted in the STAR lab, the space facility of the CubeSat team, inside an ISO7 cleanroom.

## 4.4.1 Integration and Testing

The verification strategy adopted for the project was performed through a step-by-step approach at different levels of product decomposition. Verifications were performed at equipment level, subsystem level, element/system level and overall system level. The verification process was supported by the STAR lab GSE, comprising:

- **Workstation:** PC used for software development and CTP control through minicom
- **Development board:** board used to upload code on ARM9 processors and test software functionalities
- **FLATSAT:** a 10x32 cm board with 4 104-pins connectors (Figure 29) able to host the 4 boards contemporarily and presenting 3 power supply lines (3.3 V, 5 V, 8.4 V).
- **Power suppliers for GSS:** current and voltage transformers and cables to provide power to workstation PC and other GSE (i.e. Radio, TNC)
- **Power supply units:** power supply units used to simulate the ePS energy output, to take place of batteries and as power sources for battery charge.
- **TM/TC devices:** used to allow telecommunications between the CTP or parts of it and other GSS/GSE
- **GSS:** the same GSS developed for CTP and used at ESA/ESTEC EPL was firstly developed during testing.

*Figure 29 FLATSAT board with C&DH board and Comsys board*

Software was tested during development thanks to the development board, before the system integration it was tested again on the C&DH board. Test where preliminary conducted with the FLATSAT to ensure all functionalities were supported and correct communication occurred on the various interfaces. Once all subsystems had been verified, we proceeded at the integration and testing of the platform.

The integration and verification of the platform followed the sequence defined in the AIV plan and here reported in Figure 31. Detailed instructions for the integration are reported also in the AIV plan section *11.2 Assembly sequence* and were followed literally. Before the integration all the component and elements composing the CTP as well as the tools needed for the assembly were disposed on one of the cleanroom tables and properly cleaned with isopropyl alcohol. During the integration one of the operators consulted the sequence and gave instructions to the other two operators that performed the integration. A photo shot during this phase is reported in Figure 30, showing the integration work.
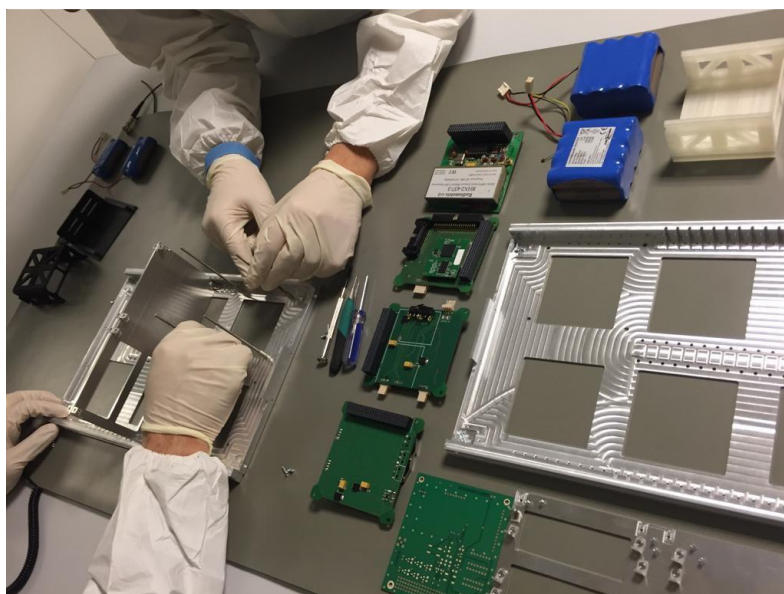


*Figure 30 CTP integration*
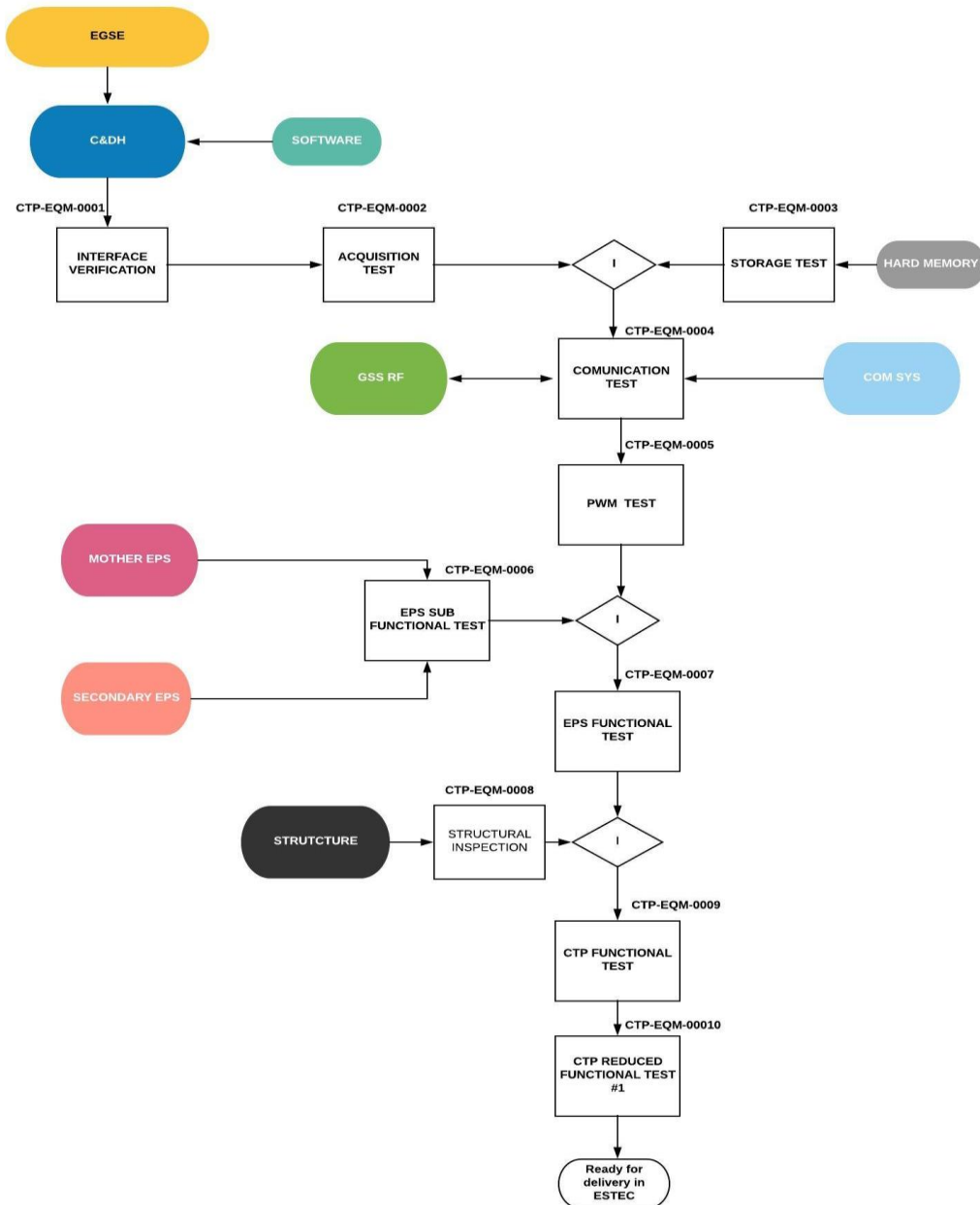
*Figure 31 Integration and Verification test*

After the integration a complete functional test (CTP-EQM-009) was performed to verify all the main functions that CTP shall accomplish to reach the goals of the ESA-PROP programme. The tested functionalities were:

- Both HL and RF communications lines towards GSS:
  - HL: UART-115200, Nominal: 12 packets/minute, Peak: 1 packet/second
  - RF: 9600bps – AFSK modulation, Nominal 2 packets/minute, Safe mode: disabled
- Storage capability (for days long test sessions)
- Data and telemetry acquisition

- Operative modes management and command execution
- Capability to detect failures/anomalies, identify faulty parts and adopt recovery actions
- Battery discharging
- Battery recharging
- Interfaces with ePS:
    - PS configuration loading in SD card (propulsion.txt)
    - Command and data handling
    - Mechanical interface
    - Electrical power feed for ePS

After the functional test had been conducted the platform was ready for shipping to ESA/ESTEC EPL, reduced functional tests (CTP-EQM-010) were conducted right before the transportation and at EPL as acceptance test. The Reduced Functional Test is foreseen as a time-saving alternative to the complete Functional Test, aiming at demonstrating correct functionality before and after transportation. The test was repeated after the CTP integration in the chamber for the same reason.

## 4.4.2 NTC characterization

As stated in Chapter 3, NTC thermistors where used as temperature sensors during phase one of the program and will continue to be used during other phases. The NTC is connected to the acquisition circuit through a couple of cables and is then placed where the temperature is to be measured. The variation in temperature will vary the thermistor resistance, and this will be detected by the acquisition circuit and transformed in what was called a 'datum', that is a 16-bit number.

The acquisition circuit is nothing else than a voltage divider with a fixed resistance of 3300 Ohm on one branch and the NTC on the other. The analogical result from the divider is fed to an ADC that transforms the signal to a digital 32-bit sequence. When interrogated by the microcontroller the ADC will send the sequences of the acquisition lines, then the microcontroller will extrapolate, by cutting out header and status bits, the 16-bits sequence composing the datum. The datum can then be related directly to a certain resistance, that is solely a function of temperature, and thus it is possible to convert it in its final form. The relation between resistance and temperature is given from the datasheet of the NTC in the form of both analytical coefficients and a table of values. From those datasheets, applying due transformations and voltage divider laws, was derived the graphic in Figure 32, that efficiently summarizes in a graphic the relationship between temperatures and respective datum.
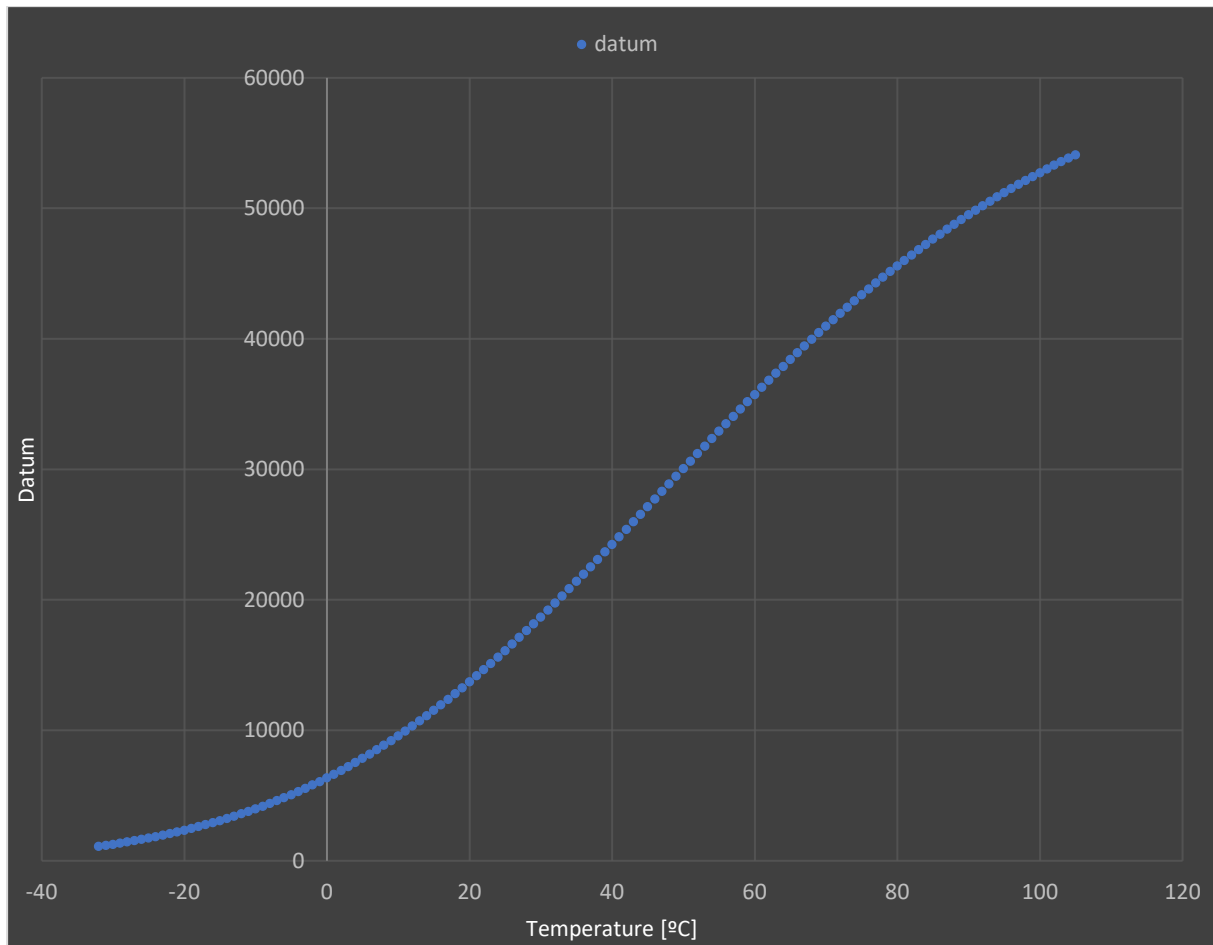
*Figure 32 Graphic summarizing NTC characterization*

It is possible to observe that the relationship is not linear, so decimals can be found either by using the analytical expression if the used NTC are given with the parameters resolving it, or by using a polygonal chain method that, having all the integer values relationships, is reasonably accurate.

## 4.5 ESA/ESTEC DELIVERY AND TEST

In conclusion of ESA-Prop phase one a meeting at ESA/ESTEC was foreseen to report for the feasibility analysis of the program and the discussion of phase two objectives. As previously stated during phase one not only a feasibility analysis was conducted, but a functioning prototype was designed and manufactured too. On the occasion of the meeting the prototype was delivered to ESA/ESTEC EPL and acceptance tests were conducted, successfully closing the phase one of the project and providing ESA with the physical prototype.

As reported in the AIV section of this chapter, the platform was integrated following the procedures at Politecnico di Torino, RFT-A1 were conducted and then PS batteries were removed due to concerns on airline company policy on battery storage in the cargo bay. PS batteries were boarded with the operators in the cabin and following the arrival and check in in ESA/ESTEC EPL facility the PS batteries were mounted again on the platform, following a slightly modified standard procedure for the occasion.

Following the re-assembly of the CTP with the PS batteries RFT-A2 were conducted on the platform in order to verify the integrity of the platform and that no damage was caused during the transfer. The platform was then partially integrated with the Small Plasma Facility vacuum chamber small hatch to test the electronic configuration and the ability of the platform to communicate with the GSE from inside the chamber. For this reason, it was necessary to modify a fit-through and to manufacture additional cables, that was done using the EPL laboratory instruments and materials, such as cables and solder, as well as test equipment. The partial integration solution can be observed in Figure 25, where a couple photos taken during integration are reported.

During the integration of the CTP inside the vacuum chamber, the GSE and GSS equipment was mounted on a desk on the exterior of SPF, and all cables connected to the fit-through. At this point RFT-B was performed to verify the platform functionality was as expected when integrated in the chamber. After successfully performing the test data storage was checked to ensure packets were saved correctly both on the on-board SD card and in a .txt file generated by the GSS.

After all the testing procedures were concluded a meeting occurred between the delegation from the Politecnico di Torino and a board of ESA customers and experts. During the meeting the ESA-Prop V1 platform was presented and shown to the board, the Phase one was declared closed and the prototype accepted by the EPL and thus moved into the laboratory storage. Also, during the meeting, the goals of the ESA-Prop project were discussed both in terms of near term, Phase two goals and of long term, complete testing facility for CubeSats with propulsion systems.

# 4.5.1 Reduced Functional Test

Reduced Functional Tests procedures have been defined for the verification of CTP in all stages of its delivery to ESA/ESTEC EPL, from STAR Lab to the integration in the chamber. Three test procedures have been defined, with some differences, to be performed in different moments:

- **RFT-A1:** Reduced Functional Test – Version A1 was the functional test to be performed prior to shipping
- **RFT-A2:** Reduced Functional Test – Version A2 was the functional test to be performed upon arrival at ESA/ESTEC EPL
- **RFT-B:** Reduced Functional Test – Version B was the functional test to be performed with CTP integrated in the vacuum chamber

The RFT-A1 and the RFT-A2 procedures are essentially the same procedure and the only difference was in the GSE used for the test, where the A1 used STAR Lab GSE the A2 used the same GSS but the other GSE was the one from the EPL. This was to confirm the lack of losses in system performances due to shipping. The procedures were composed of different parts to be performed by the operators:

- **Setup of the GSS:** the PC with the GSS was turned on, USB ports were connected to GSS serial interfaces and the GSS software was launched, initializing serial ports and communication protocol
- **Setup of the Test Bench:** operators wear latex gloves, prepare antistatic mats and bracelets and wear them
- **Setup CTP:** positioning of CTP, insertion of an SD card containing the setup data and connection of the CTP with the serial cables
- **Setup OBC Interface PC:** operators turn on the interface PC and open and setup a minicom command window to start the CTP
- **Test Start:** RBT buttons are removed and LS switch is opened. Correct activation of CTP is checked. ESA-Prop program is started and correct packet exchange between CTP and GSS is checked. Telemetry data are verified to ensure everything works fine inside CTP
- **HL Command Test:** a series of commands are given to the CTP and actuation of the command is checked and confirmed, two minutes pauses between commands ensure the previous command does not compromise CTP functioning. Commands sent to the CTP are:
  - **Set new Time:** the actual date and time is sent to CTP and correct setup is confirmed
  - **Restart:** restart command is sent and correct restart from CTP is verified. Operators should verify the configuration and the correct working of the CTP after the restart
  - **PS activation:** command to power up the propulsion system is sent to CTP and correct activation is checked

- o **Burst activation:** command to start PS burst is sent to CTP and correct activation is checked
- o **Burst deactivation:** command to stop PS burst is sent to CTP and correct deactivation is checked
- o **PS deactivation:** command to shut down propulsion system is sent to CTP and correct deactivation is checked
- o **RF link deactivation:** command to deactivate RF link is sent to CTP and correct deactivation is checked. For this part of the test only HL packets should be generated and received
- o **RF link activation:** command to activate RF link is sent to CTP and correct reactivation is checked. From this moment both HL and RF packets should be generated and received
- o **Stop:** command to stop test execution is sent to CTP and dormant mode is checked.
- **AV battery recharge:** AV batteries are connected to power generator set at 16V 1A and charge level are checked at regular intervals
- **PS battery recharge:** PS batteries are connected to power generator set at 2V 1.5A and charge level are checked at regular intervals
- **End:** when batteries are fully charged the test is concluded. LS switch is closed and RBT buttons are put back in place

The RFT-B procedures are analogue to RFT-A procedures except for the setup phases, where procedures have been modified to consider the different interfaces due to the presence of the SPF vacuum chamber. Cables are no more directly connected to the CTP but are connected to the fit-through. The satellite is then placed in the vacuum chamber, where on the bottom surface an electrostatic mat is laid and connected to ground. Interface cables are connected between the internal part of the fit-through and the CTP, and then the test proceeds as for RFT-A procedures.

## 4.5.2 Data packages

During all functional tests, as well as in normal operations when the CTP will be used for its purpose, data acquired by the on-board computer is stored in accessible text files, so that after testing the operators can access the whole record of telemetry and sensor acquisition. This is necessary to provide operators and other interested with the acquired data, enabling the study and the definition of the effects of the ePS on the platform.

Data is organized in packets, composed by a string of subsequent 8-bit or 16-bit values. The packet is then regularly written down on a .txt file on the on-board SD card. Also, this data packet is processed by the on-board computer, a header is attached before it and, in the case of TNC protocol, a closer at the end, and then sent to the GSS both using the HL and RF communication lines. The GSS is constantly reading the two serial ports in search for the headers representing the start of a data packet. When a header is recognised the GSS software saves in a temporary vector the packet, then copies it to a .txt file containing all the packets received through that line. Then it processes the packet to extrapolate data and convert them to readable values and then displays them for the ground operators. Priority for display is given to HL packets since it is the most robust communication line, and the one with the highest frequency of packages. In case HL line is deactivated or there are no packets arriving on it the RF link packets are displayed. In this case updating frequency is lower, and data displayed can be up to 20 seconds old. In Table 12 is reported the structure of data packets sent to the GSS from CTP.

*Table 12 data packet content*

| Position | Dimension [Bytes] | Content |
| --- | --- | --- |
| *1* | 7-18 | Data packet header, 7B for HL and the 18B for KISS.AX25 RF format |
| *2* | 1 | Year |
| *3* | 1 | Month |
| *4* | 1 | Day |
| *5* | 1 | Hour |
| *6* | 1 | Minutes |
| *7* | 1 | seconds |
| *8* | 4 | Telemetry pack number: the number of packets sent on the line |
| *9* | 4 | Saved packet number: the number of packets saved on-board on SD |
| *10* | 1 | Operative mode CTP is currently in |
| *11* | 1 | Last command sent to CTP |
| *12* | 1 | Number of reboots of CTP from the set-up of the test |
| *13* | 2 | 5V current |
| *14* | 2 | 3.3V current |
| *15* | 2 | Avionics battery 1 voltage |
| *16* | 2 | Avionics battery 2 voltage |
| *17* | 2 | Avionics battery 1 current |

| | | |
|---|---|---|
| *18* | 2 | Avionics battery 2 current |
| *19* | 2 | Avionics battery 1 temperature |
| *20* | 2 | Avionics battery 2 temperature |
| *21* | 2 | Avionics battery 1 charging current |
| *22* | 2 | Avionics battery 2 charging current |
| *23* | 2 | Propulsion battery 1 voltage |
| *24* | 2 | Propulsion battery 2 voltage |
| *25* | 2 | Propulsion battery 1 current |
| *26* | 2 | Propulsion battery 2 current |
| *27* | 2 | Propulsion battery 1 temperature |
| *28* | 2 | Propulsion battery 2 temperature |
| *29* | 2 | Propulsion battery 1 charging current |
| *30* | 2 | Propulsion battery 2 charging current |
| *31* | 2 | Step-up circuit current |
| *32* | 2 | Step-up circuit output voltage |
| *33* | 2 | DAC command |
| *34* | 2 | NTC sensor 1 recorded temperature |
| *35* | 2 | NTC sensor 2 recorded temperature |
| *36* | 2 | NTC sensor 3 recorded temperature |
| *37* | 2 | NTC sensor 4 recorded temperature |
| *38* | 2 | NTC sensor 5 recorded temperature |
| *39* | 2 | NTC sensor 6 recorded temperature |
| *40* | 2 | NTC sensor 7 recorded temperature |

Command packets sent from GSS to CTP share a similar structure to data packet, with a similar header followed by two 8-bit characters specifying the command. If needed, for example for data log change and time and date definition, additional positions are filled with the required information. Headers, both for data and command packets, are similar and structured on the communication standard, RF or HL. The difference is in the direction of the packet, in the header is specified who is sending the packet followed by who should receive it.

# THERMAL MODELLING OF A CUBESAT WITH EPS

As previously stated, one of the most critical aspects of electric propulsion on small CubeSat platforms is the heat management. The huge thermal loads induced by the ePS must be passively radiated from the satellite by the small external surfaces of the CubeSat. This aspect has been considered both during internal meetings and at the final review with ESA as one of the most interesting to be investigated with the program phase 2. For this reason, this work of thesis, that is generically devoted to the whole program, is specifically focused on the thermal aspects and the thermal testing of ePS.

The CTP is a platform devoted to the testing and characterization of ePS on CubeSat platform, but it is also interesting to use it in order to develop tools and competences enabling a better, faster and more efficient design of flight-ready CubeSats with propulsion systems. For this reason, a thermal model was developed able to predict the behaviour of CTP when tested with an ePS. This will enable engineers in phases 0-A of a project to predict with a fairly accurate model how different ePS will impact the system, thus focusing on the more suitable ones. It is intended to fasten design capabilities and to reduce cases in which testing and analysis conducted in subsequent phases force the designers to change ePS and thus repeat the design phases.

The thermal model has been developed with Thermal Desktop, a fluid and thermal dynamics analysis software that works as an add-on for AutoCAD. This tool enables the definition of thermal models under different conditions and is also able to simulate the orbit the satellite is in order to define the external loads. Tis has not been implemented in this model since CTP is not going to fly. It is left as an open point to develop the model in order to be as generic as possible and to provide predictions of in-orbit thermal analysis.

## 5.1 THERMAL ENVIRONMENT

Spacecrafts being launched shall withstand a wide variety of environments, going from integration facility environment to transportation conditions, launch environment and, of course, orbit environment. Since it Is usually the most critical, as well as the environment the satellite should spend most of its life time and operate, spacecrafts thermal control is usually designed with orbit conditions in mind. The whole concept of the tests to be conducted at ESA/ESTEC EPL is to replicate as closely as possible actual orbit conditions for the satellite.

## 5.1.1 Orbit environment

Heat is passively transferred thanks to three natural phenomena: conduction, convection and radiation. Conduction happens with the diffusion of heat in a solid body or the contact exchange between two bodies. Convection is a fluid thermodynamic phenomenon where heat is exchanged between a body and a moving fluid, in natural convection the process is kept in motion by density changes in the fluid due to heat exchanges, in forced convection an external motor (e.g. a fan) moves the fluid improving the heat exchange. Radiation does not need contact neither with a body nor a fluid. Everything above zero degrees Kelvin naturally emits a radiation whose intensity is a function of its temperature. Every object that is hit by the radiation, depending on its optical characteristics will partially reflect and partially absorb the radiation of other bodies.

On Earth most of heat exchange is due to conduction and convection, and usually convection or forced convection is used in technological applications to keep components at the desired temperature. In space this is not possible. Due to the almost complete vacuum experienced from spacecrafts even in LEO, convection is not a suitable method for heat dissipation. On-board heat transfer can be done passively exploiting conduction by means of active control systems such as heat pipes, thermo-electric coolers, heat exchangers. On CubeSat only passive methods and eventually heaters if needed are used, so conduction and internal radiation are really important.

Aside from the internal heat balance a spacecraft is not an isolated system, and thus it exchanges energy with the environment. This is done thanks to radiation, and optical properties of the external surfaces are the most relevant aspect to be considered. Since there are external radiative loads and internal dissipation loads to be managed, the design must consider the whole mission, where it is performed and with which power dissipation in the

various phases. External sources of energy as reported in [13] are discussed in the following of this section and depicted in Figure 33.
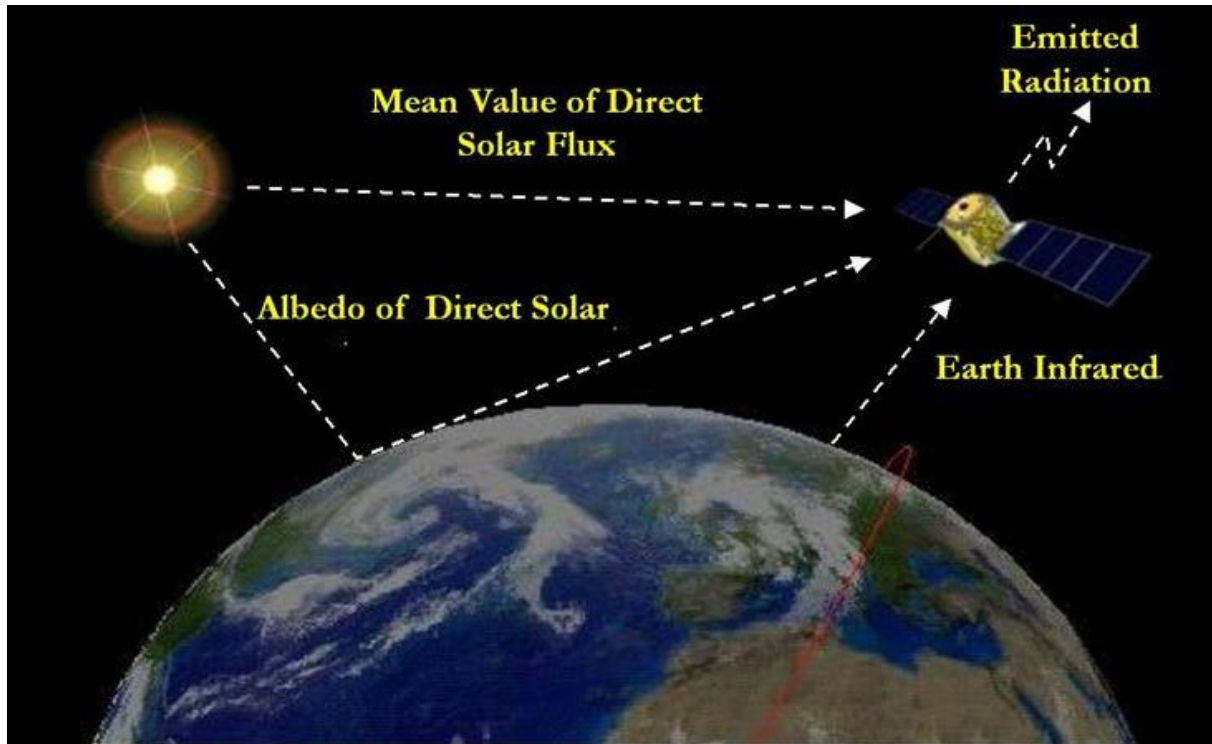


*Figure 33 Thermal loads for a satellite in orbit around the Earth*

### Direct Solar Radiation

The solar radiation is the main source of external heating for most spacecraft in Earth orbit or operating in the solar system. The Sun is quite a stable energy source, since even the solar cycle impacts on its emission for less than 1% of its power. The amount of energy reaching the spacecraft only depends on the distance between the energy source and the spacecraft. Earth orbit being elliptical causes a variation of the intensity of solar radiation during the year, with a minimum intensity at summer solstice of 1322 W/m² and a maximum at winter solstice of 1414 W/m². The intensity of solar radiation at 1AU, the mean distance between Earth and Sun, is called solar constant and is equal to 1367 W/m².

Depending on the distance from the Sun, interplanetary missions will sustain different amounts of solar radiation, and relatively to an Earth operating spacecraft inner system missions will have to cope with increased heat loads and thus will have issues with overheating while outer system missions will suffer from freezing temperatures and will need solutions to maintain heat. Some of the most complex missions exploit multiple fly-byes in order to provide the required delta-V to reach the furthest corners of the solar system. Usually those fly-byes are both in the inner and in the outer sector of the solar system, creating the really challenging need to survive both extreme heat and extreme cold.

| Celestial body | Average distance from the sun [AU] | Average Solar intensity [W/m²] |
|---|---|---|
| Mercury | 0.387 | 9116.4 |
| Venus | 0.723 | 2611 |
| Earth | 1 | 1366.1 |
| Mars | 1.523 | 588.6 |
| Jupiter | 5.202 | 50.5 |
| Saturn | 9.538 | 15.04 |
| Uranus | 19.181 | 3.72 |
| Neptune | 30.057 | 1.51 |
| Pluto | 39.44 (min 29.69 max 49.19) | 0.876 |

Solar radiation intensity also varies in function of the wavelength, with about 7% being ultraviolet, 46% visible and 47% near IR. Figure 34 shows a more accurate subdivision of the energy depending on the wavelength. Since the wavelength emitted is a function of temperature, the wavelength of heat emitted from the Sun is much shorter than that emitted from a room temperature body. This is one of the principles of thermal control, allowing designers to define optical properties in order to reflect or absorb solar radiation (depending on the need to keep it cool or to heat it up) and to emit or maintain radiative heat.
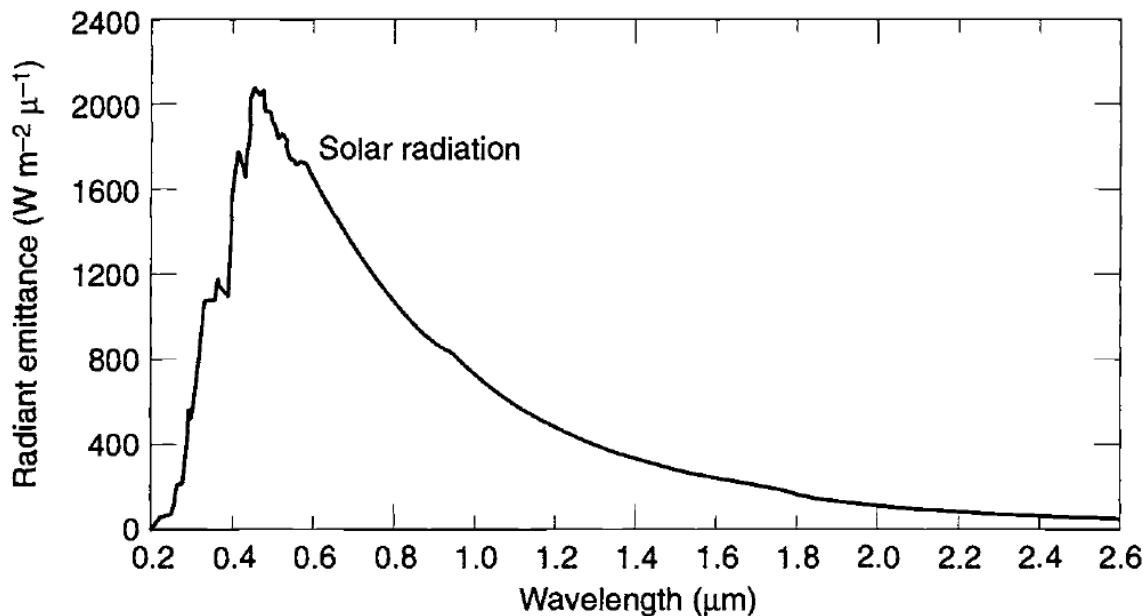


Figure 34 Solar radiation energy distribution along the wavelength spectrum

*Albedo Radiation*

74

Sunlight reflected off a planet, moon or any other celestial body is known as albedo. Of course, this occurs only when the spacecraft is in proximity of one or more celestial bodies and is neglectable during interplanetary transfers. Planet albedo is not a constant of its own but is usually expressed as a fraction of the incident sunlight. This represents the amount of such radiation that is not absorbed but is reflected to space.

Albedo is by nature extremely variable, since it depends on the surface of the planet and/or the atmosphere right beneath the spacecraft. Usually it is higher over continental regions than it is over oceanic regions, but it also depends on clouds and ice or snow (that increase reflectivity) as well as the solar elevation angle. Thus, selection of albedo fraction is highly variable and comes with great uncertainty.

*Planetary IR*

Planets and other celestial bodies behave exactly as the spacecraft, and thus emits IR radiation depending on their temperature. While the balance on a global scale is quite stable, it can vary considerably depending on local surface temperature and cloud coverage. The variation in IR radiation, while considerable, are much less significant than albedo variations.

The issue with planetary IR radiation is that most celestial bodies are at similar temperatures than the spacecraft orbiting around them. As an example, Earth has an average effective temperature of about -18°C. Thus, the wavelength of IR radiation is longer than solar radiation, and in the order of the emitted IR from the spacecraft itself. This causes surface finish designed to dissipate heat to absorb most of the planetary IR, since emissivity and absorptivity at a certain wavelength are the same. Since the spacecraft is usually at higher temperatures even if not by much, dissipation effectiveness is still positive, but significantly lowered for surfaces facing a celestial body. Although planetary IR is actually a single thermal exchange depending on the temperature difference between spacecraft and planet surfaces, usually especially for the early design superposition principle is applied. The surface flux is given by the balance between the radiated flux, computed as if the surface is radiating to deep space, and the incoming flux, considered as a constant depending on the planet, the satellite orbit and the seasonal fluctuation.

*Free Molecular Heating*

Free molecular heating is the result of the bombardment of the spacecraft by individual molecules moving at high relative velocities. Even if there is vacuum in space, this is not a perfect vacuum. The atmosphere does not simply stop at a certain altitude, but it becomes more and more rarefied, to the point only a few particles can escape from it. At this point fluid models are not applicable and a single particle impact for both aerodynamic drag and thermal

exchanges must be applied. This is significant mostly during the final phases of the launch, after the fairing is ejected, and for satellites in particularly low orbits.

*Charged Particles Heating*

Charged particles are another source of heating, although weak compared to the ones discussed before. It is usually neglectable in the design of common systems and it is usually only accounted for in the design of cryogenic systems. It is due to the charged particles trapped in certain areas of space, such as the Van Allen belts, that hitting the spacecraft can release energy and increase the system temperature.

# 5.1.2 Test environment

Tests with ESA-Prop will be conducted, as seen before, inside a vacuum chamber at ESA/ESTEC EPL. Vacuum chambers are a tool that enables the most accurate possible simulation of the space environment for thermo and fluid dynamics. They are needed for propulsion tests since the thruster performances are strongly affected by the external pressure. Most chemical thruster work on pressure differential, and thus are much more efficient in vacuum than for atmospheric flight. Some electric thrusters are even not usable in atmosphere due to the requirement of rarefied gas in order to work. If low-pressure, rarefied propellant is provided in space the pressure differential is still outflowing from the thruster, allowing its working, but in atmosphere, at 1 bar, the air would enter the thruster and prevent its functioning.

The simulated environment of a vacuum chamber can accurately reproduce the hard-vacuum conditions that the spacecraft will sustain in space. From a thermodynamic point of view this successfully disables convection. Anyway, the vacuum chamber alone is not able to simulate space conditions. As for the radiated heat towards the planet, the exchange depends on the difference in temperature between the two bodies. Deep space radiation is almost perfect, with the effective temperature of deep space being of about 3.5 K. For a spacecraft in a vacuum chamber the radiation happens between the spacecraft itself and the internal walls of the chamber, that will be at room temperature. To prevent this from happening thermo vacuum is often used when thermal design is concerned, this way the vacuum chamber walls temperature can be changed. Specifically, a flux of liquid nitrogen is used to cool the internal walls. This reduces the temperature but is not enough to recreate the 3.5 K of deep space, since liquid nitrogen is only 77 K.

Another limitation of the vacuum chamber is the lack of the external loads that would be present in space. While free molecular and charged particle heating can be omitted due to their low impact, solar radiation is characterizing for the environment the spacecraft will operate.

This can be simulated using sun simulators, that radiate to the spacecraft in the chamber an equal amount of energy than the one the spacecraft would receive in its orbit. Depending on the solar simulator radiation can be more or less coherent with actual solar radiation, with the best simulators emitting energy in the same wavelengths of the Sun. Sun simulators provide both thermal environment and EPS testing if the spacecraft uses solar panels for electric production. The introduction of a sun simulator is foreseen as part of ESA-Prop phase 3. It is interesting to consider that even with liquid nitrogen cooling and the sun simulator the test is not actually representative since there will not be the planetary effects (albedo, IR emission) and there will instead be vacuum chamber effects (reflection of simulated sunlight off the internal walls, low emission from the cooled internal walls). To achieve actual simulation data will need to be post processed to consider differences between the simulated environment and the actual space environment.

The thermal model at the moment will feature the spacecraft in a radiative environment characterized by the walls at room temperature. Through parameters changes the vacuum chamber walls temperature can be defined in order to reflect the decision to use the cooling circuit or not for the test. Subsequent updates of the model will likely feature a radiative model for the sun simulator according to design choices during phase 3 of the program. Other possible future upgrades of the model could see the definition of an in-orbit simulator to help with early design of electric propelled CubeSats.

## 5.2 THERMAL PROPERTIES OF THE MATERIALS

The thermal behaviour of a spacecraft is defined by its geometry, the applied thermal loads and the materials and finishes used. For the materials it is important to consider the conductive properties and the inertial mass for the internal transmission of heat and the temperature changes, and the optical properties of the surfaces for radiative transmission. The strong dependence from the surface properties makes it possible for thermal engineers to have a great impact at relative low cost by varying paintings, finishes and surface treatments.

The use of certain surfaces enables the spacecraft both to regulate the intensity of thermal loads acquired from the different external sources, and to define the rate at which internal heat is dissipated to space. It can also be important for internal heat transmission and sometimes heat can be actually passed from an external surface to another, depending on spacecraft layout. This usually occurs when there are elements that are deployed on the exterior of the spacecraft's main volume such as solar panels, antennas and other instrumentation.

Different materials have different physical properties, but the optical properties can easily be changed even for the same material. A polished surface will perform differently than an opaque surface of the same material. If this is not enough it is possible to apply several different paints, use insulating coats like MLI or Kapton blankets, cover with a spray of gold or silver particles, or even mix two or more of those options allowing a quite fine tuning to the necessity of the specific mission. By varying the optical parameters of the materials this model will allow thermal engineers to predict the outcome of different materials and coatings in order to select the most useful for the actual mission, even in the early phases of the mission. This will enable to save time and costs in later phases, by setting the path for the design of the TCS.

Of course, the CTP v1 has already been designed and manufactured, and thus its physical properties are well defined and can only be changed by adding thermal insulation such as MLI blankets or Kapton tape. For this reason, the thermal model is based on the present architecture of the CTP and shall be modified according to architecture and materials changes as the program develops.

*Table 14 Material properties used in the thermal model*

| Material Property | Measurement Unit | Description |
|---|---|---|
| *Density* | Kg/m³ | The density of a material represents the mass per unit of volume. It is important in thermal analysis since it is important in thermal inertia calculation. |
| *Specific Heat* | J/(K·m³) | The specific heat represents the amount of energy needed, at constant pressure, to change the temperature of one volumetric unit of one degree. This value is also used for thermal inertia calculation, combined with density and dimensional data. |
| *Thermal Conductivity* | W/(m·K) | Thermal conductivity represents the efficiency with which heat is transferred in a certain material. Good conductors like metals have high thermal conductivity, good insulating materials have low thermal conductivity and can be used to limit heat exchanges. |

| | | |
|---|---|---|
| *Emissivity* | - | Emissivity is the effectiveness of a certain material in emitting energy as thermal radiation. Depending on the temperature the energy is emitted at different wavelengths, comprising the bands of the thermal infrared and visible light. Emissivity equals absorptivity for a certain wavelength, so it is to be used in calculations between surfaces at similar temperatures. |
| *Absorptance* | - | Absorptance is the effectiveness of a certain material in absorbing incident radiant energy. As for emissivity absorptance depends on the wavelength of the radiation, thus for our study the absorptance coefficient used is that of the peak power of solar emission, corresponding to visible light. |

The CTP is manufactured with a limited amount of materials. The structure is made with machine worked aluminium alloys, while the boards are composed by the plastic matrix of the PCB and many different electronic components ranging from resistances and capacitors to integrated circuits and solid-state memories. Batteries are made from plastic and lithium ions materials. Thermal characteristics of PCB and batteries are esteemed from empirical data or standard values used for first approximations are used.

For the battery cells thermal properties the reference values used are those obtained in [14], a thesis work from a student at Politecnico di Milano Energy department. In this work empirical data is collected in order to derive the thermal characteristics of the battery cell. This is done to various extents, considering the anisotropic nature of the Lithium-Ion batteries. For this thermal model an average, first approximation value had been selected, able to approximate the batteries properties in terms of mean temperatures, if not in actual spatial distribution on the inside. The exterior of the battery pack is covered in blue solder mask, a plastic material often used for this application. Optical properties of the battery pack used by the model are those of blue solder mask.

For the PCB thermal modelling had been performed with parameters derived from [15], featuring a summary of various articles about thermal behaviour of integrated circuits and boards. PCB are also anisotropic since the copper printing are good heat conductors while the

plastic matrix is an insulator. For this reason, heat is easily spread on the plane while it is harder for it to pass the thickness of the board. The thermal model uses the simplified values for fr4 (boards printed on 4 layers) as thermal properties.

The primary structure is manufactured from a block of Al6061 while lateral faces composing the secondary structure are made of Al 5005. Thermal properties have been defined accordingly, with values taken from [16], a professional website dedicated to materials. The ePS mock-up was also considered to be made of Al6061 to reflect the thermal load emulator, but this can be changed to reflect actual materials composing the ePS to be studied. Other materials used in the CTP are PEEK for the PS batteries drawer and stainless steel for the filleted bars and the screws. In order to change the material, it is enough to create a new entry in the *Thermophysical Properties* and *Optical Properties* tabs of Thermal Desktop with the desired values. Then it is possible to assign those materials to the ePS through the *Edit* tab, replacing the previous material properties.

# 5.3 THERMAL DESKTOP ANALYTICAL MODEL

The model was developed with Thermal Desktop, a Cullimore and Ring software that uses AutoCAD to model the analysis object. It enables accurate thermo- and fluid-dynamics simulations and is particularly suited for spacecraft thermal analysis thanks to its ability to simulate external loads on the satellite by providing orbital parameters and attitude of the spacecraft. The program uses a FEM model to simulate the heat exchanges and derive the temperature map of the test object. A simplified FEM of the CTP v1 has been created in Thermal Desktop, and a preliminary mock-up of an ePS has been inserted in the model.

First thing the materials composing the CTP have been identified and corresponding properties have been defined in Thermal Desktop. In the *Edit Optical Properties* tab, shown in Figure 35, different optical behaviour of the various surfaces composing CTP have been defined. For each entry *absorptivity* and *emissivity* values have been defined, and the program then automatically calculates the *a/e* rapport. The optical properties used in the model are aluminium surfaces, composing the structure and the ePS, fr4 surfaces for the electronics, blue solder mask surfaces for the batteries and a hybrid property defined as a mean property of the PEEK drawer and the PS batteries blue solder mask. For the latter, surface had been estimated to be about 70% PEEK and 30% blue solder mask. Those properties have been used during the modelling phase to define the optical properties of the platform's surfaces.

If new entries are ever needed to represent new components, insulations or surface finishing, particularly for the engine models or updates in the CTP avionics, it will be enough to type the new material name in the *New property to add:* bar and then click on *Add*. Another tab will appear which requires entries on the optical properties of the material. Once relevant properties values have been inserted, the user will be able to confirm the insertion and the new optical surface will be added to the list of usable optical properties.
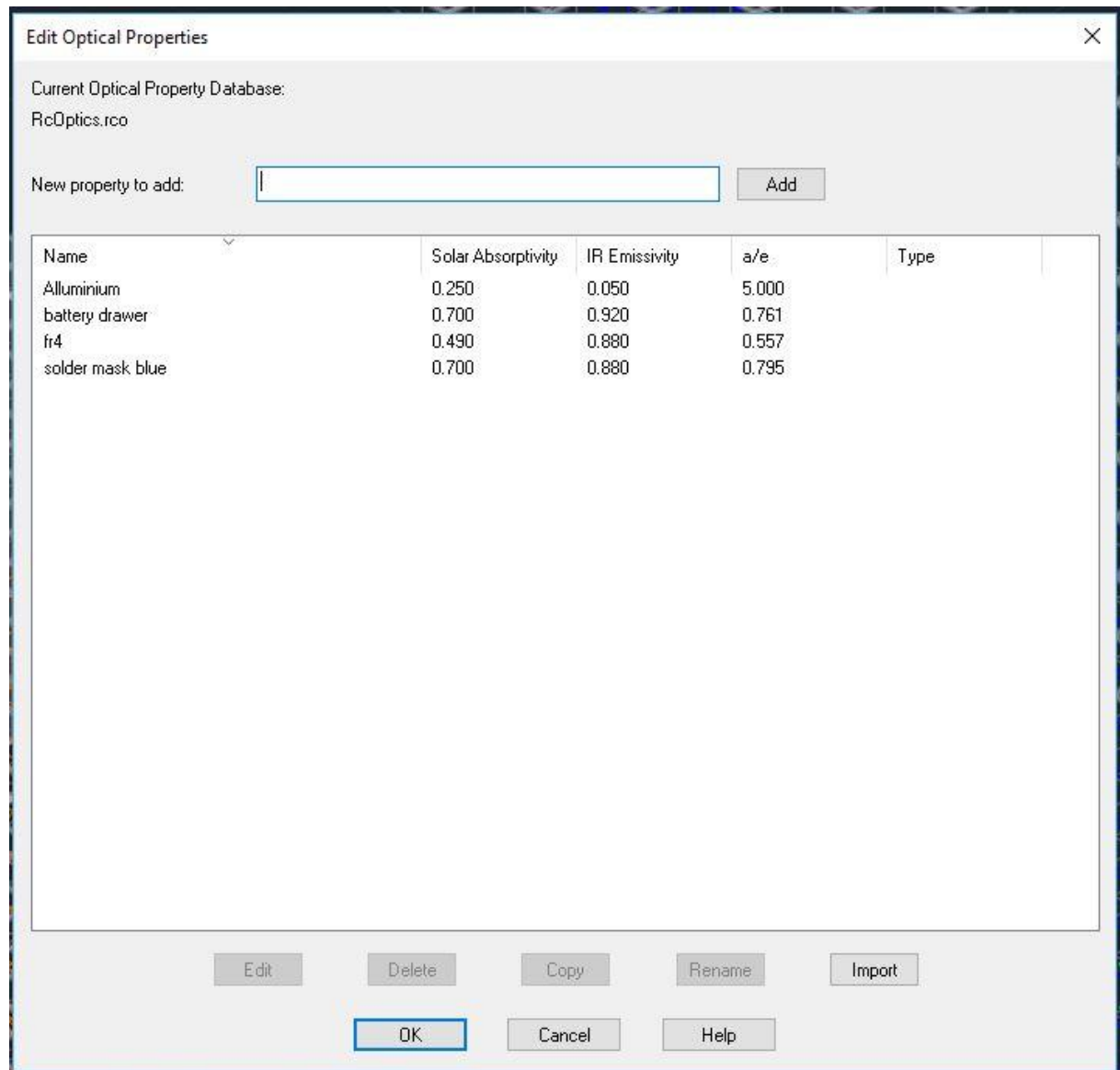


*Figure 35 Optical Properties Tab from TD model*

In the *Edit thermophysical properties* tab, shown in Figure 36**Errore. L'origine riferimento non è stata trovata.Errore. L'origine riferimento non è stata trovata.**, the physical properties of the materials that are relevant for thermodynamics simulation, except those related to optics and radiation, are defined. In this model two aluminium alloys, Al5005 and Al6082, have been defined since they have a slightly different thermal conductivity. Batteries material thermal properties have been based on an empirical

characterisation of Li-Ion battery cells[14]. The boards material has been modelled from [15]. Stainless steel has also been characterized to model connectors representing screws and filleted bars. PEEK has also been inserted in the model and is used for the drawer containing the PS batteries. The Battery/Drawer material is a weighted mean value of the thermophysical properties of PEEK and Li-ion batteries.

As for the optical properties, if the need arises to add new materials, just type the new material's name in the *New property to add:* bar and press *Add.* A new tab will open where it will be possible to insert values for the properties and at the end to confirm the new entry. At that point the material will be available in the list of thermophysical properties to be used in the model.
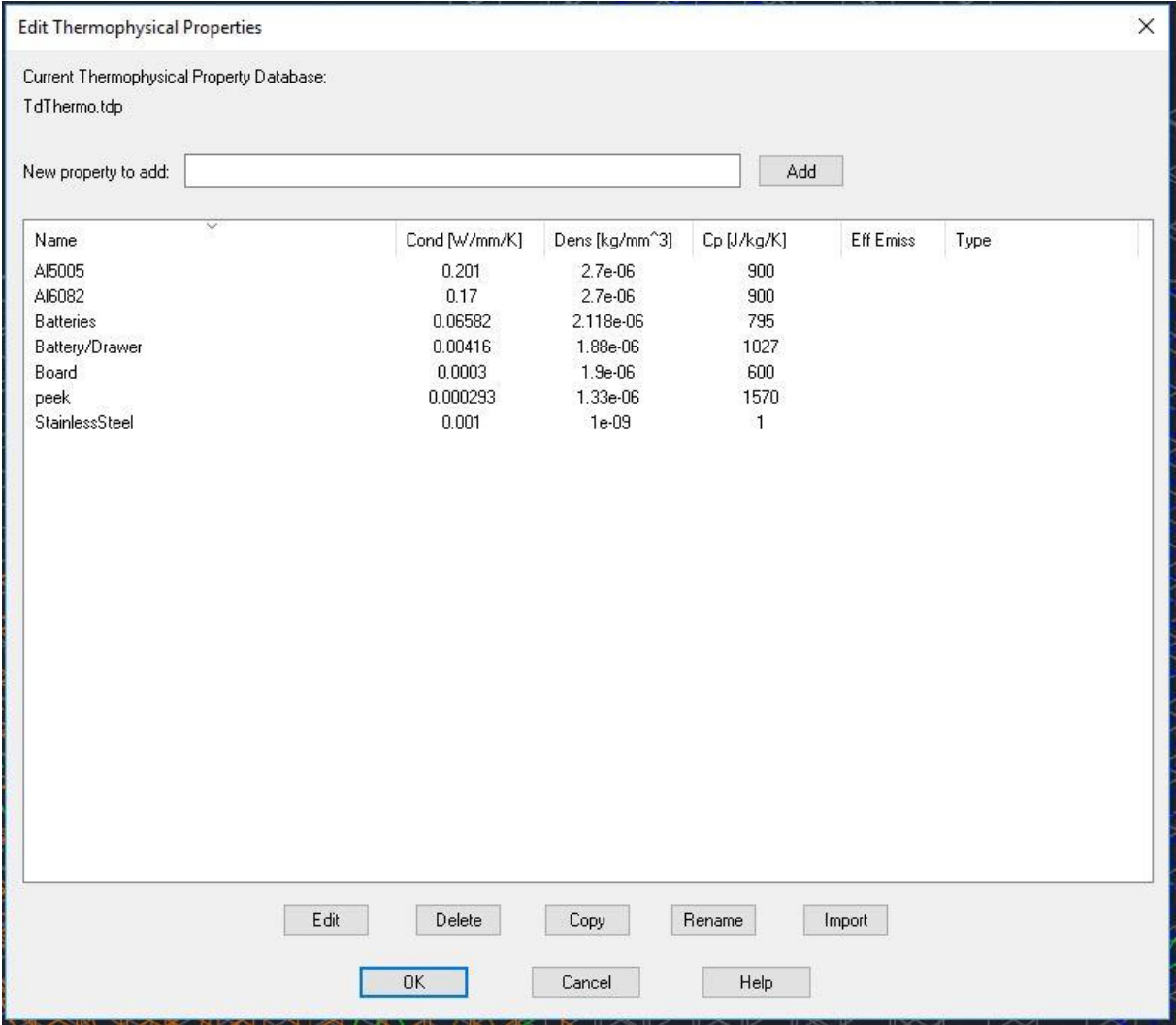


*Figure 36 Thermophysical Properties Tab from TD model*

The overall philosophy adopted during the modelling was to keep it simple and easy to interact with. In order to enable any future user to understand the model and adapt it to the actual test object of the moment, different elements groups had been defined. Figure 37 shows the model browser, this subdivision enables to operate quick changes affecting only a certain

portion of the model. It is the optimal tool to keep the model ordered and every element traceable. To enhance the model also at a visual level Layers have been assigned to different elements groups, with dedicated colours, as shown in Figure 38. This enables the quick recognition of different elements of the platform.

After the material definition the actual modelling of the platform begun. The first thing to be modelled was the structure of the CTP, that was approximated with aluminium plates composing a box with the dimensions of the actual platform. The structure is contained into its own submodel and is distributed into different layers all sharing grey colour, allowing the user to only visualise parts of the structure.
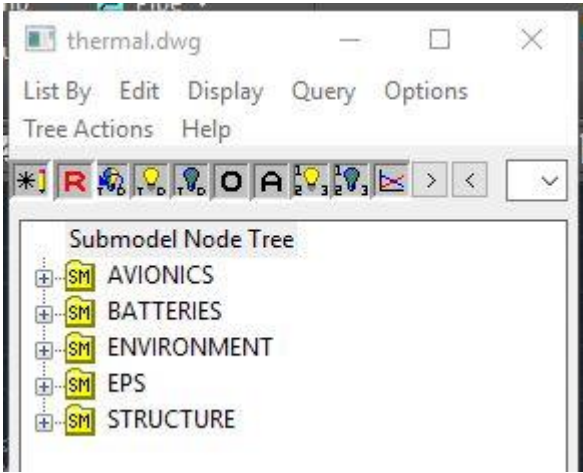


Figure 37 Model Browser from TD model



Figure 38 Layers of the Thermal Desktop model

The structure is composed by a *Bottom plate* and a *Top plate*, that are the 6U surfaces of the platform and are created with a *FEM plate* of 346x226 mm. Bottom and Top plates are parallel and 100mm away from each other. They are connected by the *lateral plates*, 3 vertical plates connecting the former two on the 3U sides and on the service module 2U side. On the

ePS module 2U side there are two plates with a centred gap for the ePS. To model the *bulkhead* separating the Service Module from the Propulsion module a vertical aluminium plate was used. While the horizontal and lateral plates are connected by performing the equivalence of the nodes, the bulkhead is connected to the other plates via a contactor. The contactor connecting the bulkhead to the primary structure mimics the actual configuration, and thus is positioned on the Top and Bottom plates, and has a total area considered for the exchange equal to that of the feets connecting the bulkhead to the surface. To reflect real model's materials Top and Bottom plates and the bulkhead are made of Al6082 while lateral plates are made of Al5005. Properties relative to materials and thermal calculations of the two kinds of elements are reported in Figure 39Figure 40Figure 41Figure 42.
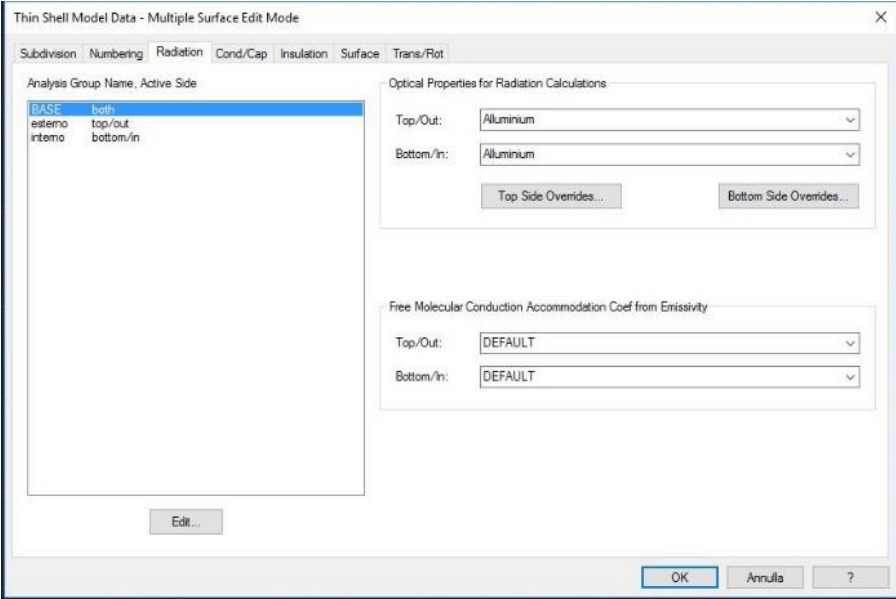


*Figure 39 Radiation tab from the properties of Top Plate*
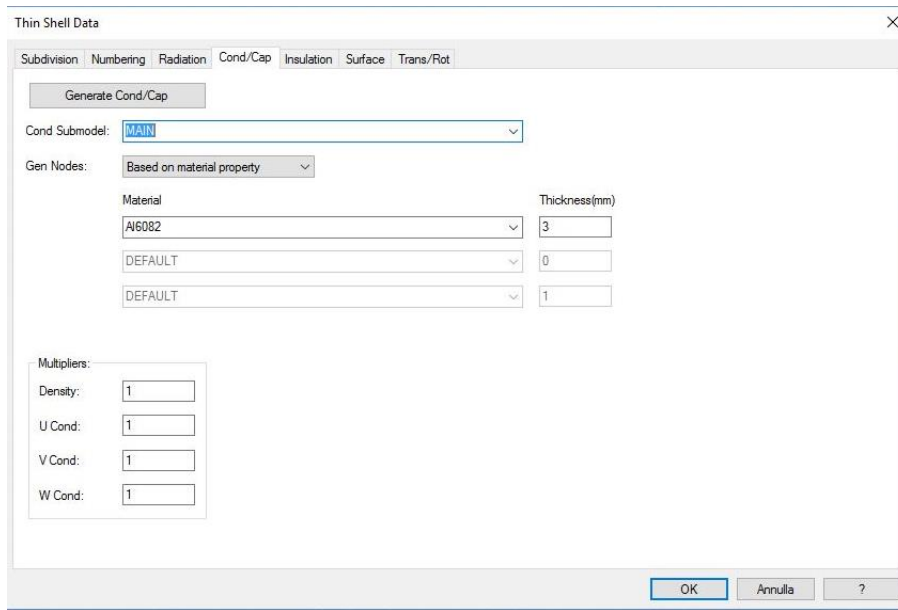
*Figure 40 Cond/Cap tab from the Properties of Top Plate*
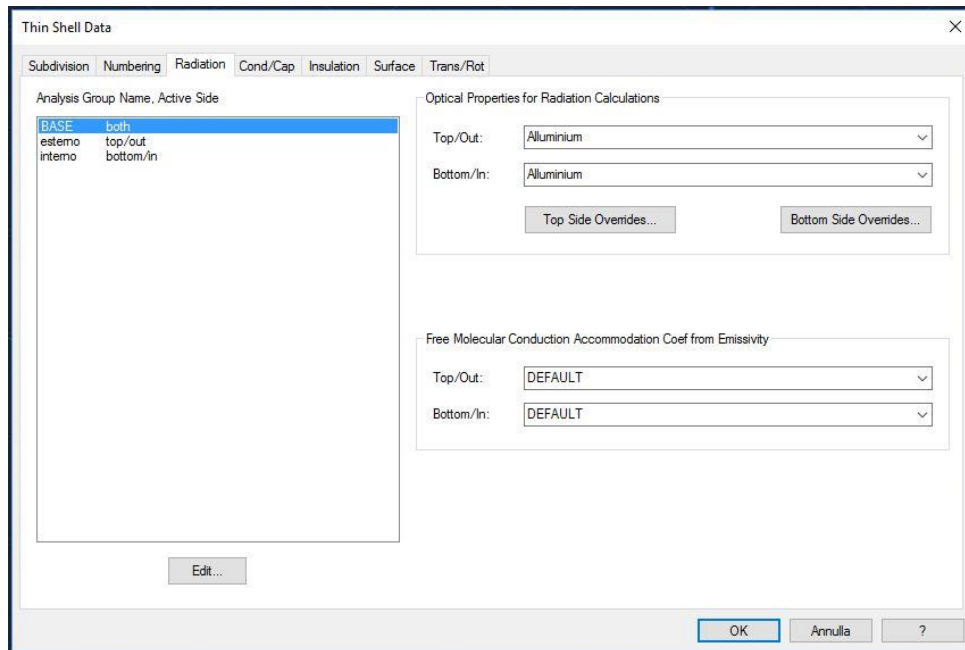


*Figure 41 Radiation tab from the Properties of Lateral faces*
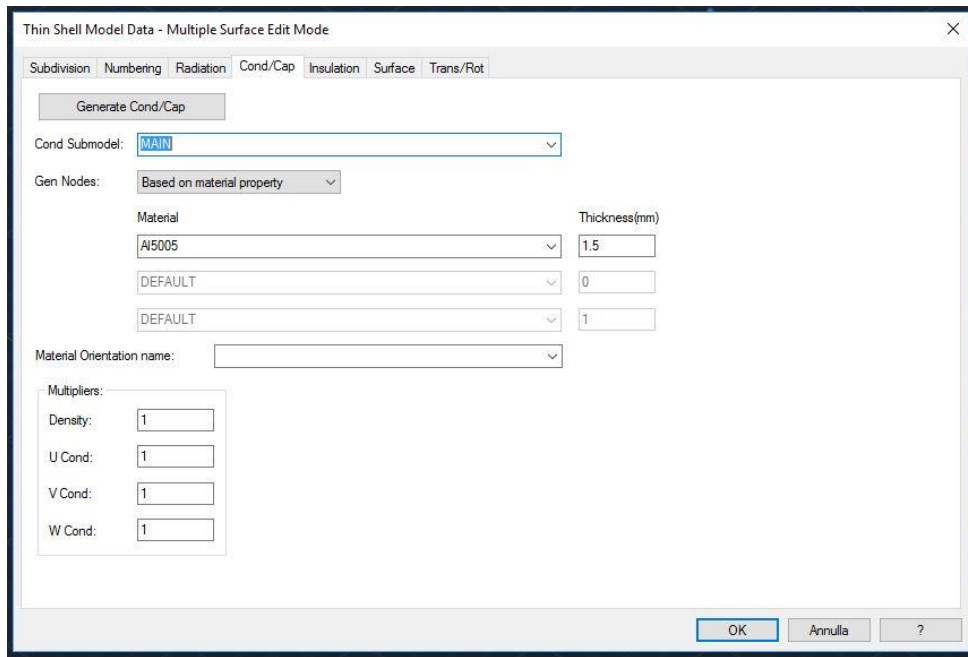
*Figure 42 Cond/Cap tab from the Properties of Lateral faces*

All structural plates had been divided in edge type finite elements, with 10 elements for each unit of the side. The thickness considered is an average of the actual different plate thicknesses. The configuration of the structure mirrors the real configuration of the CTP, and from a structural point of view is that shown in Figure 44. The contactors modelling the connection between the bulkhead and the primary structure is also visible, and its details are reported in Figure 43.
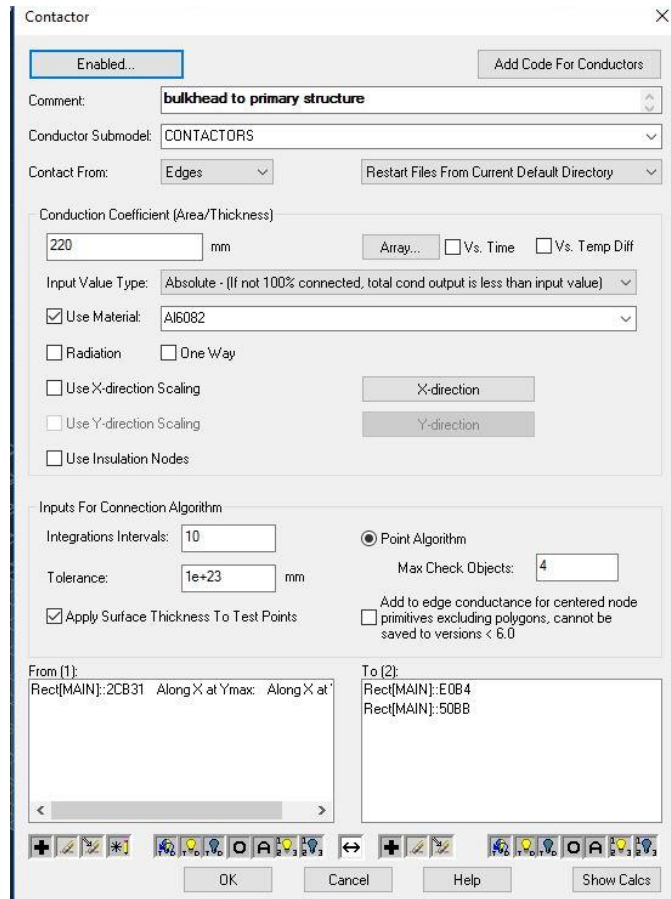
*Figure 43 Details of the connector between the bulkhead and the primary structure*
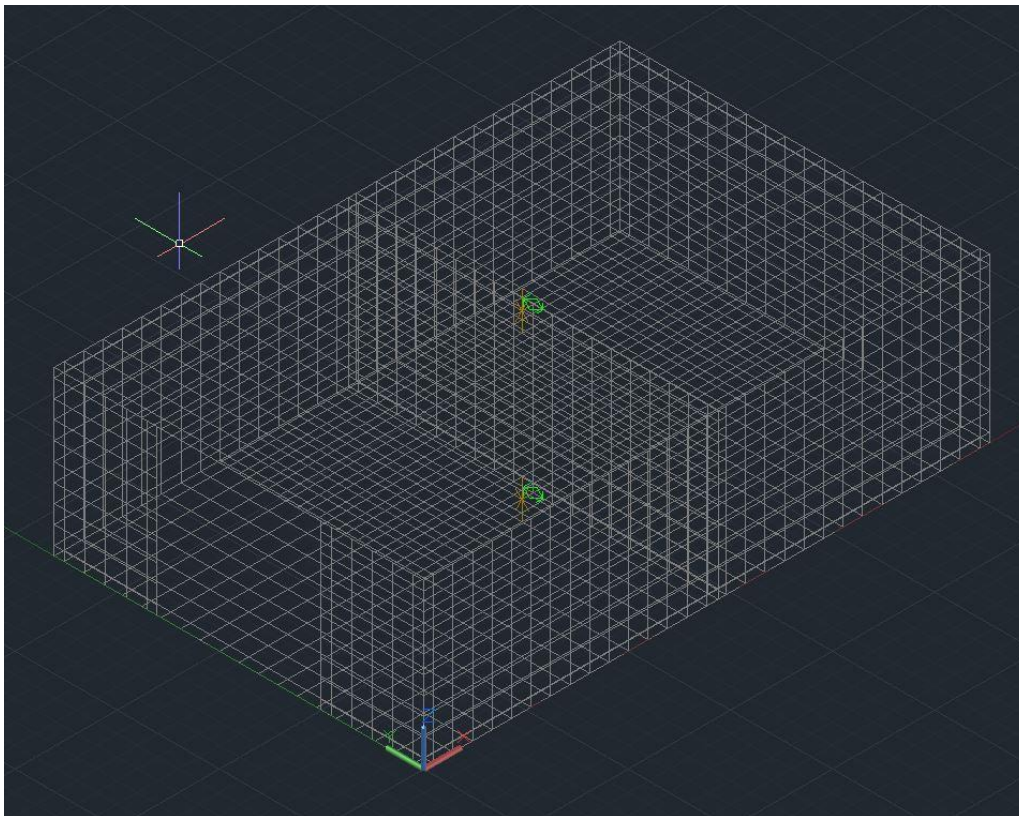


*Figure 44 TD model Structure*

Once the structure of the platform was modelled into Thermal Desktop the focus moved to the avionics. The first thing modelled were the electronic boards, sticking to the platform design. In the CTP real model, the avionics box containing the electronic boards is composed by 4 PCB stacked on top of each other with 4 stainless steel filleted bars for structural strength. In TD model PCB are created with FEM surfaces stacked one on top of the other and connected with 4 stainless steel filled cylindric FEM bars. Each single board, as shown in Figure 45, have the optical properties defined for fr4 on both sides, and its activated radiation group is the one for internal calculations. The board physical properties are those of the board material, previously explained, with a thickness of 1.5mm, as shown in Figure 46. Electronics have their own submodel and layer and are visualised with the colour green, as are the connectors associated. To make filleted bars models as similar to reality as possible, the TD model uses a cylinder passing through the whole CTP height. The four components are filled FEM cylinders and are connected to the filleted bar through node equivalence. The material of the cylinder is Stainless Steel and it is connected to the structure's Top and Bottom plates. The cylinder has a diameter of 2.5mm and is divided in 10 elements along its height. The integrated model with the structure and the electronics is shown in Figure 47.
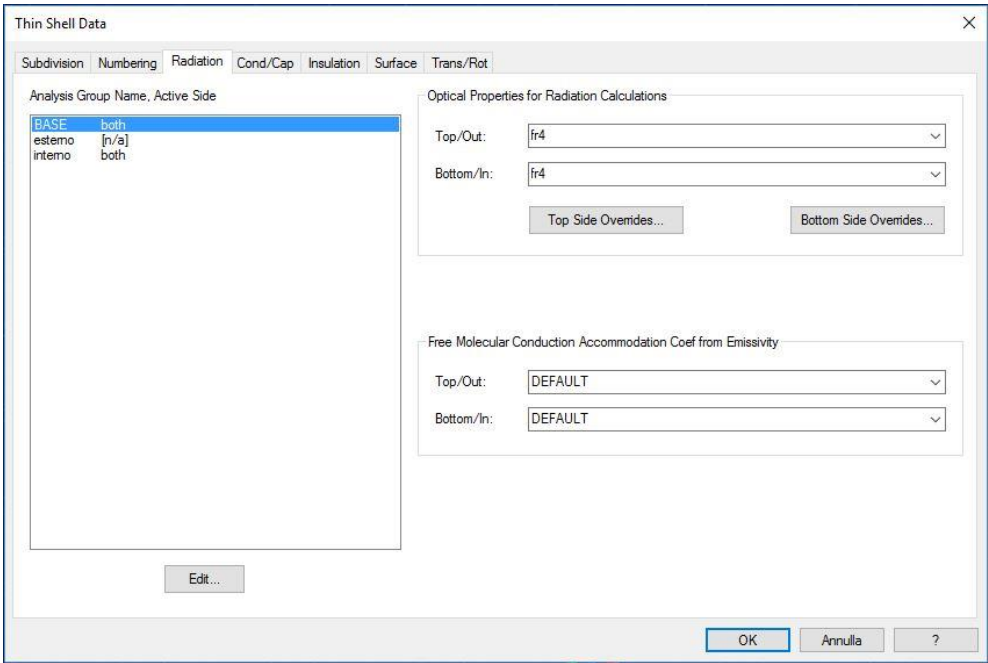


*Figure 45 Radiation tab of Electronic Boards properties from TD model*
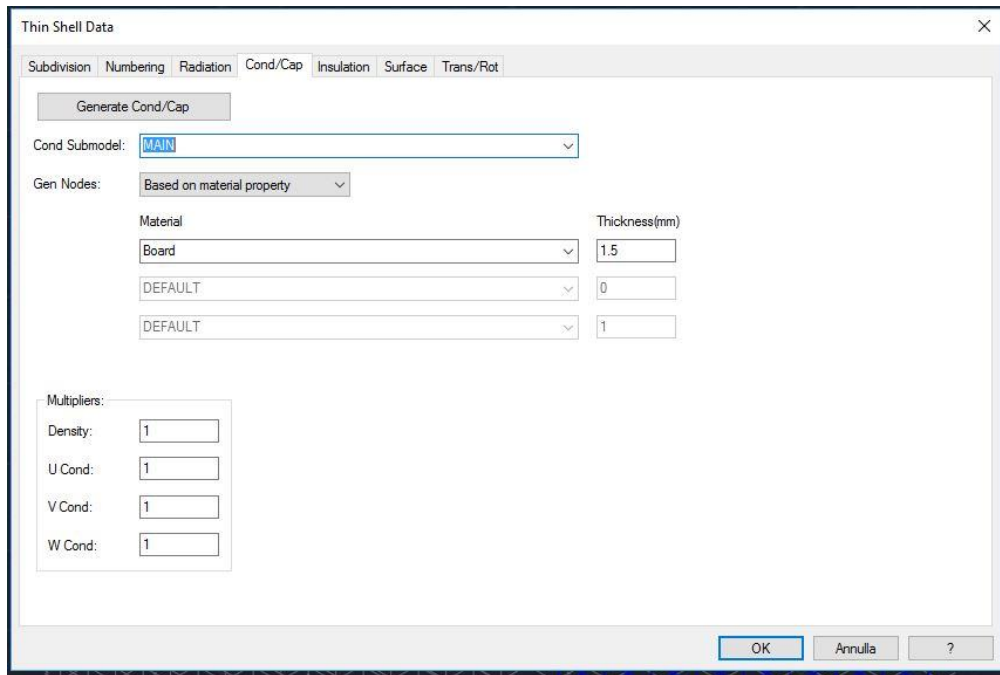
*Figure 46 Cond/Cap tab of Electronic Boards properties from TD model*
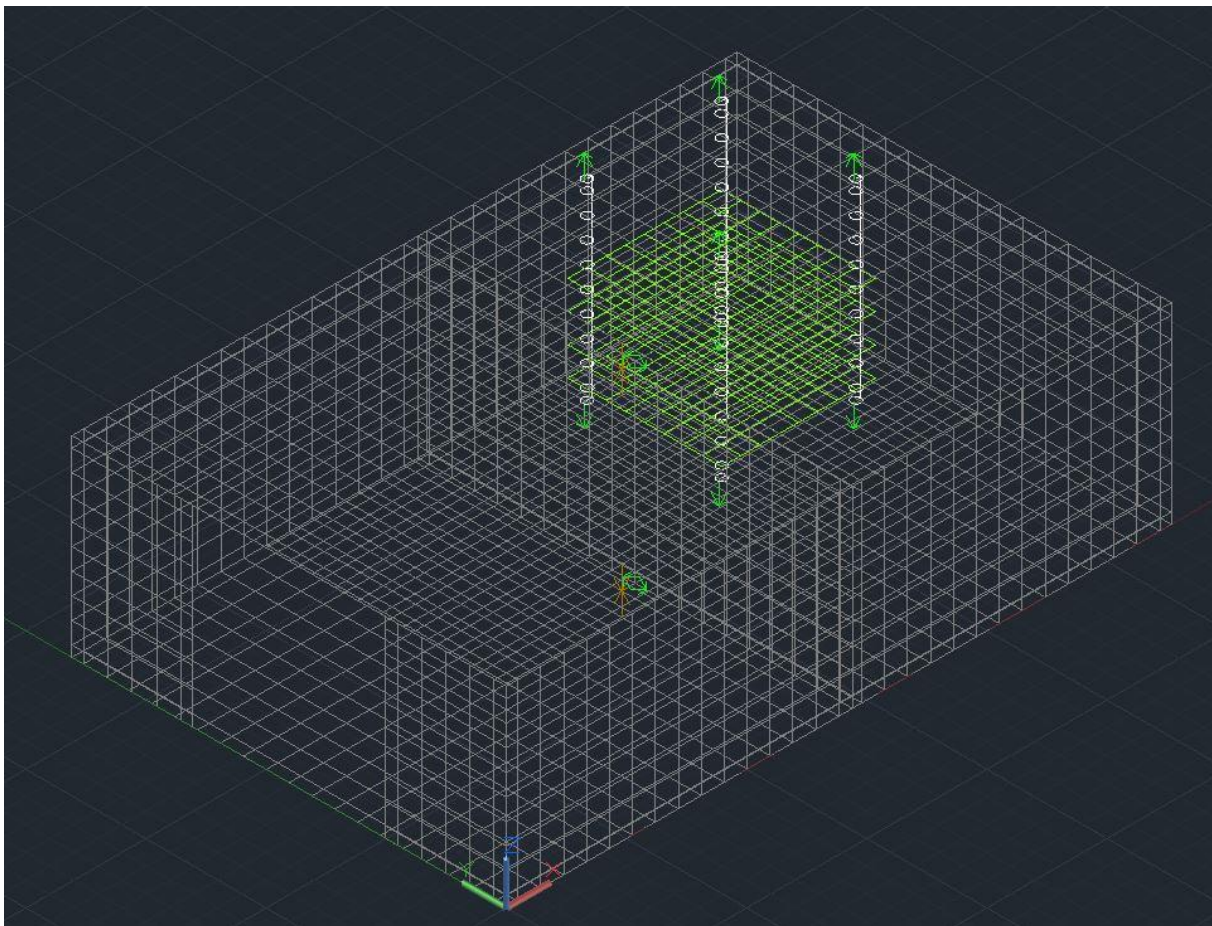


*Figure 47 TD model with Structure and Electronic Boards*

The CTP has 4 battery packs, grouped two by two in avionics batteries, mounted on top of the avionics box, and propulsion batteries, mounted next to the avionics box. Batteries have

been modelled as FEM solid bricks, with their own layer coloured blue. As for the electronic boards, Avionic Batteries are connected to the filleted bars running through the Avionic box, while the PS batteries are connected to the Bottom plate via a contactor, similarly to that of the bulkhead. The contactor is calculated for the -Z face, that is the one touching the plate, and the material considered is PEEK to mirror the operative model of the CTP that will mount a 3D printed PEEK drawer. In Figure 48 and Figure 49 the model with electronics and batteries is reported, with a focused front view on the interior of the service module. In Figure 50 it is possible to consult the properties of the contactor between the PS batteries and the Bottom plate.
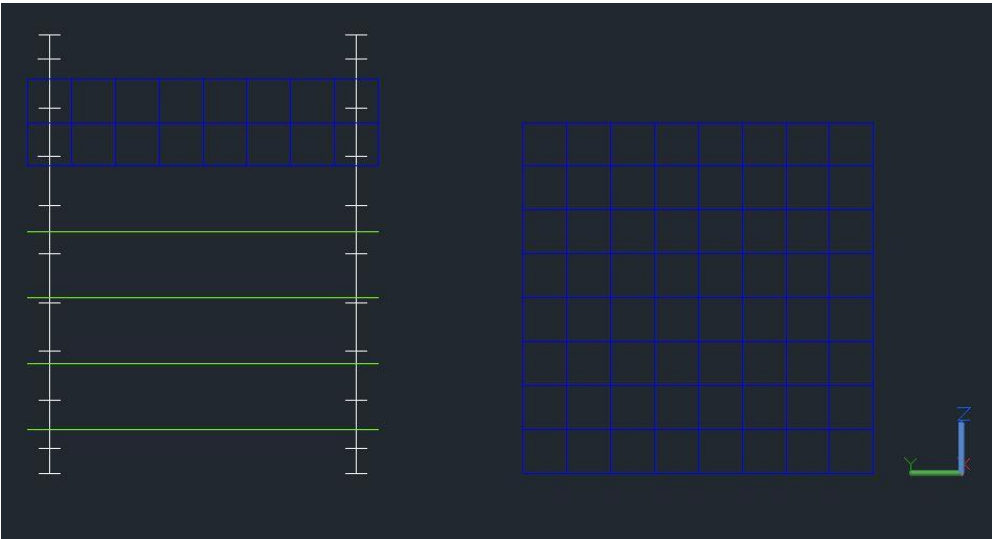


*Figure 48 Front view of electronics and battery packs with their contactors*
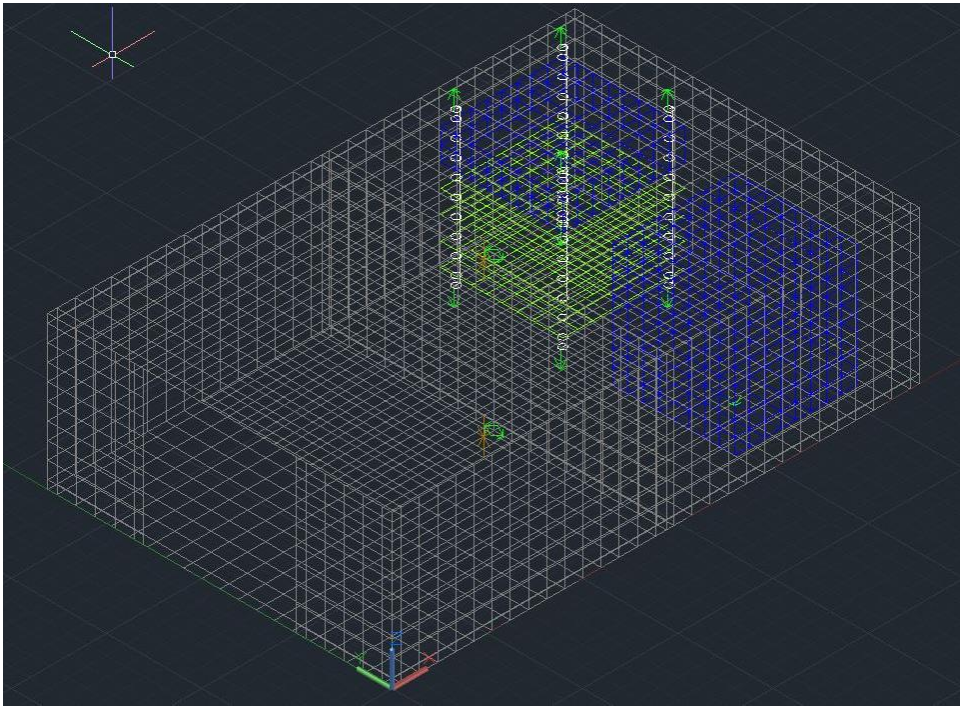


*Figure 49 Thermal Desktop model with Structure, Electronics and Batteries*
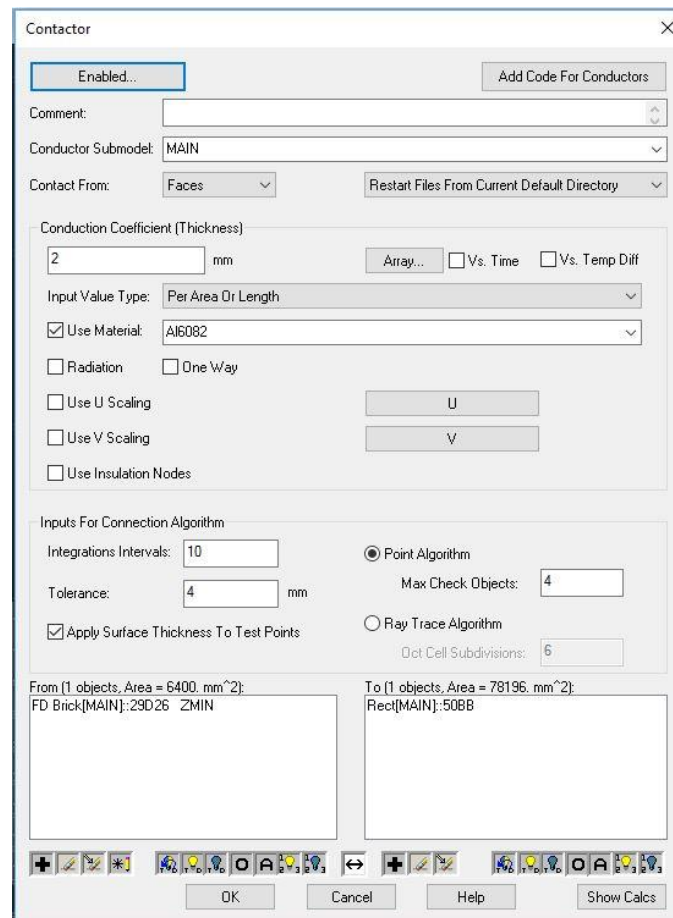
*Figure 50 PS batteries contactor with the Bottom plate properties*

After the definition of the structure and the service module, the payload had to be modelled. The ePS was modelled after T4i's REGULUS since it is expected to be the first integrated propulsion system and it is the one which had more data available. This is a 1.5U ePS with 1U dedicated to the thruster and 0.5U to the tank, fuel lines and controls. The TD model ePS was created with FEM plates to model its external structure, and the edge nodes were unified through node equivalence. The internal of the ePS is divided into the thruster section and tank section through another FEM plate, connected to the external structure through contactors. In the thruster section a FEM cylinder running horizontally between the two plates was modelled to represent the thruster, and the heat load of the ePS was placed on its internal surface. The cylinder was then connected through contactors to the two vertical plates. All the structures composing the ePS were considered to be aluminium, and this will be changed when more detailed information about materials are known. The ePS has its own layer with the colour orange and can be scaled to the occurrence in order to simulate various ePS.

To mirror the real model, the ePS is connected to the Top and Bottom plates through 6x2.5mm screws on each side. This was approximated in the model with a contactor between

ePS model and Top and Bottom plates with a coefficient that is derived from the actual contact area. Also, to mimic the real behaviour, inside the ePS has been inserted a FEM brick with a boundary node at 360K, simulating the heated tank. For REGULUS to work propellant shall be heated prior to thruster shooting, and this is done in the warm-up phase, that goes from the normal temperature of the tank to about 360K. The ePS model is shown, complete with the Heat load that will be discussed later, in Figure 51. The TD model complete with the ePS is shown in Figure 52.
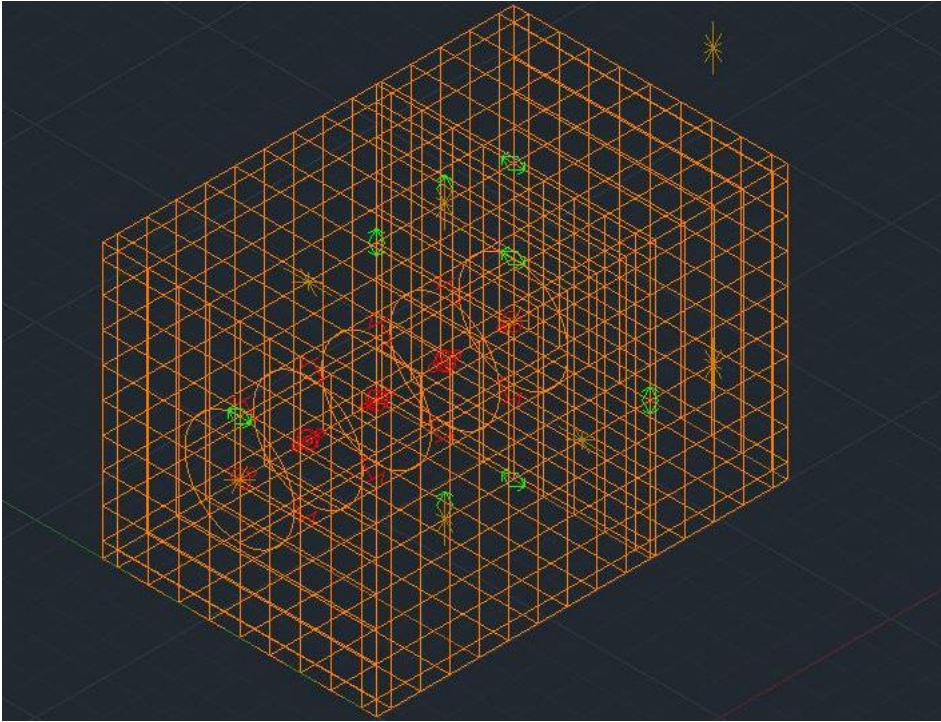


*Figure 51 ePS model for REGULUS from TD model*
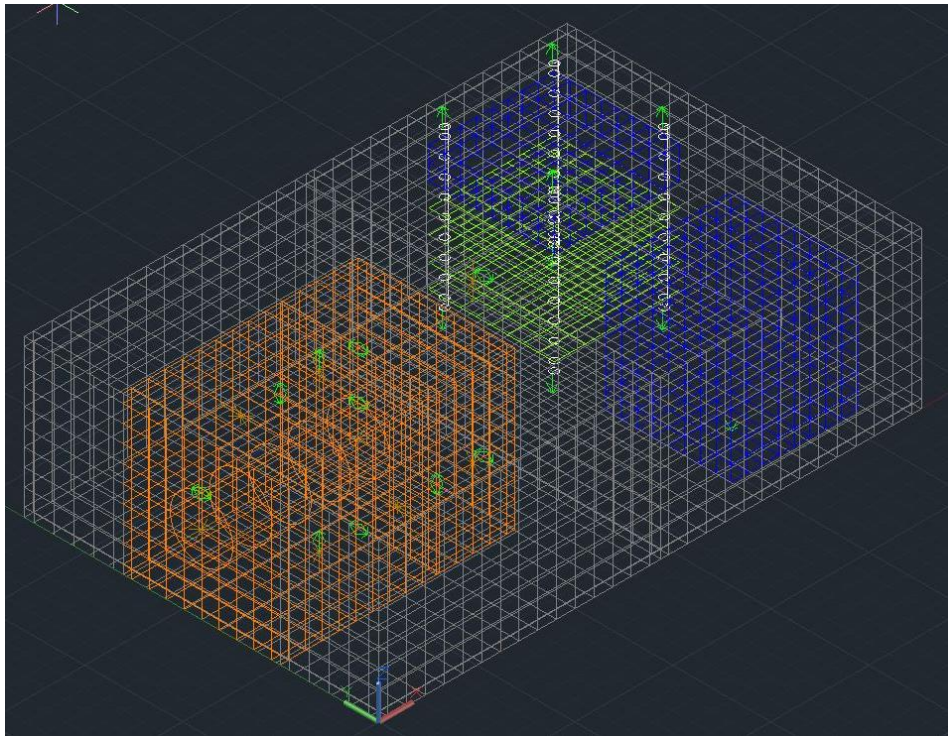
*Figure 52 Thermal Desktop model with Structure, Electronics, Batteries and ePS*

Once the geometry and properties of the model had been defined, it was necessary to identify and insert the thermal loads. Almost all components in the platform, except for the structures, generates a certain heat load due to power dissipation. Heat loads have thus been analysed and modelled into the system. Figure 53 shows how the different heat loads have been integrated on the TD model.
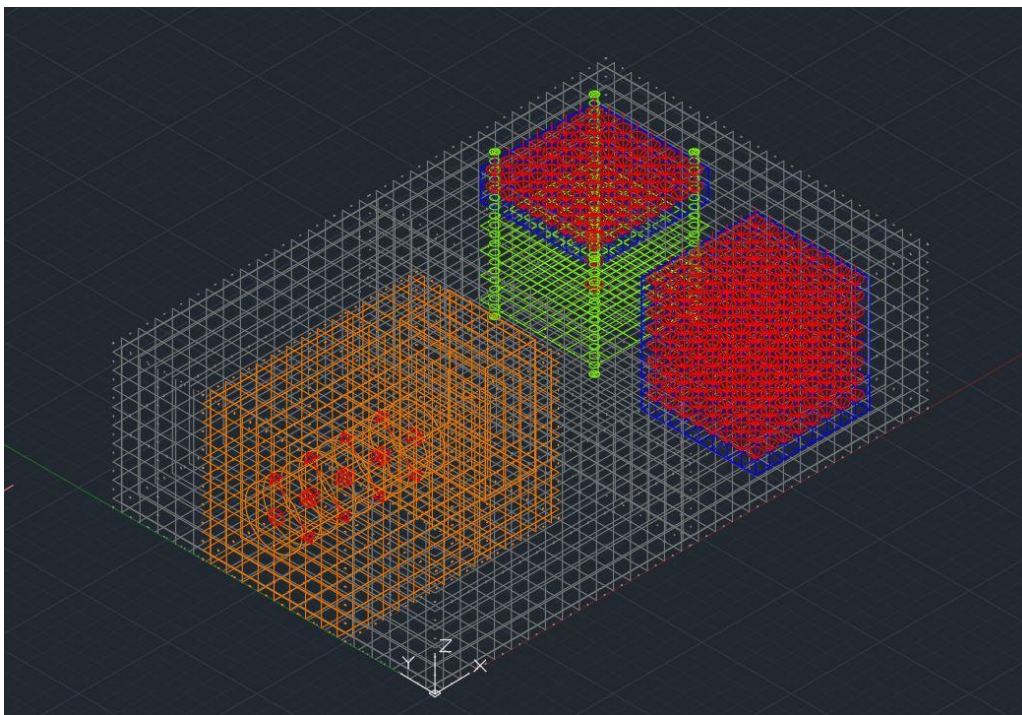


*Figure 53 Thermal Desktop complete model with heat loads*

The first heat source identified is the ePS, which will likely be the highest load applied on the platform. If we see the ePS at a system level, considering it as a black box, it will take a certain power as input and it will provide a certain force as an output. The conversion of the electrical power into the force is not ideal. The sum of all the different energy losses is called thermal efficiency and represents the fraction of power that is effectively converted into thrust. the remaining fraction is converted into heat. In the TD model all the power dissipated had been applied to the thruster model, since it is likely the most prominent heat source in the ePS.

The electronic boards are also a source of heat. They use power for data processing and even power management, but as from the third law of thermodynamics, that is no idea process and so a fraction of that power is dissipated into heat. There are four boards, the C&DH, the COMSYS, the EPS-M and the EPS-D. The C&DH board main power user is the microprocessor, and when operative its recorded power consumption is of 1.75W. The COMSYS board presents peak power consumption with low efficiency during packet transmission, every 30 seconds. Transmission takes 1.5W to provide a 0.5W signal, thus dissipating 1W into heat, but this is for a few seconds every 30s. The EPS-M is the board managing the PS batteries and the ePS power supply, its main source of dissipation is the step-up circuit, that have an efficiency of 0.95. This means that 5% of the power provided to the ePS is dissipated locally to heat, this is 2.5W of heat dissipation on the board. The EPS-D provides regulated power for the other boards and will have minor dissipation proportional to other boards power needs. For each board the heat load had been defined and charged on a central node of the board, thus simulating a chip dissipation. This causes the results to be much less accurate in that precise point but enables at least a mean value consideration without the need to model every single component and their dissipations.

The batteries are also heat sources since charge and discharge processes have an intrinsic dissipation. For this model battery efficiency has been considered to be 0.95 and thus we will have heat loads proportional to the system power needs. The heat loads on the batteries have been modelled as distributed volumetric loads, and thus the power is dissipated constantly on all the nodes composing the element.

All the heat loads are singularly modelled and belong to their own layer in order to allow user to easily change them. This is the easiest way to change parameters of the simulation to represent different operative modes or phases, and even to try variations on power consumption due to different ePS with similar geometry. The values for this simulation are reported in Table 15. Warm-up dissipated power refers to the value the power has in the first 10 minutes of the simulation, the burst dissipated heat is the value the loads assume from 10 minutes to the end of the simulation.

Table 15 Heat loads values of the TD model

| Component | Power consumed / managed [W] | Heat Warm-up [W] | Heat Burst [W] |
|---|---|---|---|
| ePS | 50 | 0 | 7 |
| C&DH | 1.75 | 0.15 | 0.15 |
| COMSYS | 1.5/30s | 0.3 | 0.3 |
| EPS-M | 50 | 1 | 2.5 |
| EPS-D | 3 | 0.2 | 0.2 |
| Avionic Batteries | 3 | 0.2 | 0.2 |
| PS Batteries | 50 | 1 | 2.5 |

To complete the TD model the environment was needed. While Thermal Desktop has built in tools for orbit modelling, and the user can easily set the environment once mission details are known, for this model the Vacuum chamber was needed. Since the CTP is completely closed inside the vacuum chamber and exchanges heat only with it via radiation. The vacuum chamber was modelled as a cylinder surrounding the model, composed by 8 elements. The radius and height of the cylinder is the same as the actual small hatch of the SPF at ESA/ESTEC. The circular plates have been used to close the cylinder on the edges, thus completely enclosing the CTP in the chamber, as shown in Figure 54. The nodes composing the cylinder and the circular plates were modified to boundary nodes, thus making temperature constant.
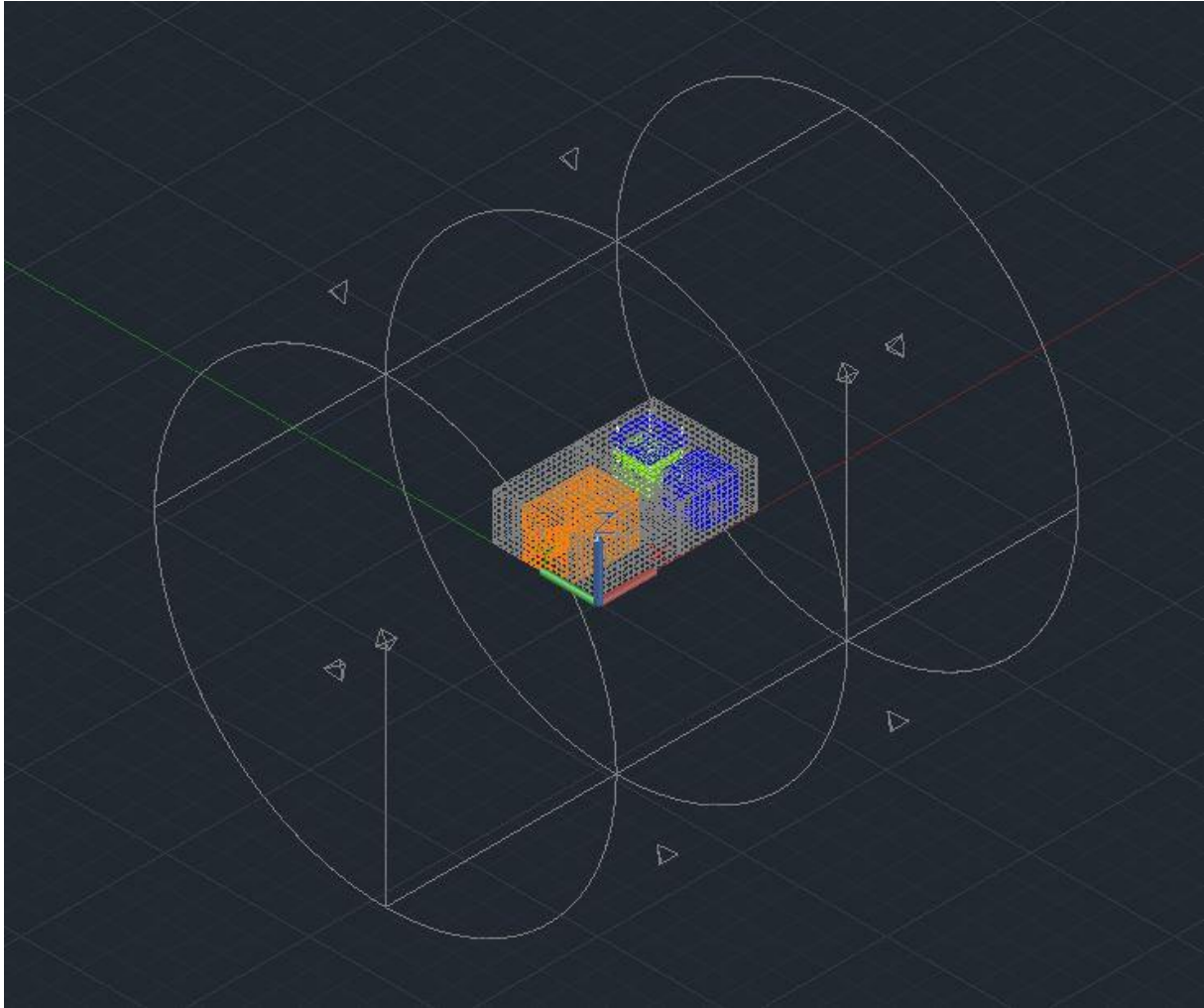
*Figure 54 TD model of the CTP with SPF small hatch environmental model*

Boundary nodes are the most common exploit used in thermal simulations to represent the external dissipation. The boundary condition on the node means no matter how much power is transferred to it, it will maintain its temperature. This makes it possible to model a thermostat, in its thermodynamic definition of an element with an infinite thermal inertia. For practical applications a thermostat is any element that has a thermal inertia high enough, related to the analysis conducted, that is not visibly influenced by the heat loads applied. This is the case for the ocean when modelling a ship, the air when modelling the heat profile of a beer can, a planet or deep space when considering a spacecraft. In this model the vacuum chamber will be a thermostat, even if it is not completely applicable to the reality. Actually, a liquid Nitrogen cooled vacuum chamber can be considered to be almost a thermostat, provided the nitrogen flow is high enough to quickly dissipate all the heat. A simple vacuum chamber, where a metal wall is in contact only with the air, will likely slightly increase its temperature over time if a source of heat is inserted.

The internal walls of the chamber are added to the external radiation calculation group, and its properties are set to match those of an aluminium surface. This way the solver will

calculate view factors and radiation exchanges for the calculations. the bounded temperature of the chamber was set for this simulation either to 90K or to 293.15K. The former represented a nitrogen cooled vacuum chamber, while the latter a simple vacuum chamber at room temperature. The values can be easily changed to any other boundary condition by selecting the environment submodel and editing the nodes.

# 5.4 THERMAL ANALYSIS

After the definition of the model and the loads the thermal analysis can be set and then launched. Thermal Desktop will create the matrices for nodes and connections and then send them to the solver, SINDA/FLUINT. The solver then uses numerical calculations to solve the set of problems provided by the user. The results are then feedback to Thermal Desktop that allows the visualisation and postprocessing of the data. Thermal Desktop can perform steady state simulation and transient simulations. While the first is much less computational power and thus time demanding, the second is the one needed for most applications. The steady state analysis only gives the thermal balance, and most of the real cases does not reach equilibrium, but rather undergoes cycles. For this specific case study, a steady state simulation would provide an unrealistically high temperature range, that would be reached in a long operational time but is not significant of actual operations since damage preventing mechanisms would intervene before that increase.

According to ECSS-E-ST-35C [17], treating the general requirements of propulsion, every propulsion system should be tested with a burst of a duration that is the same of the highest duration manoeuvre considered for the mission. For this reason, propulsion systems are provided with the maximum burst duration, that is the one it has been tested for. Since the CTP will be used for test and qualification of ePS, it will have to undergo the longest non-stop burn established from the manufacturer. This can prove quite stressing from a thermal point of view for the platform, and thus predictive thermal analysis is used.

During the final phases of this thesis the first test of the CTP was foreseen, and the simulations were modelled accordingly. The first test object, as said, will be T4i's REGULUS, upon which the ePS itself is modelled. Before the manoeuvre REGULUS needs the propellant to be at 90ºC and for this reason it will use a heater on the tank. For this purpose, a boundary node has been used for the tank, and to simulate the conducted heat from the tank to the platform 10 minutes of the transient have been conducted with propulsion off. The expected mean manoeuvre for REGULUS is expected to have a duration of 30 minutes, while the upper

limit is expected to be at 2 hours. It is still uncertain if the tests are going to be conducted in a thermal vacuum environment (tvac) or in a simple vacuum environment. Tvac refers to a 90K walled chamber, while vac to a 293.15K walled chamber. Four simulations have been run:

- 10-minute warm-up + 30-minute burst in tvac (**tvac-30**)
- 10-minute warm-up + 30-minute burst in vac (**vac-30**)
- 10-minute warm-up + 2-hours burst in vac (**vac-120**)
- 10-minute warm-up + 2-hours burst in tvac (**tvac-120**)

The latter were the most extreme test condition possible and were performed to verify the ability of the platform to sustain the test, either in normal vacuum or in thermal vacuum conditions.

## 5.4.1 Analysis setup

The setup of the different analysis is quite similar, and the only differences are the temperature of the boundary nodes between tvac and vac simulations and the time the simulation runs. The geometrical model as well as the calculation method are the same. All the different case sets rely on similar assumptions. One of the assumptions is that of the environmental boundary on the chamber walls, the other is on the tank. The boundary node at 360K on the tank that is considered to be kept constant during the whole transient.

Thermal Desktop allows the user to define different analysis case sets, and to define how the cases should perform the analysis. For this analysis a case set was created, shown in Figure 55, where only the Transient simulation is performed. The duration of the transient is either 2400s for 30-min burst and 7800s for 120-min burst, both with a 600s warm-up phase. The time step of the calculation was set to 0.5s to make the simulation run quicker. To make the simulation run smoother, Thermal Desktop allows the user to differentiate different aspects in different analysis groups. For this analysis two groups have been defined to represent the two separate environments. The first is the exterior, and it is the analysis group concerning the radiated heat between the CTP and the internal walls of the vacuum chamber. This exchange only interests the external surfaces of the structural box containing the platform and the built-in radiator of Regulus. For this reason, it comes with no advantage to perform the calculation for the internal nodes and coming to the result that there is no exchange, making the simulation run slower with no reason. The other group is the is the interior group, and it is about the exchanges happening between the elements composing the platform. Again, it would come to no advantage to make calculations for the exchange between internal component and the facility walls. By dividing the two environments computational power is saved.

Both environments are operated with *radk*, that is a tool provided by Thermal Desktop that enables the calculation of radiated energy without having to define the view factors. Those are calculated by the tool via the simulation of a certain number of rays radiating from each element and eventually intercepted by other elements. After view factors calculations the software sends those, along with materials, areas and starting temperatures to the solver, SINDA/FLUINT, that simulates the transitory and provides the results.
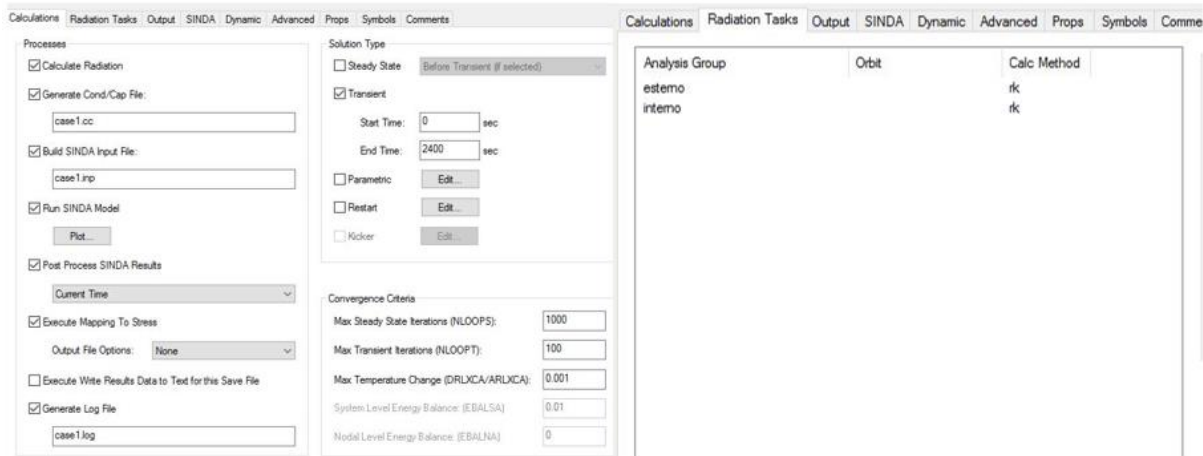


*Figure 55 case set from TD model*

## 5.4.2 Analysis results

There are two main output of this transient simulation, the temperature map at the end of the simulated period and the evolution of those temperatures with time. The first is useful in this case because it represents the maximum reached after a prolonged heat load is applied, while it is not significative in case of cyclic or variable loads. The evolution over time is significant in every case since it shows the thermal history of the platform and enables to understand how the loads affected the temperature maps over time. From now on, whenever a thermal map is shown, it will refer to the end time of the simulation (either 2400 or 7800 seconds), while some graphs about thermal variation are also reported. Results will be analysed for each submodel group. Transient graphs are only reported for the two-hour simulations since from those alone it is possible to derive the 30 minutes simulation graphs as well.

*Avionics*

The avionics are a delicate part of the platform, since they are all packed in a small environment and they all dissipate power. For this specific case there is also a power dissipation that is much higher than that usually found on CubeSat boards. This can prove to be an issue, especially for tests with long duration burns. Figure 56 and Figure 57 shows the resulting thermal maps of

the avionics from the different simulations. It is interesting to focus on Figure 56, where it is possible to notice that the tvac-30 and vac-30 thermal maps are really similar in their form but differ from each other of about 5 degrees. This is due to the higher ability of tvac in extracting the heat generated by the CTP. In both cases temperatures rise well up on the limits of the board in specific points where the load is applied, but this is due to a numerical problem of this load model, while the actual significant temperatures are those more distant from the nodes. Both cases at 30 minutes burst show temperatures that are in the operative ranges, and thus for short tests it is of little concern the environmental cooling. For the 120 minutes burst however temperatures rise to dangerous levels on most of the surface, and thus further analysis should be conducted on the possibility of performing vac test to the thruster limit. While limiting the temperature reached, tvac simulation also reaches dangerous temperatures. A more detailed model for the avionics should be used to be safe or a TCS should be implemented to dissipate heat from the boards more efficiently.
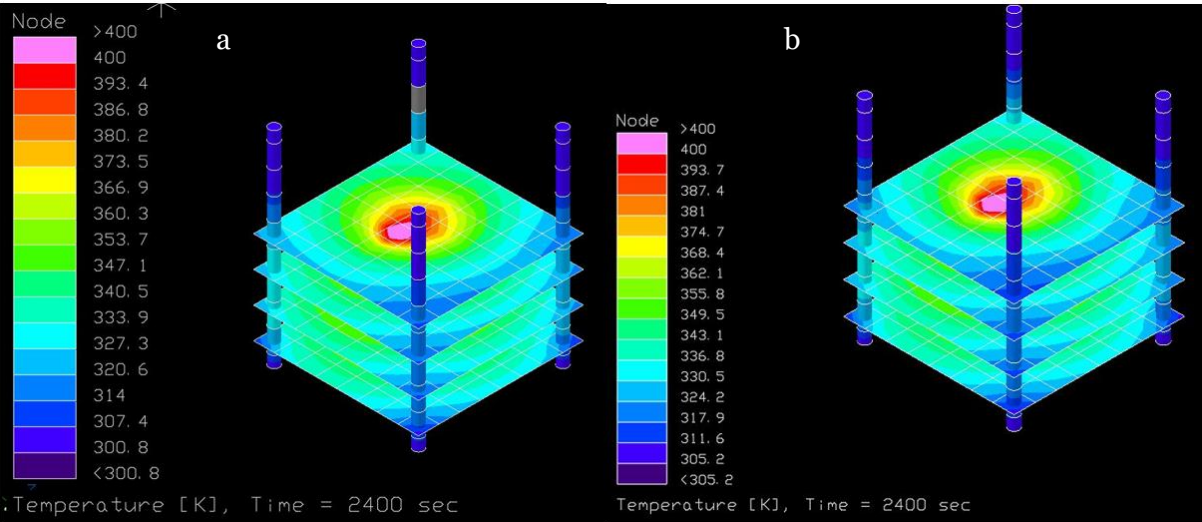


*Figure 56 Thermal map of the Avionics boards from tvac-30 (a) and vac-30 (b) simulation*
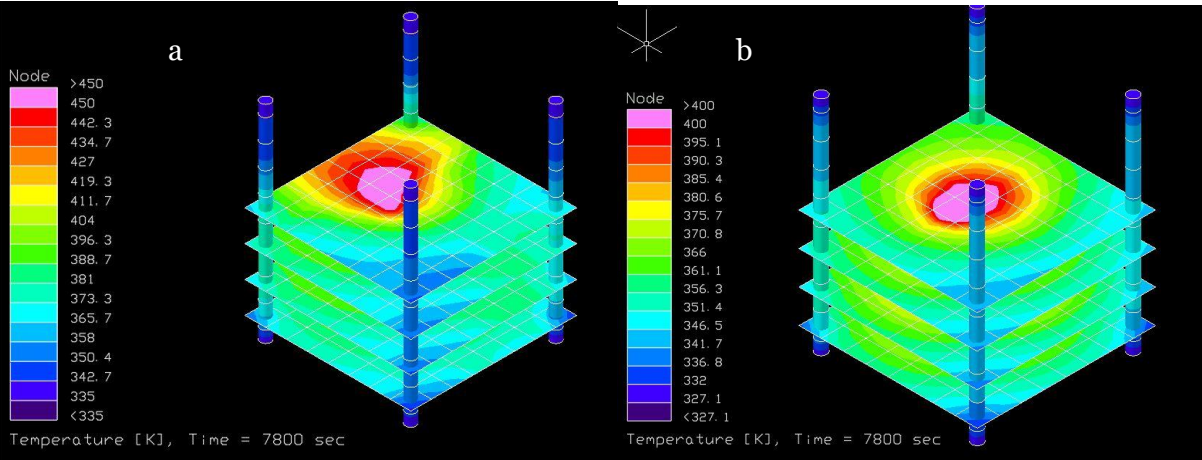


*Figure 57 Thermal map of the Avionic boards from vac-120 (a) and tvac-120 (b) simulation*

100

Figure 58 shows the transient graphics for the vac-120 and tvac-120 minutes. It is possible to see how, after an equilibrium reached during warm up, the temperature tends to increase as the time passes and the load persists. this shows how the high-power loss on the EPS-D board is greatly affecting the survivability of the system over long duration bursts.
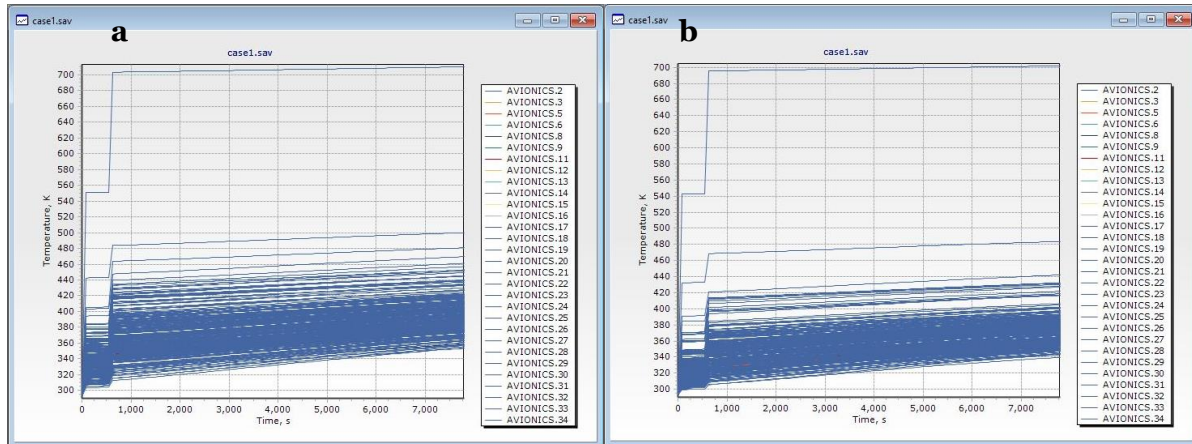


*Figure 58 Transient graphic of the temperatures of Avionics boards for vac-120 (a) and tvac-120 (b)*

### Batteries

Batteries are usually the most delicate element in a spacecraft, greatly suffering both cold and hot environment to the point that not only their performances, but also their integrity quickly degrades. For this reason, particular care should be used when considering battery design. Figure 59 shows the thermal maps of the batteries for the tvac-30 and vac-30 simulations. As for the avionics the differences are minimal, and the batteries are completely inside their operative limits. Thus, there is no need for tvac for short burst tests. As for Avionics the situation is more critical in the case of uncooled long bursts. As shown in Figure 60 temperatures up to 76ºC are reached by the batteries, and that could prove dangerous for their survivability. This is especially true for the avionic batteries, and thus it is reasonable to think that a TCS able to dissipate avionics heat more efficiently could also solve the problem on the batteries. In case it is not enough it could be useful to add some insulating material between the avionics and the batteries. From the tvac simulation it is obvious that thermal vacuum alone could be not enough to preserve the components.

From the transient graphic in Figure 61 it is possible to see how the batteries keep heating up as the simulation goes on in vac-120 it is possible to see the tendency of the PS batteries to reach an equilibrium temperature, while the avionics batteries warm up due to avionic heat dissipation. From the results of the analysis it is likely that the addition of some kind of insulation such as MLI between the avionics and the batteries could prove useful in limiting the heat passing to the batteries.
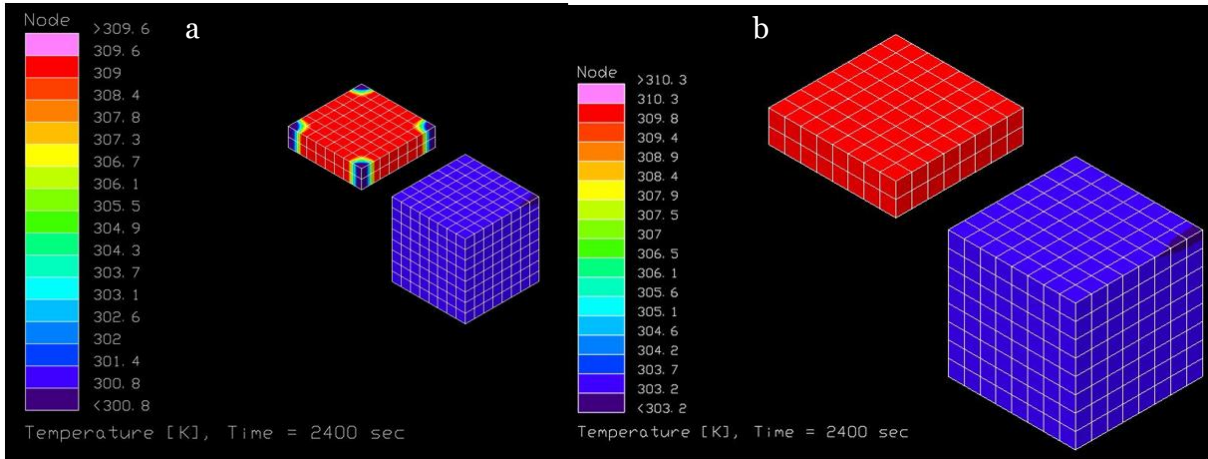
*Figure 59 Thermal map of the Batteries from tvac-30 (a) and vac-30 (b) simulations*
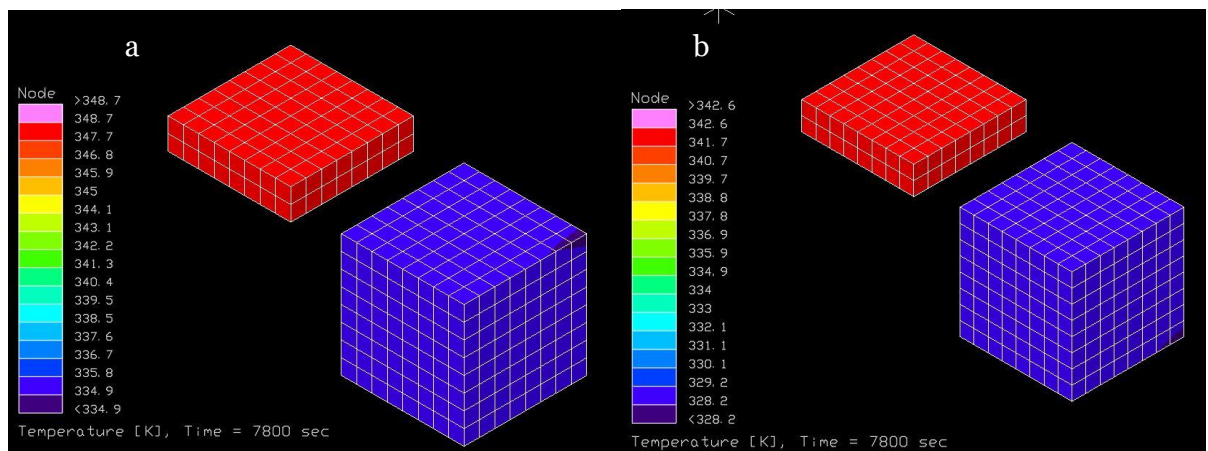


*Figure 60 Thermal map of the Batteries from the vac-120 (a) and tvac-120 (b) simulation*
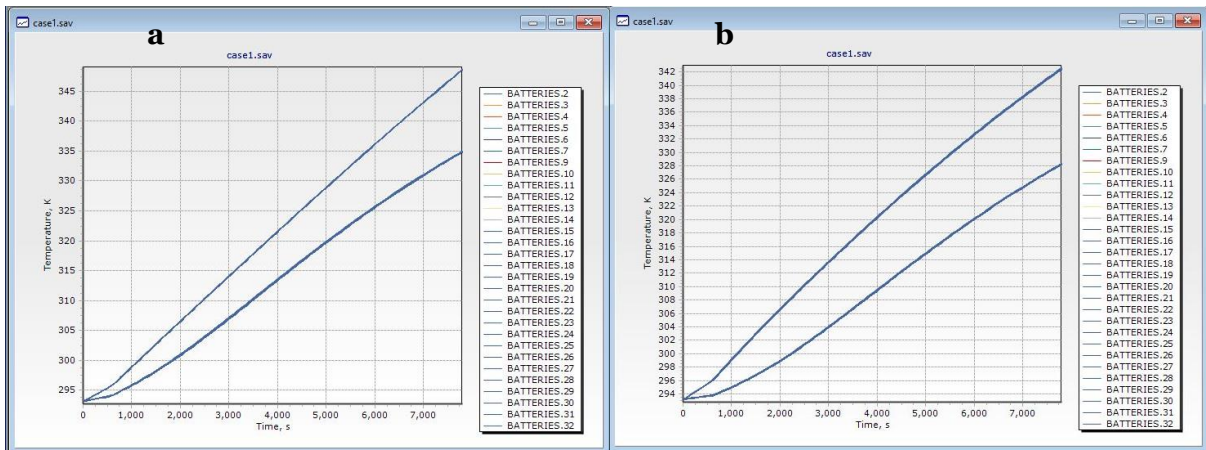


*Figure 61 Transient graphic of the temperatures of Batteries for vac-120 (a) and tvac-120 (b)*

*Electric Propulsion System*

102

The electric propulsion system is obviously a great source of heat, even if not the most critical one. Anyway, its positioning and heat dissipation through radiation makes it less critical than the avionics in the end. As shown in Figure 62 and Figure 63 the ePS has an increase of temperature that is bonded partially to the thruster, but very much to the heating of the tank. This leaves an open point to be investigated on the eventual insulation of the tank and how it reduces heat dissipation. However even a not insulated model as this shows how the tank heating, summed with the thruster dissipation, is not able to make the ePS too hot to work. Of course, this is quite obvious since the manufacturer of each ePS will obviously perform a detailed thermal analysis to ensure the safety of the system. For this reason, the ePS is of actual little concern for this thesis work and is only used to see how it impacts on the other components. A detailed thermal analysis of the ePS is expected to be provided prior to the test and the model will be modified accordingly in order to simulate it in a more accurate way. Figure 64 shows the transient analysis of the ePS. It is possible to see that it closes to equilibrium in the two-hour simulation time.
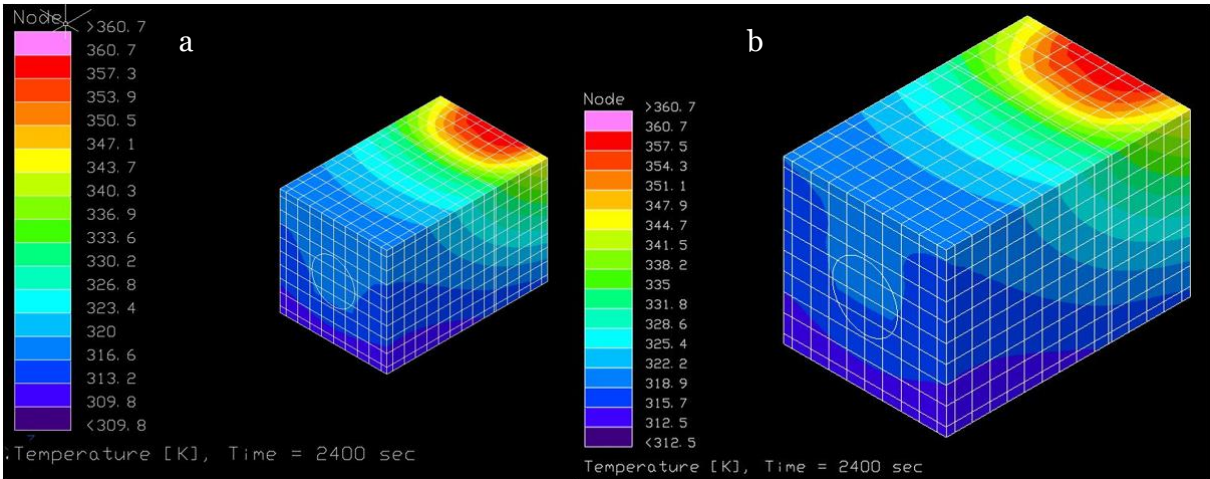


*Figure 62 Thermal map of the ePS from tvac-30 (a) and vac-30 (b) simulations*
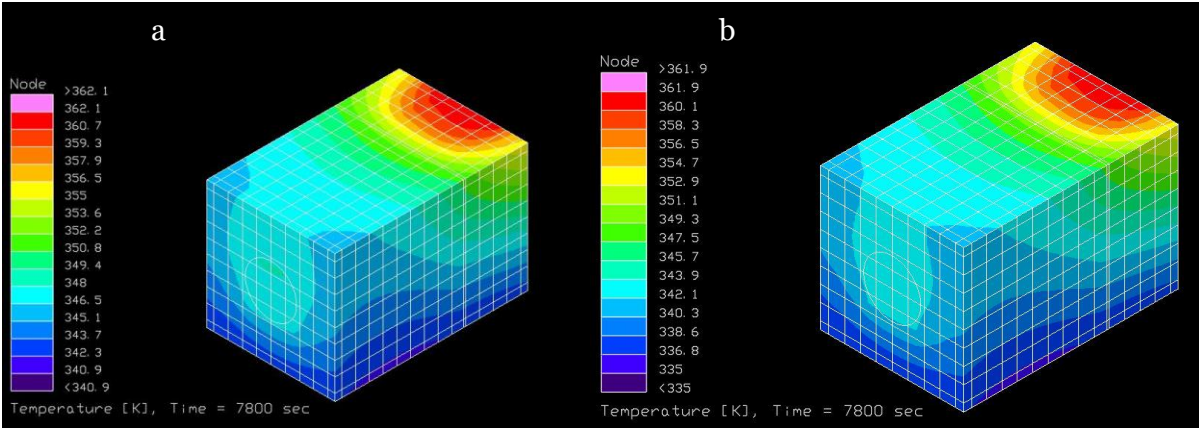


*Figure 63  Thermal map of the ePS from vac-120 (a) and tvac-120 (b) simulations*
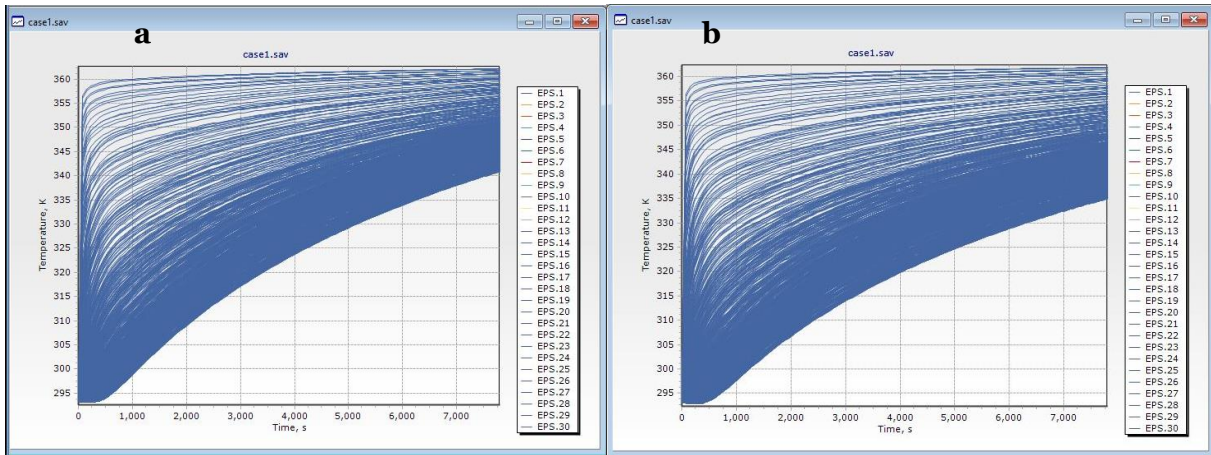
*Figure 64 Transient graphic of the temperatures of ePS for vac-120 (a) and tvac-120 (b)*

*Structure*

The structure of the CTP is the less sensitive part of the platform, since temperatures able to damage it would mean the internal components are not only passed their operative temperature ranges, but also their survivability range. It is however an important part, since it is, with the integrated radiator of the ePS, the only part of the platform facing the external environment. Thus, the heat produced in the platform is dissipated through it, and the amount of heat dissipated is directly proportional to the temperature of the structure itself. This way, the more the temperature of the structure rises, the more heat is dissipated. Therefore, at a certain point equilibrium is reached by each power dissipating object.

In Figure 65 The structure's thermal map is shown for the 30 minutes cases. As for the other cases the tvac case shows slightly lower temperatures than the vac simulation. This is due to the nature of radiative exchange, where heat is exchanged from the hot surface to the cold surface proportionally to the difference in temperature. This becomes even more evident after 2 hours of simulation, as shown in Figure 66. As time passes and internal element dissipate power getting warmer, the same is true for the external structure. As it is possible to see from Figure 68, showing the variation in time, the more the time passes the more the structure heats up. Due to the higher heat dissipation towards the vacuum chamber, the heat rate of the structure decreases over time, but equilibrium is still to be reached 2 hours into the simulation. It is possible to see from the pictures, especially from Figure 67, that the connection between the ePS and the structure transforms the latter into an effective radiator for the heat generated by the thruster. If ever a TCS is added to help cooling the avionics, it will also exploit the structure as a radiator, and thus it will need some kind of connection to the structure itself or changes in the structure internal optical properties to increase radiated heat absorption.

104
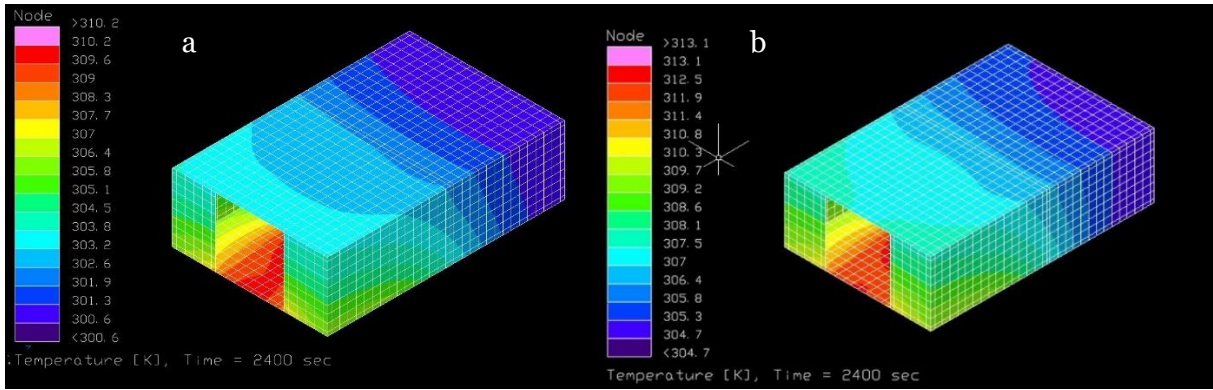
*Figure 65 Thermal map of the Structure from tvac-30 (a) and vac-30 (b) simulations*
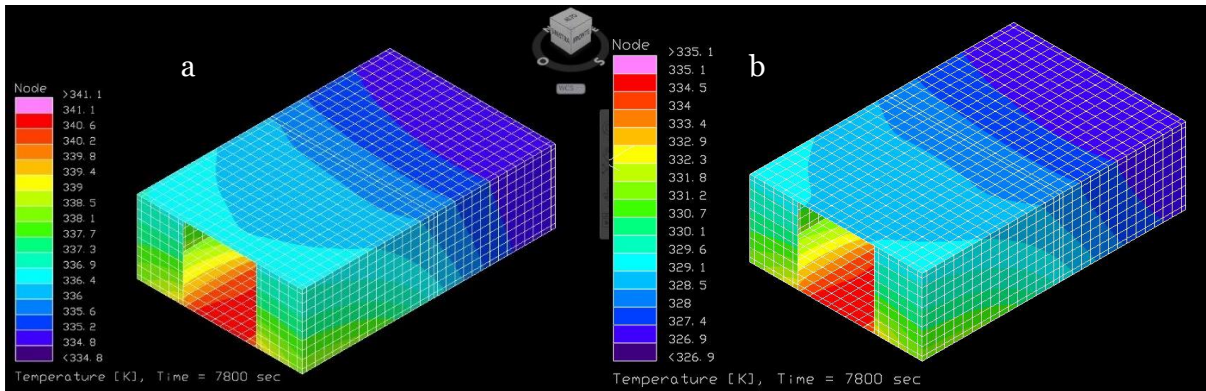


*Figure 66 Thermal map of the Structure from vac-120 (a) and tvac-120 (b) simulations*
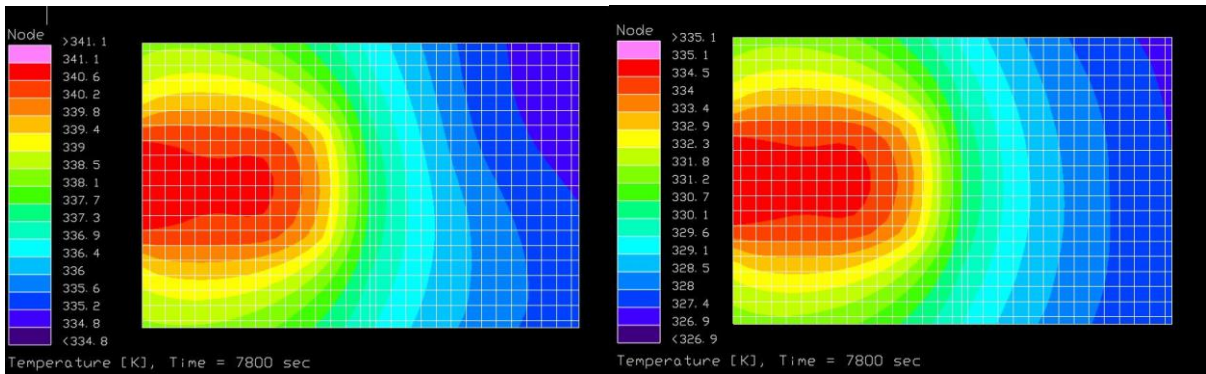


*Figure 67 Thermal map of the Structure bottom view from vac-120 (a) and tvac-120 (b) simulations*
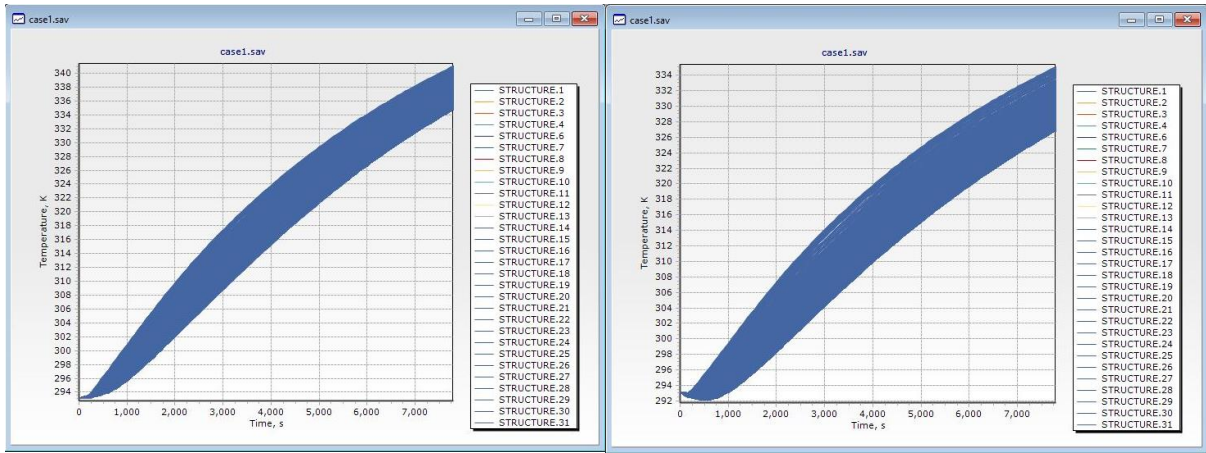
*Figure 68 Transient graphic of the temperatures of Structure for vac-120 (a) and tvac-120 (b)*

## 6.1 RESULTS AND CONCLUSIONS

With their potential and the interest and effort both agencies and privates are putting into their development, it is of little doubt that CubeSats will have a major role in the upcoming space exploration and commercial space market, both as a support and as a standalone platform. The work concluded to this point can prove to be a significant help to the development of one of the capabilities required to fulfil these roles. It is likely that in the upcoming few years there will be a strong demand for a quick, proved qualification procedure for small spacecraft propulsion, and this work, along with the program it is part of, bring this reality one step closer to being completed. As the ultimate goal of the ESA-Prop program, new tailored ECSS for CubeSat propulsion could be developed starting from this work.

The scene of miniaturised electric propulsion had been analysed and found mature enough to perform a multitude of roles in the upcoming years. Those roles have been identified and associated with different propulsion technologies, while keeping in strong regard the technical issues CubeSat platforms will suffer from each different technology. From this analysis the development of a test platform and relative procedures is being carried on and will go on with the next phases of the project and with the platform usage from ESA. The major issues the platform will face and the measurements that will prove necessary for the qualification of an electric propulsion system have been identified, as well as some of the sensors and methodologies to measure them.

With the knowledge acquired from the first phase of the program a prototype test platform has been designed and manufactured. It was integrated and tested to ensure its functionality, thus demonstrating the feasibility of the program higher goals. The platform has been delivered to ESA/ESTEC Electric Propulsion Laboratory and was accepted by the agency as a proof of concept. Thus, the program is advancing towards a more complete platform building on the previous experience and expanding the knowledge matured in the first phase.

For this reason, a preliminary thermal analysis has been conducted, simulating the tests performance as expected, identifying some criticalities that will need to be addressed with the operative version of the platform. The analysis has also highlighted that, at least from a thermodynamic point of view, ePS integration on a CubeSat platform will actually need to be assessed with appropriate care and knowledge. The impact of the system on the platform is huge for such a small platform, but is not unbearable, assuming the designers keep it into account when designing it.

## 6.2 OPEN POINTS AND FUTURE WORK

As previously stated, this thesis is not the conclusion of the ESA-Prop program neither for the Politecnico di Torino nor the European Space Agency, an it is in fact the very beginning of the most important phase. For this reason, the work will need to be carried on both with the identification of the needed sensors and preliminary analysis of the remaining impacts of the ePS and with the actual design and manufacture of the operative platform.

Test procedures will also need to be defined, and both the platform and those procedures will need to be put to the test with an actual ePS test. This has partially already been assessed or is under investigation at the moment of the writing of this chapter, since even with the end of this thesis the actual work on the program still goes on.

Regarding more in detail the work presented in this document, some open points remain to be assessed:

- The SoA of electric propulsion and the matrix connecting ePS and mission capabilities should be regularly updated to keep track of variation in design, upgraded performances and even new actors on the scene
- The TD model should be modified to reflect the properties of CTP operative version, when its design is completed
- The simulation should be repeated with data coming from the actual ePS detailed thermal analysis as soon as it is provided, in order to adjust the results to the specific case.
- The simulation should be repeated for different ePS models each time a different test is expected

# REFERENCES

[1] "Technology CubeSats." [Online]. Available: http://www.esa.int/Our_Activities/Space_Engineering_Technology/Technology_Cub eSats.

[2] M. A. C. Silva, D. C. Guerrieri, A. Cervone, and E. Gill, "A review of MEMS micropropulsion technologies for CubeSats and PocketQubes," *Acta Astronaut.*, vol. 143, pp. 234–243, 2018.

[3] J. Yanhui, Z. Tianping, W. Chenchen, and K. Yujun, "The Latest Development of Low Power Electric Propulsion for Small Spacecraft," *Jia*, 2017.

[4] K. Lemmer, "Propulsion for cubesats," *Acta Astronaut.*, vol. 134, pp. 231–243, 2017.

[5] J. Mueller, R. Hofer, and J. Ziemer, "Survey of propulsion technologies applicable to cubesats," 2010.

[6] D. Rafalskyi and A. Aanesland, "A Neutralizer-Free Gridded Ion Thruster Embedded Into A 1U Cubesat Module," in *International Electric Propulsion Conference*, 2017, vol. 10, p. 48.

[7] A. Tummala and A. Dutta, "An overview of cube-satellite propulsion technologies and trends," *Aerospace*, vol. 4, no. 4, p. 58, 2017.

[8] R. Walker *et al.*, "Deep-space CubeSats: thinking inside the box," *Astron. Geophys.*, vol. 59, no. 5, pp. 5–24, 2018.

[9] E. A. Woeppel *et al.*, "The Near Earth Object (NEO) Scout Spacecraft: A low-cost approach to in-situ characterization of the NEO population," 2014.

[10] C. Foster, H. Hallam, and J. Mason, "Orbit determination and differential-drag control of Planet Labs CubeSat constellations," *arXiv Prepr. arXiv1509.03270*, 2015.

[11] E. Gill, P. Sundaramoorthy, J. Bouwmeester, B. Zandbergen, and R. Reinhard, "Formation flying within a constellation of nano-satellites: The QB50 mission," *Acta Astronaut.*, vol. 82, no. 1, pp. 110–117, 2013.

[12] K. Dannenmayer, "TEC-MP-EPL/P002 EPL General Description." .

[13] D. G. Gilmore, "Spacecraft Thermal Control Handbook, Fundamental Technologies, vol. I The Aerospace Press/American Institute of Aeronautics and Astronautics." Inc, 2002.

[14] M. Muratori, "Thermal Characterization of Lithium-Ion Battery Cell," Politecnico di

Milano, 2009.

[15]    "Electronics Cooling." [Online]. Available: electronics-cooling.com.

[16]    "matweb." [Online]. Available: www.matweb.com.

[17]    "ECSS-E-ST-35C - Propulsion General Requirements." .